A SPECTRAL-PERTURBATION MODEL OF WATER-DRIVEN OIL FLOW IN POROUS MEDIA

Peter T. Kallay

New Mexico Institute of Mining and Technology

This independent study
has been submitted
in partial fulfillment of the
requirements for the degree
Master of Science in Hydrology.

ABSTRACT

The flow of two immiscible fluids through porous media occurs in many physical situations, in particular during waterflood oil recovery. Perturbation of governing equations followed by application of the Spectral Representation Theorem allows stochastic modeling of two-phase flow in heterogeneous porous media. The spectral-perturbation method is applied to both two-dimensional and three-dimensional flow, as well as to the effective velocity of water. The application of the spectral-perturbation method to two phases is a new development, and thus many simplifying assumptions are made; however, the method shows promise of developing into an effective tool for stochastic modeling of heterogeneous reservoirs. Further work to reduce the restrictiveness of some of the assumptions is recommended.

Computer programs were written to compute spectral densities and covariances for two-dimensional pressure and log saturation, variances of three-dimensional pressure and log saturation, and the effective velocity of water. Sensitivity analyses for the variances and effective velocity to various parameters were carried out. The variances of pressure and log saturation are lower for three dimensions than for two dimensions. The variance of log saturation increases toward an asymptotic value, while the variance of pressure decreases substantially as the log-saturation gradient increases. The sensitivity of log saturation and pressure to correlation length is not very great, but variance of log saturation decreases and variance of pressure increases with increasing correlation length. Effective velocity showed little sensitivity to correlation length, but increased as the absolute value of the log saturation gradient increased.

ACKNOWLEDGMENTS

The author would like to gratefully acknowledge the many sources of help without which this work could not have been completed. Those who have helped are too numerous to cite here, but a few must be specifically mentioned. First, the author would like to acknowledge the large amounts of time and patient effort spent in support of this project by his advisor, Allan Gutjahr, and professor, John Wilson. The financial support provided by the U. S. Department of Energy (DOE) is gratefully acknowledged. Much helpful assistance was given by fellow students Tony Zimmerman and Annette Schafer-Perini. Many hours were spent typing and revising the manuscript by Elly Adair.

The author would also like to acknowledge the patience and financial support given by his mother and father, Eva and Chuck Kahn. The author also appreciates the patience and understanding of his wife, Comfort, and daughter, Cynthia.

Finally, the author wishes to gratefully acknowledge the talents and opportunities bestowed on him by his Creator. There are many on this earth who will never have the opportunities given to the author, and the author trusts that his Creator will give him strength and guidance that he may unselfishly share the fruits of this work with others, particularly those who may never have the opportunities given to him.

TABLE OF CONTENTS

LIST OF FIGURES

LIST OF NOTATIONS

A = Anisotropy Ratio

A_C = Exponent of saturation in approximating function for total mobility

A_O = Parameter in approximating function for relative permeability to oil

A_w = Exponent of saturation in approximating function for relative permeability to water

B_C = Exponential constant in approximating function for total mobility

C = Covariance function

C_o = Parameter in approximating function for relative permeability to oil

C_w = Exponential constant in approximating function for relative permeability to water

E = Expected value operator

e = Base of the natural logarithms

F = Mean of logarithm of permeability

f = Random fluctuations of logarithm of permeability

G = Expected value of the gradient of the natural logarithm of saturation

i = The unit pure imaginary complex number (0.0,1.0)

J = Expected value of the gradient of pressure

k = Intrinsic permeability

k_{ro} = Relative permeability to oil

k_{rw} = Relative permeability to water

M = Total mobility

M_i = Mobility of fluid i

P_C = Capillary pressure

P_o = Oil pressure

$\bar{P}_o$ = Mean of oil pressure

P_o' = Random fluctuations of oil pressure

P_w = Water pressure

$\underline{r}$ = Spatial distance vector in wave number space

S = Water saturation

S_B = Mizell's spectral density "B" for permeability

S_{ff} = Spectral density of permeability

S_{pp} = Spectral density of pressure

S_{YY} = Spectral density of natural log of saturation

$\underline{V}_o$ = Darcy velocity vector for oil

$\underline{V}_w$ = Darcy velocity vector for water

Y = Natural logarithm of saturation, S

$\bar{Y}$ = Mean of natural log of saturation

Y' = Random fluctuations of natural log of saturation

Z_f = Complex process uniquely associated with permeability

Z_p = Complex process uniquely associated with pressure

Z_Y = Complex process uniquely associated with saturation

z = Axial distance variable in cylindrical coordinate system

α = A distance parameter related to the integral scale

θ = Angular variable in cylindrical coordinate system

λ_1 = Correlation length in first cartesian coordinate direction (horizontal)

λ_2 = Correlation length in second cartesian coordinate direction (horizontal)

λ_3 = Correlation length in third cartesian coordinate direction (vertical)

μ_o = Oil viscosity

μ_w = Water viscosity

ξ = Distance variable in the real domain

π = Ratio of circumference of a circle to its diameter

ρ = Specific mass, or density, of a fluid

ρ = Radial distance variable in cylindrical coordinate system

σ_f = Variance of permeability

σ_Y = Variance of natural log of saturation

Φ = Porosity

∇ = Del operator, or gradient operator

$*$ = Complex conjugate

1. INTRODUCTION

NATURE OF PROBLEM

The flow of two immiscible fluids through porous media occurs in a wide variety of physical situations. Among the most common in the subsurface environment are waterflooding of an oil reservoir, water flow through the vadose zone, and organic liquids flowing in an aquifer.

Human activities often create or alter these flows, resulting in substantial changes from the original flow regimes. To aid in our understanding of the physical processes involved, understand flow behavior in regions where no data is available, and predict future behavior, it is generally desirable to model these fluid flows in some manner. In fact, modeling is almost always used before large-scale activities designed to modify fluid flows are undertaken.

Modeling of the subsurface flow, in general, consists of representing the fluid phases in the heterogeneous environment in some simplified manner while still allowing a reasonably accurate representation of fluid behavior. Most commonly, a mathematical model is used. To be useful, a mathematical model must be amenable to some sort of a solution technique.

Because the different situations involving flow of two fluid phases can differ greatly depending on relative importance of gravity, phase changes, compressibility, chemical changes, adsorption, and numerous other factors, this model will be developed in the context of a particular physical situation - the horizontal flow of oil and water. More specifically, the situation of interest generally involves water pushing oil ahead of it and within it. In this study, the term "two-phase flow" will always refer to two distinct, immiscible fluid phases being present

in the system. While the solid-phase matrix is always present, the two phases being referred to are not to be construed as including this phase.

While the topic of this study may appear to be of interest primarily to petroleum engineers, it, in fact, presents a situation of interest to a number of disciplines dealing with flow in porous media. For example, a somewhat similar situation is faced by hydrologists investigating immiscible fluids displacing groundwater, which often occurs in refined oil product spills. An even more similar situation occurs if flushing of this oil product with water is used as a cleanup strategy after such a spill.

This chapter introduces the fundamental physical relationships which govern two-phase flow. It is shown that stochastic models, and in particular the spectral-perturbation approach, are appropriate for modeling two-phase flow when it is desired to model the heterogeneity of the reservoir.

PURPOSE OF THIS WORK

This study seeks to show that stochastic methods are suitable for modeling fluid behavior in heterogeneous porous media when it is desired to include such heterogeneity in the model. More specifically, the spectral-perturbation approach is developed as a useful technique for increasing our understanding of fluid behavior in the framework of waterflooding of an oil reservoir. Within this context, the purpose is twofold: to demonstrate the applicability and usefulness of the spectral-perturbation approach for modeling two-phase flow, and to draw conclusions from the application of this model to such flows.

This paper presents a newly-developed extension of the spectral-perturbation technique to two-phase flow from its former use only for single-phase flow. This being a new development, the simplifying assumptions arè restrictive in some instances. This study does not intend to show a highly refined, perfected model. In this type of work, it is suggested that the attention be focused on the validity of the method being developed, and possibilities in its application to two-phase flow. Once this approach is recognized as being valid, further research to extend this method to more accurate models with less restrictive assumptions will make the model more useful.

WATERFLOODING OF AN OIL RESERVOIR

Waterflooding most commonly takes place during oil production. In oil production, oil is usually pumped from a reservoir, which is an oil-bearing geologic formation, to the surface. In order to maintain a high rate of oil flow to the production wells, waterflooding is very often used. Water serves the dual purposes of maintaining high oil pressures while physically pushing oil toward production wells [Ewing, 1983]. The term "waterflooding" is usually applied to cases in which water is artificially forced into reservoirs, usually via injection wells. A similar situation may also occur naturally. If there is sufficient water adjacent to a reservoir and permeability is high enough to allow a good flow rate, water may move into the reservoir fast enough without the need for pumping it.

In most real oil reservoirs at least two, and often three, fluid phases are present. In many cases, oil and water predominate, this

usually being the case in reservoirs while waterflooding is being carried out.

Crude oil generally contains volatile components which will vaporize when fluid pressure drops below the bubble-point pressure. Bubble-point pressure is the pressure, at a given temperature, below which a significant portion of an oil's components vaporize. Any drop of pressure below this point allows formation of gases. It has been shown that the amount of oil recovered during a waterflood is at a maximum when the pressure is maintained at the bubble-point pressure [Singh, 1982]. Therefore, waterfloods are often designed so as to maintain pressure just above bubble-point, to preclude formation of gases [Morel-Seytoux, 1969]. As long as oil and water are the only two significant fluid phases present, these fluids can be modeled as slightly compressible [Huyakorn and Pinder, 1983]. When such flow is principally horizontal, pressure ranges are usually small relative to average reservoir pressure, making compressibility relatively unimportant.

SIMPLIFICATIONS FOR MODELING

Any model for describing fluid behavior in natural geologic materials requires simplifications for it to be usable. While such simplifications are necessary, it is still a desirable goal to include enough physical information for the model to be reasonably realistic and accurate.

A highly simplified approach to modeling oil displacement by water is to use single-phase flow equations. In this approach, the media is assumed to be originally completely saturated with oil, and then the oil

is assumed to be completely displaced by water in a piston-flow type model [Scheidegger, 1960]. However, this is an oversimplified model which bears little relation to reality.

More realistic models may incorporate more than one fluid phase, different properties for each fluid, various rock properties, heterogeneities, and other complicating factors [Scheidegger, 1960]. Each of these extensions makes the mathematical representation more complex and the solution more difficult to obtain.

While virtually all multiphase fluid flows involve some dissolution of compounds from one fluid into the other fluid, the term "immiscible" means that there is a presence of two clearly distinct fluids having a sharp interface at their common boundaries. When the quantity of one fluid dissolved in the other is much less than the quantity of each separate fluid, such dissolution is usually considered negligible for purposes of modeling bulk fluid flow and hence is neglected in this work. Of course, in many cases, such dissolution may be important for other reasons.

Another simplification made in this model is to neglect capillary pressure. Capillary pressure is usually of substantial importance in laboratory-scale experiments, but can sometimes be neglected in field-scale flow modeling [Welge, 1952]. Therefore, the capillary pressure (and hence the capillary pressure gradient) are taken to be zero in this field-scale model. A more complete list of simplifying assumptions is given in Chapter 3, where the relations are derived in detail.

THE GOVERNING EQUATIONS

The basic relation governing flow in porous media at velocities normally encountered in nature is Darcy's law, discovered by Henry D'Arcy, a French hydraulic engineer, in 1856. This principle is applicable to water, oil, and most other fluids normally encountered in the subsurface.

The simplest statement of Darcy's law is for single-phase flow. The following equation is in a form commonly used in petroleum reservoir engineering.

$$\underline{V} = \frac{-k}{\mu} \nabla [P + \rho g z] \tag{1.1}$$

where $\underline{V}$ = Darcy velocity vector

k = Intrinsic permeability

μ = Dynamic viscosity of fluid

P = Pressure of fluid

ρ = Density of the fluid

g = Acceleration of gravity

z = Distance in the vertical direction

We wish to develop a model for two-dimensional, essentially horizontal flow. For such a model, Darcy's law is first written separately for each of the two phases, these being oil and water in the context of waterflood oil production. The following equations are statements of Darcy's law for each phase [Morel-Seytoux, 1969].

$$\underline{V}_w = \frac{-kk_{rw}}{\mu_w} \nabla P_w \tag{1.2a}$$

$$\underline{V}_o = \frac{-kk_{ro}}{\mu_o} \nabla P_o \tag{1.2b}$$

where V, k, μ and P have the same meanings as in (1.1), except the subscript w refers to water only and the subscript o refers to oil only.

$k_{rw} \equiv k_{rw}(S)$ = Relative permeability to water

$k_{ro} \equiv k_{ro}(S)$ = Relative permeability to oil

$S \equiv S_w$ = Water saturation

Conservation of mass can be expressed in continuity equations written for each phase, dissolution of one fluid in the other being considered negligible. These forms are valid for incompressible fluids [Collins, 1976].

$$\phi \frac{\partial S}{\partial t} + \nabla \cdot \underline{V_w} = 0 \tag{1.3a}$$

$$-\phi \frac{\partial S}{\partial t} + \nabla \cdot \underline{V_o} = 0 \tag{1.3b}$$

Now, equations (1.2) are substituted into (1.3) to give:

$$\phi \frac{\partial S}{\partial t} - \nabla \left[\frac{k k_{rw}}{\mu_w} \nabla P_w \right] = 0 \tag{1.4a}$$

$$-\phi \frac{\partial S}{\partial t} - \nabla \left[\frac{k k_{ro}}{\mu_o} \nabla P_o \right] = 0 \tag{1.4b}$$

RELATIVE PERMEABILITIES AND MOBILITY

Relative permeability is a fundamental concept in immiscible multiphase fluid flow. The need for this concept arises because each fluid occupies only a fractional portion of the total pore space. Thus, each fluid behaves in some sense like a single fluid phase in a similar porous medium, but with a lower porosity. Relative permeability for a fluid phase i is defined as:

$$k_{ri}(S) = \frac{k_i(S)}{k} \tag{1.5}$$

where $k_i \equiv k_i(S)$ is the effective permeability of phase i

k is the intrinsic permeability of the medium

Note that the use of the word "effective" in connection with permeability, which is in accordance with the petroleum literature, may differ from the use of this term in hydrologic usage, where it is most often used to mean an equivalent average value.

Intrinsic permeability is a function of porous medium properties only. Effective permeability is a function primarily of saturation. While several factors affect it to some degree, numerous experimental results indicate that treating effective permeability as a function of saturation only is a good approximation [Scheidegger, 1960].

While the numerical values of relative permeabilities at a given saturation differ for fluids in different media, the basic shapes of these curves generally follow similar patterns. For some examples, compare Bear [1979], Huyakorn and Pinder [1983], and Amyx, et al [1960].

The ratio of the relative permeability of a fluid to its viscosity is defined as the mobility of that fluid. Thus, for a fluid i, the mobility is:

$$M_i = \frac{k_{ri}}{\mu_i} \tag{1.6}$$

Mobility is a function of the saturation, temperature, and pressure of a fluid. Total mobility is defined as the sum of the mobilities of the fluids which are present.

The viscosities and relative permeabilities of oil and water vary over a substantial range under reservoir conditions, due to a number of factors. Consequently, mobilities vary over a wide range. We have assumed a constant oil-water viscosity ratio of 30:1 for this study, this being a commonly occurring value. At this viscosity ratio, water mobility is several times that of oil [Craig, 1971]. Total mobility

equals oil mobility plus water mobility for our two-phase system. At the oil-water viscosity ratio being used, the total mobility curve does not differ greatly in shape or magnitude from the water mobility curve.

HETEROGENEITIES

All real petroleum reservoirs exhibit some degree of heterogeneity, of both permeability and porosity. Furthermore, each of these heterogeneities occur on various scales and to various degrees [Dagan, 1986]. In the above equations, k is a function of x for a heterogeneous reservoir, and also of direction if the reservoir is anisotropic. The heterogeneity of porosity is not treated in this work.

Heterogeneity is generally a difficult phenomenon to treat satisfactorily in most models. Many models ignore heterogeneities completely, treating an entire reservoir as if it were homogeneous. This may be necessary if only one exploratory well is drilled into a reservoir, since the fluid and rock properties determined there may have to be extrapolated to the whole reservoir. In other cases, various procedures are used to obtain "representative", mean, average, or effective parameter values -- single parameter values which are used to replace the entire range of values which actually exist, and yet supposedly allow reasonably accurate modeling of reservoir behavior. However, no matter how accurately these single parameter values are determined, a model which neglects heterogeneities cannot accurately represent certain phenomena which are known to occur specifically because of the presence of heterogeneities.

One of the motivations for the development of different approaches to solving multiphase flow equations is to deal more adequately with

heterogeneities. In fact, this is the primary motivation for the development of stochastic models.

APPROACHES TO SOLVING THE TWO-PHASE FLOW EQUATIONS

The history of modeling has shown that all techniques involve trade-offs between accuracy and solvability. Simple models are easily solved, but represent reservoir behavior too simplistically. More complex models may be more accurate, but solutions to them may be difficult to obtain, or else they may require more data than can practically be obtained to make their use worthwhile.

Analytic: Practical analytic solutions are currently available only for the single-phase flow model, equation (1.1). While obtaining an analytical solution is always desirable, such solutions have not yet been found for two-phase, multi-dimensional flows. Therefore, for real oil reservoir modeling problems, analytical solutions are not presently available, particularly if heterogeneities are to be considered.

Numerical: In numerical modeling, the governing equations are discretized and then usually solved for each block on a digital computer. This allows the solution of equations for which analytic solutions are not available. Such models can even incorporate crude modeling of large-scale heterogeneities. Numerical models have the following advantages and disadvantages:

Advantages:

* Multiphase, multidimensional flow equations can be solved
* Large-scale heterogeneities can be modeled approximately
* Anisotropy can be modeled to some extent

Disadvantages:

* Solutions are only approximate
* Small-scale heterogeneities can only be modeled poorly, if at all
* Finding solutions may require much time and powerful computers
* Varying of conditions and parameters is difficult because each change requires a completely new solution
* It is virtually impossible and certainly impractial to obtain sufficient data to take full advantage of the heterogeneity modeling capabilities of numerical models

With their advantages, numerical models have enjoyed widespread use in the oil industry. "Black oil codes" model two and three-phase flow without taking account of phase changes. More sophisticated numerical codes even incorporate modeling of phase changes.

Stochastic: Stochastic models attempt to overcome some of the disadvantages of analytic and numerical models, particularly those relating to modeling of heterogeneities. Clear advantages of stochastic models include:

* Heterogeneities on various scales can be modeled quite accurately
* It is not necessary to obtain parameter values at all points in the reservoir which is to be modeled. Only enough data to establish the statistical behavior of parameter values needs to be gathered.

Stochastic models are the subject of the next chapter, where they are more fully discussed.

2. THE STOCHASTIC MODEL: SPECTRAL-PERTURBATION APPROACH

This chapter begins with the introduction of probability concepts, reasons for using the spectral-perturbation approach, and details of application of this approach. Then, the perturbation approach is introduced, and relative permeabilities and total mobility are represented by approximating functions suitable for incorporation into our mathematical model.

WHY USE A STOCHASTIC MODEL?

Geologic formations are made up of randomly distributed geologic materials, and their various properties are also randomly distributed. Intuitively, it makes sense to use a model which takes the statistical distribution of parameter values into account.

As discussed in the previous chapter, deterministic models have serious limitations in modeling heterogeneities. For instance, it is not practical to obtain as many reservoir property measurements as there are nodes in a numerical model. Even if this were possible, all heterogeneities would not be accounted for, since heterogeneities occur on many scales [Dagan, 1986].

Another very important point is that a realistic model of the true nature of heterogeneities is needed in order to model certain types of phenomena. Probably the most important of these is fingering of one fluid within another which is specifically due to heterogeneities in permeability of the reservoir matrix. Fingering consists of the formation of long, narrow zones of the displacing fluid moving forward along certain pathways into the bulk of the fluid being displaced.

Closely related to fingering is the fact that when water is used to displace oil, some oil remains virtually unmoved while water flows around it along certain pathways. Since this phenomenon has a direct bearing on the amount of oil that can be produced economically, it is of fundamental concern to the petroleum reservoir engineer.

BASIC PROBABILITY CONCEPTS

When a property is said to be randomly distributed in space, it means that the value of that property cannot be represented by an algebraic function or other simple deterministic relation. Rather, its value is represented by the laws of probability, and the associated distribution of these values is called a random field.

The most basic properties of a random field are its mean and variance. Another important property is that random fields of concern to us possess covariance structure. That indicates how closely the value of a property at one location is related to its value at another location, as a function of distance and possibly direction. The autocovariance. $C(\underline{x}_1, \underline{x}_2)$, of a property V is a function of two locations $\underline{x}_1$ and $\underline{x}_2$:

$$C(\underline{x}_1, \underline{x}_2) = E\left\{ \left[V(\underline{x}_1) - E\{V(\underline{x}_1)\} \right] \left[V(\underline{x}_2) - E\{V(\underline{x}_2)\} \right] \right\} \qquad (2.1)$$

where E( ) represents expected value.

The autocovariance will be simply referred to hereafter as the covariance.

Expected value is the first-order moment, or mean, of a random function at a particular point:

$$E\{V(\underline{x})\} = m(\underline{x}) \tag{2.2}$$

An important property associated with the spatial random fields we consider is stationarity. This is the property of random fields which states that the statistical parameters (such as mean and variance) do not vary from one location to another, and covariance depends only on the separation vector, $\underline{x}_1 - \underline{x}_2$. Strict stationarity involves all joint distributions in a field, which is very difficult to prove. In most practical work, second-order stationarity is used, and is usually sufficient for most applications [Journel and Huijbregts, 1978]. More precisely, a random field is second-order stationary, or statistically homogeneous, if [Journel and Huijbregts, 1978]:

(1) The mathematical expectation, $E(V(\underline{x}))$ exists and is a constant for all $\underline{x}$,

(2) The covariance exists and only depends on the separation vector $\underline{x}_1 - \underline{x}_2$. (2.3)

i.e.

$$\text{cov}\left(V(\underline{x}_i),\ V(\underline{x}_{i+l})\right) \equiv C(\underline{x}_{i+l} - \underline{x}_i) \tag{2.4}$$

Another concept often invoked in applied statistics is ergodicity, which states that averaging over an ensemble is equivalent to averaging over one realization. An ensemble is a group of realizations (often hypothetical) which are related by having been formed by similar random processes.

The ergodic assumption implies that the ensemble probabilistic parameters can be estimated from a single realization or reservoir. In

addition, it is often used to justify the application of ensemble results to averaged results connected with particular reservoirs.

STOCHASTIC APPROACHES

An early attempt to incorporate probability into models was by use of parameter variation. This method suffers by not incorporating correlation of parameters.

The most important stochastic approaches used today for fluid flows in geologic formations are geostatistics, Monte Carlo simulation, and the spectral-perturbation approach. These approaches are neither mutually exclusive nor directly comparable. Rather, they may often be used in conjunction with each other, each serving a different purpose.

Geostatistics, in the sense of regionalized variables developed by Matheron and others, is particularly useful for working with actual field data. It is employed to predict values over a field based on known values at some locations. Values must, in general, be either known or must be generated in order to make good use of geostatistics. Its greatest value is as an operational technique rather than being of great importance for theoretical studies [Journel and Huijbregts, 1978].

Monte Carlo simulation is particularly suitable for studies which involve the generation of numerous realizations of a statistical field [Smith and Brown, 1982]. It is often applied to problems for which other methods of determining means and variances of output variables are not readily available or are not practical. It generally is computationally expensive - in some cases, prohibitively so.

The spectral-perturbation approach affords some unique advantages which make it very useful for scientific study of the behavior of random variables:

* Since the perturbed equations are solved analytically, actual data is not used. Consequently, the various problems associated with data collection or generation are initially avoided [Bakr, et al, 1978].
* The variables are related through stochastic differential equations. Such equations act as a smoothing mechanism which filters out much of the noise present in model parameters [Neumann, 1982].
* Given an input covariance for the permeability field, the covariance fields of related parameters may be found [Bakr, et al, 1978].
* The spectral approach can be applied in any number of dimensions [Bakr, et al, 1978].

Because of these reasons, the spectral-perturbation approach was considered to be the most appropriate as an initial step for modeling relations between parameters in two-phase flow.

APPLYING THE SPECTRAL-PERTURBATION METHOD

The spectral-perturbation approach is carried out via the following steps:

1) Develop relations among variables of interest using applicable governing equations and mathematical operations.
2) Perturb random variables as in equations (2.9), shown later. Perform indicated multiplications, dropping products of

perturbations, as appropriate, by assuming that they are negligible. This gives us the perturbation equation.

3) Take the expected values of all terms in the equation resulting from perturbation. Subtract this equation from the perturbation equation. This results in the mean-removed equation.

4) Use the Spectral Representation Theorem to represent each random field in the mean-removed equation as a unique complex stochastic process.

5) Perform all indicated differentiations under the integral signs. Drop all integrals based on the uniqueness implied in the Spectral Representation Theorem.

6) Solve for the complex representations of the random fields of interest.

7) Obtain the spectral densities of these random fields by taking the absolute value of the complex processes, squaring them and taking expected values.

8) The covariance of the random field is obtained by taking the inverse Fourier transform of the corresponding spectral density. This may be done analytically, if possible, or by using a numerical Fast Fourier Transform (FFT) algorithm. If only the variance is desired, this is obtained by simply integrating the spectral density expression.

9) Sensitivity analyses may now be performed. If analytical relations are developed, this can be done by studying the expressions. If numerical solutions are used, sensitivities

can be studied by varying input parameter values in steps 7 and 8 above.

SETTING UP THE EQUATIONS FOR PERTURBATION

First, (1.4a) and (1.4b) can be incorporated into a single equation. This is done by adding the two equations and noting that $P_o = P_w$ because of our assumption of zero capillary pressure. Thus

$$-\nabla\left[k\left(\frac{k_{rw}}{\mu_w} + \frac{k_{ro}}{\mu_o} \right) \nabla P_o \right] = 0 \tag{2.5}$$

We define total mobility as:

$$M(S) = \frac{k_{rw}(S)}{\mu_w} + \frac{k_{ro}(S)}{\mu_o} \tag{2.6}$$

which when substituted into (2.5) gives:

$$\nabla \cdot (kM\nabla P) = \nabla(kM) \cdot \nabla P_o + kM\nabla^2 P_o = 0. \tag{2.7}$$

Dividing through by kM gives us:

$$\nabla \ell n\ (kM) \cdot \nabla P_o + \nabla^2 P_o = 0 \tag{2.8}$$

Here, we have used the fact that $\nabla \ell n\ V = \frac{\nabla V}{V}$.

THE PERTURBATION APPROACH

In this approach, a random field which is assumed to be stationary is represented in two parts: its mean, and a zero-mean term which contains all of the random fluctuations of the original variable. We make use of these perturbations in this work:

$$\ell n[k(\underline{x})] = F + f \tag{2.9a}$$

where $E\{\ell n[k(\underline{x})]\} = F$ and $E\{f\} = 0$

$$\ell n[S(\underline{x})] \equiv Y = \bar{Y} + Y' \tag{2.9b}$$

where $E\{Y\} = \bar{Y}$ and $E\{Y'\} = 0$

$$P_o(\underline{x}) = \bar{P}_o + P_o' \tag{2.9c}$$

where $E\{P_o\} = \bar{P}_o$ and $E\{P_o'\} = 0$

Additionally, the following notations are used for convenience:

$$\underline{G} \equiv E\{\nabla Y\}$$
$$\underline{J} \equiv E\{\nabla P_o\} \qquad (2.10)$$

The next step is to substitute the perturbation representations into the equations. Multiplications are performed and it is then usual to assume that the products of perturbations are small enough to be negligible.

Before we perturb, we need to express relative permeabilities and total mobility in forms suitable for inclusion into an equation. This means that we need to represent them as functions of S.

FUNCTIONS FOR RELATIVE PERMEABILITIES AND MOBILITY

Relative permeabilities are different for each porous medium and cannot be represented exactly by any function. However, expressions of the form (2.11), below, have been shown to represent experimental data well in many cases [Scheidegger, 1960]. $\ell n\ k_{rw}$ can be approximately represented by a function of the form:

$$\ell n(k_{rw}) = C_w + A_w\ Y \qquad (2.11)$$

or, in exponential form, recalling that $Y = \ell n(S)$:

$$k_{rw} = e^{C_w}\ S^{A_w} \qquad (2.11a)$$

An expression of a different form was found to better fit the oil relative permeability curve:

$$k_{ro} = \frac{A_o}{S} + C_o S \qquad (2.12)$$

As stated in Chapter 1, with our assumption of an oil-water viscosity ratio of 30, the total mobility curve does not differ greatly in form or values from the water relative permeability curve. Consequently, we will fit an expression similar to (2.11) to total mobility:

$$\ell n(M) = B_c + A_c\, Y \tag{2.13}$$

where M = total mobility.

In exponential form, we have:

$$M = e^{B_c}\, S^{A_c} \tag{2.13a}$$

Relative permeability values for a number of formations, different oil-water viscosity ratios, and as determined by various techniques are shown in Amyx, et al [1960]; compare also curves shown in Bear [1979] and Huyakorn and Pinder [1983].

For our purposes, reasonable values for the parameters in equations (2.11), (2.12), and (2.13) were determined as follows. Three graphs of oil-water relative permeability curves were obtained, one each from Amyx, et al [1960], Bear [1979], and Huyakorn and Pinder [1983]. Values of the water and oil relative permeabilities at several different values of saturation were estimated from these graphs. Then these values were averaged at each value of saturation. Values for the total mobility curve at these saturations were computed from these averaged values using the sum of oil and water mobilities as defined in equation (1.6). Then, best least-squares fits of equations of the forms (2.11), (2.12), and (2.13) were fitted to the averaged values of water relative permeability, oil relative permeability, and total mobility. The shapes of these fitted curves were compared to curves in the references cited above to ensure that they had similar shapes and comparable values over the entire lengths of the curves which were of interest. Only the portions of the curves representing water saturations between 0.25 and 0.8 were considered because it is assumed that water is always present within this range of saturation values. These fitted curves are shown

in Figure 2.1. The values found for the parameters were $C_w = 0.0$, $A_w = 3.0$, $A_0 = 0.162$, $C_o = -0.253$, $B_c = -0.17$, and $A_c = 2.6$.

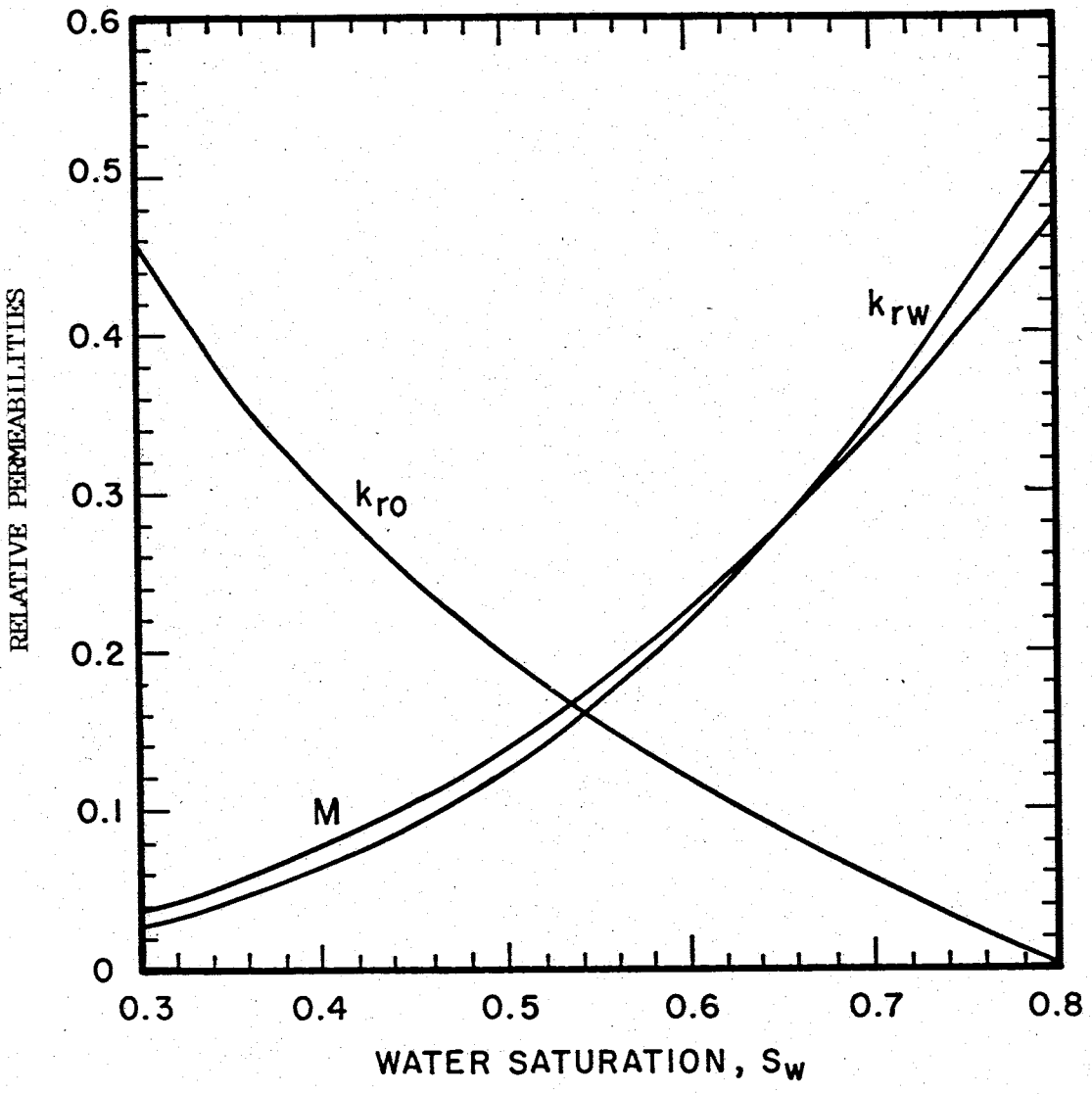

$$k_{rw} = e^{C_w S^{A_w}} = e^{0.0 S^{3.0}}$$

$$k_{ro} = \frac{A_o}{S} + C_o S = \frac{.162}{S} - .2535$$

$$M = e^{B_C S^{A_C}} = e^{-.17 S^{2.61}}$$

Figure 2.1. Curves for Relative Permeabilities and Mobility

3. DEVELOPMENT OF THE TWO-DIMENSIONAL MODEL

In this chapter, the spectral relations for the log permeability and pressure are developed. The preliminaries introduced in the two previous chapters are used in deriving the relationships. Perturbation and the assumption that products of perturbations are negligible are used repeatedly. The development of the equations is presented in full detail.

Perturbation is the representation of a random variable as the sum of its mean and its fluctuations. By using perturbation, a random quantity is decomposed into its deterministic mean and purely random, mean-zero parts.

ASSUMPTIONS

A number of assumptions are made for this model. The most important ones are listed here for convenience.

Physical Assumptions

* Capillary pressure, $P_c(S) = P_o - P_w = 0$. Thus, $P_o = P_w$, and thus $\nabla P_o = \nabla P_w$.
* The only fluids present in significant quantities are oil and water.
* Water saturation remains between 0.25 and 0.8 at all times.
* Oil and water are incompressible.
* The oil/water viscosity ratio remains constant.
* No temperature gradient exists. Injected water is at the same temperature as fluids already in the reservoir.
* Dissolution of one fluid into the other is negligible.

* Flow is strictly horizontal. Gravity can be neglected.
* Flow conditions are at steady state.
* k_{ro} and k_{rw} are functions of saturation only.
* Exponential functions of S are valid approximations of water relative permeability and total mobility.
* The saturation and pressure gradient vectors are parallel.

Statistical Assumptions

* $\ell n(k(x))$ is statistically homogeneous.
* P_o' is a random field such that $P_o' = P_o(x) - E[P_o(x)]$ is statistically homogeneous.
* $\ell n(S)$ is a random field such that $Y' = \ell n(S) - E[\ell n(S)]$ is statistically homogeneous.
* $\underline{J} = E[\nabla P_o(\underline{x})] = \nabla E[P_o(\underline{x})]$ is a constant vector.
* $\underline{G} = E[\nabla \ell n S]$ is a constant.
* The initial saturation profile in the reservoir is nonrandom.

PERTURBATION OF THE CONTINUITY EQUATION FOR WATER

Equation (1.4a) can be rewritten as follows after using the chain rule. P_o has been substituted for P_w, as these are equal by our assumption of zero capillary pressure.

$$\phi \frac{\partial S}{\partial t} = \frac{-kk_{rw}}{\mu_w} \left[\nabla \ell n(kk_{rw}) \cdot \nabla P_o + \nabla^2 P_o \right] \tag{3.1}$$

Now, looking at the first term in (2.8), perturbations as shown in (2.9) and expression (2.13) are substituted as follows:

$$\nabla \ell n(kM) = \nabla \ell n(k) + \nabla \ell n(M) = \nabla F + \nabla f + \nabla B_c + \nabla(A_c Y) \tag{3.2}$$

The mean of permeability, F, is assumed to be a constant and hence the gradient is also zero. Using notation defined in (2.10) and introducing the perturbation of Y as defined in (2.9), (3.2) becomes:

$$\nabla \ell n(kM) = \nabla f + A_c \nabla \bar{Y} + A_c \nabla Y' = \nabla f + A_c \underline{G} + A_c \nabla Y' \tag{3.3}$$

We next multiply (3.1) by $-\mu_w$ and expand the first gradient. By the laws of logs, $\ell n(kk_{rw}) = \ell n(k) + \ell n(k_{rw})$.

$$-\mu_w \Phi \frac{\partial S}{\partial t} = kk_{rw} \left[\nabla\left(\ell n(k) + \ell n(k_{rw}) \right) \cdot \nabla P_o + \nabla^2 P_o \right] \tag{3.4}$$

Using relations (2.9) and (2.11), the following are obtained:

$$k = \exp \{F + f\} \tag{3.5a}$$

$$k_{rw} = \exp \{C_w + A_w Y\} \tag{3.5b}$$

Substituting perturbations (2.9) and (3.5) into (3.4) yields the following, after moving some exponential terms to the left-hand side:

$$-\mu_w \Phi \exp \{-F - C_w - A_w Y\} \frac{\partial S}{\partial t} =$$

$$e^f \left[(\nabla F + \nabla f + \nabla C_w + A_w \nabla Y) \cdot \nabla P_o + \nabla^2 P_o \right] \tag{3.6}$$

By (2.9b) and the properties of derivatives of exponentials, we have:

$$\frac{-\partial}{\partial t} \frac{\exp\left[-(A_w-1)Y\right]}{A_w-1} = -\left(-e^{-A_w Y} e^{Y} \frac{\partial Y}{\partial t} \right) = e^{-A_w Y} \frac{\partial}{\partial t} e^{Y} = e^{-A_w Y} \frac{\partial S}{\partial t} \tag{3.7}$$

Substituting (3.7) into (3.6) and dropping the gradients of constants, gives:

$$\frac{\mu_w \exp\{-F - C_w\}}{A_w-1} \frac{\partial}{\partial t} \left\{ \exp\left[-(A_w-1)Y \right] \right\} =$$

$$e^f \left\{ \left[\nabla f + A_w \nabla Y \right] \cdot \nabla P_0 + \nabla^2 P_0 \right\} \tag{3.8}$$

Introducing perturbations of additional variables we have:

$$\frac{\mu_w}{A_w-1}\exp(-F-C_w)\frac{\partial}{\partial t}\left\{\exp\left[-(A_w-1)(\bar{Y}+Y')\right]\right\} = e^f\left\{\left[\nabla f + A_w\nabla(\bar{Y}+Y')\right]\cdot\nabla\left(\bar{P}_0+P_0'\right) + \nabla^2\left(\bar{P}_0+P_0'\right)\right\} \tag{3.9}$$

Separating exponential terms and using the associative law to regroup terms:

$$\frac{\mu_w}{A_w-1}\exp(-F-C_w)\frac{\partial}{\partial t}\left\{\exp\left[-(A_w-1)\bar{Y}\right]\exp\left[-(A_w-1)Y'\right]\right\} = e^f\left\{\left[\nabla f + A_w\nabla\bar{Y} + A_w\nabla Y'\right]\cdot\nabla\left(\bar{P}_0 + P_0'\right) + \nabla^2\left(\bar{P}_0 + P_0'\right)\right\} \tag{3.10}$$

The three-term Taylor series approximation of e^f is substituted and since $\nabla\bar{P}_0$ is a constant, $\nabla^2\bar{P}_0 = 0$.

$$\frac{\mu_w}{A_w-1}\exp(-F-C_w)\frac{\partial}{\partial t}\left\{\exp\left[-(A_w-1)\bar{Y}\right]\exp\left[-(A_w-1)Y'\right]\right\} = \left(1+f+\frac{f^2}{2}\right)\cdot\left\{\left[\nabla f + A_w\nabla\bar{Y} + A_w\nabla Y'\right]\cdot\nabla\left(\bar{P}_0 + P_0'\right) + \nabla^2 P_0'\right\} \tag{3.11}$$

Introducing the convenient notations shown in (2.10), rearranging the left-hand side and expanding the right-hand side:

$$\frac{\mu_w}{A_w-1}\exp(-F-C_w)\frac{\partial}{\partial t}\left\{\exp\left[-(A_w-1)\bar{Y}\right]\exp\left[-(A_w-1)Y'\right]\right\} = \left(1+f+\frac{f^2}{2}\right)\cdot\left\{\nabla f\cdot\underline{J} + \nabla f\cdot\nabla P_0' + A_w\underline{G}\cdot\underline{J} + A_w\underline{G}\cdot\nabla P_0' + A_w\nabla Y'\cdot\underline{J} + A_w\nabla Y'\cdot\nabla P_0' + \nabla^2 P_0'\right\} \tag{3.12}$$

The last factor on the left-hand side is moved to the right.

$$\mu_w\exp\left[-F-C_w+(1-A_w)\bar{Y}\right]\frac{\partial Y'}{\partial t} = \exp\left[(A_w-1)Y'\right]\left(1+f+\frac{f^2}{2}\right)\cdot\left\{\nabla f\cdot\underline{J} + \nabla f\cdot\nabla P_0' + A_w\underline{G}\cdot\underline{J} + A_w\underline{G}\cdot\nabla P_0' + A_w\nabla Y'\cdot\underline{J} + A_w\nabla Y'\cdot\nabla P_0' + \nabla^2 P_0'\right\} \tag{3.13}$$

Multiply through by the Taylor Series approximation of e^f. Terms higher than second-order are dropped:

$$\mu_w \exp\left[-F - C_w + (1-A_w)\bar{Y}\right] \frac{\partial Y'}{\partial t} = \exp\left[(A_w-1)Y'\right] \cdot \tag{3.14}$$

$$\left\{\nabla f \cdot \underline{J} + \nabla f \cdot \nabla P_o' + A_w \underline{G} \cdot \underline{J} + A_w \underline{G} \cdot \nabla P_o' + A_w \nabla Y' \cdot \underline{J} + A_w \nabla Y' \cdot \nabla P_o' + \right.$$

$$\left. \nabla^2 P_o' + f\,\nabla f \cdot \underline{J} + f\,A_w \underline{G} \cdot \underline{J} + f\,A_w \underline{G} \cdot \nabla P_o' + f A_w \nabla Y' \cdot \underline{J} + \frac{f^2}{2} A_w \underline{G} \cdot \underline{J} + f \nabla^2 P_o' \right\}$$

Now, replace $\exp\left[(A_w - 1)Y'\right]$ by its three-term Taylor Series approximation. We multiply through and drop terms higher than second-order. This is the perturbation equation.

$$\mu_w \exp\left[-F - C_w + (1-A_w)\bar{Y}\right] \frac{\partial Y'}{\partial t} =$$

$$\left\{\nabla f \cdot \underline{J} + \nabla f \cdot \nabla P_o' + A_w \underline{G} \cdot \underline{J} + A_w \underline{G} \cdot \nabla P_o' + A_w \nabla Y' \cdot \underline{J} + A_w \nabla Y' \cdot \nabla P_o' + \right.$$

$$\nabla^2 P_o' + f\,\nabla f \cdot \underline{J} + f\,A_w \underline{G} \cdot \underline{J} + f\,A_w \underline{G} \cdot \nabla P_o' + f A_w \nabla Y' \cdot \underline{J} + \frac{f^2}{2} A_w \underline{G} \cdot \underline{J} + f \nabla^2 P_o' + \tag{3.15}$$

$$\nabla f \cdot \underline{J}(A_w-1)Y' + A_w \underline{G} \cdot \underline{J}(A_w-1)Y' + A_w \underline{G} \cdot \nabla P_o'(A_w-1)Y' + A_w \nabla Y' \cdot \underline{J}(A_w-1)Y' +$$

$$\left. \nabla^2 P_o'(A_w-1)Y' + f A_w \underline{G} \cdot \underline{J}(A_w-1)Y' + A_w \underline{G} \cdot \underline{J} \frac{\left[(A_w-1)Y'\right]^2}{2} \right.$$

Now, we take the expected value of (3.15) to get the mean equation:

$$\mu_w \exp\left[-F - C_w + \bar{Y}(1-A_w)\right] E\left[\frac{\partial Y'}{\partial t}\right] =$$

$$E[\nabla f \cdot \underline{J}] + E\left[\nabla f \cdot \nabla P_o'\right] + A_w E[\underline{G} \cdot \underline{J}] + A_w E\left[\underline{G} \cdot \nabla P_o'\right] + A_w E\left[\nabla Y' \cdot \underline{J}\right] + \tag{3.16}$$

$$A_w E\left[Y' \nabla P_o'\right] + E\left[\nabla^2 P_o'\right] + E[f \nabla f \cdot \underline{J}] + A_w E[f \underline{G} \cdot \underline{J}] + A_w E\left[f \underline{G} \cdot \nabla P_o'\right] +$$

$$A_w\left[f \nabla Y' \cdot \underline{J}\right] + E\left[f \nabla^2 P_o'\right] + A_w E\left[\frac{f^2}{2} \underline{G} \cdot \underline{J}\right] + (A_w - 1) E\left[\nabla f \cdot \underline{J} Y'\right] +$$

$$(A_w - 1) A_w E\left[\underline{G} \cdot \underline{J} Y'\right] + A_w (A_w - 1) E\left[\underline{G} \cdot \nabla P_o' Y'\right] + A_w (A_w - 1) E\left[\nabla Y' \cdot \underline{J} Y'\right] +$$

$$(A_w - 1) E\left[\nabla^2 P_o' Y'\right] + A_w (A_w - 1) E\left[f \underline{G} \cdot \underline{J} Y'\right] + \frac{A_w (A_w - 1)^2}{2} E\left[\underline{G} \cdot \underline{J} (Y')^2\right]$$

After dropping terms which are zero, the mean equation becomes:

$$0 = E\left[\nabla f \cdot \nabla P_o'\right] + A_w \underline{G} \cdot \underline{J} + A_w \cdot E\left[Y' \cdot \nabla P_o'\right] + \underline{J} \cdot E[f \cdot \nabla f] + A_w \underline{G} \cdot E\left[f \cdot \nabla P_o'\right] +$$

$$A_w \underline{J} \cdot E[f \cdot \nabla Y'] + E\left[f \cdot \nabla^2 P_o'\right] + \frac{A_w \underline{G} \cdot \underline{J}}{2} E[f^2] + (A_w - 1) \underline{J} \cdot E\left[\nabla f Y'\right] + \tag{3.17}$$

$$A_w \underline{G} (A_w - 1) \cdot E\left[\nabla P_o' Y'\right] + A_w (A_w - 1) \underline{J}\, E(Y' \nabla Y') + (A_w - 1) E\left(Y' \nabla^2 P_o'\right) +$$

$$A_w \underline{G} \cdot \underline{J} (A_w - 1)\, E[f Y'] + \frac{A_w \underline{G} \cdot \underline{J} (A_w - 1)^2}{2} E\left[Y'\right]^2$$

Now, (3.17) is subtracted from (3.15) to give the mean-removed equation:

$$\mu_w \exp\left[-F - C_w + (1 - A_w) \bar{Y}\right] \frac{\partial Y'}{\partial t} =$$

$$\nabla f \cdot \underline{J} + \nabla f \cdot \nabla P_o' - E\left[\nabla f \cdot \nabla P_o'\right] + A_w \underline{G} \cdot \nabla P_o' + A_w \nabla Y' \cdot \underline{J} + A_w Y' \nabla P_o' -$$

$$A_w E\left[Y' \cdot \nabla P_o'\right] + \nabla^2 P_o' + f\, \nabla f \cdot \underline{J} - \underline{J} \cdot E[f \nabla f] + f A_w \underline{G} \cdot \underline{J} + f A_w \underline{G} \cdot \nabla P_o' -$$

$$A_w \underline{G} \cdot E\left[f \nabla P_o'\right] + f A_w \nabla Y' \cdot \underline{J} - A_w \underline{J} \cdot E[f \nabla Y'] + f \nabla^2 P_o' - E\left[f \nabla^2 P_o'\right] + \tag{3.18}$$

$$\frac{f^2}{2} A_w \underline{G}\cdot\underline{J} - \frac{A_w \underline{G}\cdot\underline{J}}{2} E\left[f^2\right] + \nabla f\cdot\underline{J}(A_w-1)Y' - (A_w-1)\underline{J}\cdot E\left[\nabla f Y'\right] +$$

$$A_w \underline{G}\cdot\underline{J}(A_w-1)Y' + A_w \underline{G}\cdot\nabla P_0'(A_w-1)Y' - A_w \underline{G}(A_w-1)\cdot E\left[\nabla P_0' Y'\right] + A_w \nabla Y'\cdot\underline{J}(A_w-1)Y' -$$

$$A_w \underline{J}\cdot(A_w-1)E\left[\nabla Y' Y'\right] + \nabla^2 P_0'(A_w-1)Y' - (A_w-1)E\left[\nabla^2 P_0' Y'\right] + f A_w \underline{G}\cdot\underline{J}(A_w-1)Y' -$$

$$A_w \underline{G}\cdot\underline{J}(A_w-1)E\left[f Y'\right] + \frac{A_w \underline{G}\cdot\underline{J}}{2}\left[(A_w-1)Y'\right]^2 - \frac{A_w \underline{G}\cdot\underline{J}}{2}(A_w-1)^2 E\left[Y'\right]^2$$

Finally, the second-order terms are dropped, leaving the following approximate relation:

$$\mu_w \exp\left[-F - C_w + \bar{Y}(1-A_w)\right] \frac{\partial Y'}{\partial t} =$$

$$\underline{J}\cdot\left[\nabla f + A_w \nabla Y'\right] + A_w \underline{G}\cdot\nabla P_0' + \nabla^2 P_0' + A_w \underline{G}\cdot\underline{J} f + A_w \underline{G}\cdot\underline{J}(A_w-1)Y' \qquad (3.19)$$

This completes the development of the perturbation equations. Note that the second order perturbations were carried along in order to get consistent results. Namely, if only $1 + f$ is used to approximate e^f, one actually loses terms from the final expression and obtains an inconsistent result.

SPECTRAL REPRESENTATION

The next step is to represent the random fields by Fourier-Stieltjes integrals using the Spectral Representation Theorem. Although we are dealing with purely random quantitites, use of spectral representation allows us to work with these quantities mathematically in wave number space as if we were dealing with deterministic quantities [Lumley and Panofsky, 1964].

The assumptions necessary to allow spectral representation are stationarity of the field, and continuity and absolute integrability of the covariance. These are relatively weak assumptions which are sufficiently unrestrictive to be permissible in many physical situations [Lumley and Panofsky, 1964].

The Spectral Representation Theorem states that with the assumptions given above, a complex stochastic process exists with probability of one which uniquely represents a random function. [Lumley and Panofsky, 1964].

For a random process $V(\underline{x})$, the Spectral Representation Theorem can be formally stated as:

If:

* $V(\underline{x})$ is second-order stationary
* $E[V(\underline{x})] = 0$
* $C(\underline{s}) = \mathrm{Cov}((\underline{x}+\underline{s}), V(\underline{x}))$
* $C(\underline{s})$ is continuous at $\underline{s} = 0$

Then there exists a unique (with probability one) complex stochastic process such that:

$$V(\underline{x}) = \int_{-\infty}^{\infty} e^{i\underline{r}\cdot\underline{x}}\, dZ_v(\underline{r})$$

Also,

$$C(\underline{s}) = \int_{-\infty}^{\infty} e^{i\underline{r}\cdot\underline{s}}\, S_{vv}(\underline{r})\underline{dr}$$

is the covariance function, where

$$S_{vv}(\underline{r}) = E\left[dZ_v(\underline{r}) \cdot dZ_v^*(\underline{r})\right]$$

is the spectral density function.

Based on these statements, all of the random fields in (3.19) are now represented by stochastic Fourier-Stieltjes integrals. We make the

necessary assumptions for use of the Spectral Representation Theorem.

$$H \frac{\partial}{\partial t} \int_{-\infty}^{\infty} e^{i\underline{r}\cdot\underline{x}} dZ_Y =$$

$$\underline{J} \cdot \left[\nabla \int_{-\infty}^{\infty} e^{i\underline{r}\cdot\underline{x}} \, dZ_f + A_w \nabla \int_{-\infty}^{\infty} e^{i\underline{r}\cdot\underline{x}} \, dZ_Y \right] + A_w \underline{G}\cdot\underline{J} \int_{-\infty}^{\infty} e^{i\underline{r}\cdot\underline{x}} \, dZ_f + \tag{3.20}$$

$$A_w \underline{G}\cdot\underline{J}(A_w - 1) \int_{-\infty}^{\infty} e^{i\underline{r}\cdot\underline{x}} \, dZ_Y + A_w \underline{G}\cdot\nabla \int_{-\infty}^{\infty} e^{i\underline{r}\cdot\underline{x}} \, dZ_p + \nabla^2 \int_{-\infty}^{\infty} e^{i\underline{r}\cdot\underline{x}} \, dZ_p$$

where

$$H = \mu_w \exp\left[-F - C_w + \bar{Y}(1 - A_w) \right]$$

Now, differentiation under the integral signs is performed. The integrals may be dropped since the Spectral Representation Theorem implies that the spectral components are unique [Lumley and Panofsky, 1964].

$$-H \frac{\partial}{\partial t} dZ_Y = \underline{J}\left[i\underline{r}\cdot dZ_f + i\underline{r}\cdot A_w dZ_Y \right] + i\underline{r}\cdot A_w \underline{G} dZ_p + \tag{3.21}$$

$$A_w \underline{G}\cdot\underline{J} \, dZ_f + A_w \underline{G}\cdot\underline{J}(A_w - 1) \, dZ_Y + (-r^2) \, dZ_p$$

Regrouping terms of the complex representations, we have:

$$-H \frac{\partial}{\partial t} dZ_Y = (A_w \underline{G}\cdot\underline{J} + i\underline{J}\cdot\underline{r}) \, dZ_f +$$

$$\left[A_w \underline{G}\cdot\underline{r} i - r^2 \right] dZ_p + \left[i A_w \underline{J}\cdot\underline{r} + A_w \underline{G}\cdot\underline{J}(A_w - 1) \right] dz_Y \tag{3.22}$$

PERTURBATION OF THE TOTAL MOBILITY EQUATION

Now, to reduce the number of different complex increments in (3.22), we develop an expression for dZ_p using an equation for total mobility. This is done by adding equations (1.4), which results, as shown in the previous chapter, in (2.8):

$$\nabla \ln [kM] \cdot \nabla P_o + \nabla^2 P_o = 0 \tag{2.8}$$

Introduce perturbations (2.9) into (2.8):

$$[\nabla F + \nabla f + \nabla B_C + A_C \nabla Y] \cdot \nabla\left(\bar{P}_o + P_o'\right) + \nabla^2\left(\bar{P}_o + P_o'\right) = 0 \qquad (3.23)$$

Drop the products of perturbations and the gradients of constants, and introduce $\underline{J} = E[\nabla \bar{P}_o]$ and $\underline{G} = E[\nabla \bar{Y}]$:

$$\nabla f \cdot \underline{J} + A_C \underline{G} \cdot \underline{J} + A_C \nabla Y' \cdot \underline{J} + A_C \underline{G} \cdot \nabla P_o' + \nabla^2 P_o' = 0 \qquad (3.24)$$

Finally, taking the expected value of (3.24) gives us the mean equation. Subtracting this from (3.24) yields the mean-removed equation:

$$\nabla f \cdot \underline{J} + A_C \nabla Y' \cdot \underline{J} + A_C \underline{G} \cdot \nabla P_o' + \nabla^2 P_o' = 0 \qquad (3.25)$$

Again, the spectral representation theorem is used to allow Fourier-Stieltjes integral representations of each random variable in equation (3.25):

$$\underline{J} \cdot \nabla \int_{-\infty}^{\infty} e^{i\underline{r} \cdot \underline{x}}\, dZ_f + A_C \underline{J} \cdot \nabla \int_{-\infty}^{\infty} e^{i\underline{r} \cdot \underline{x}}\, dZ_Y + A_C \underline{G} \cdot \nabla \int_{-\infty}^{\infty} e^{i\underline{r} \cdot \underline{x}}\, dZ_p + \nabla^2 \int_{-\infty}^{\infty} e^{i\underline{r} \cdot \underline{x}} dZ_p = 0 \qquad (3.26)$$

After taking the indicated derivatives, the integrals are dropped on the basis of uniqueness, as mentioned previously:

$$i[dZ_f + A_C dZ_Y]\underline{r} \cdot \underline{J} + \left[iA_C \underline{G} \cdot \underline{r} - r^2\right] dZ_p = 0 \qquad (3.27)$$

We thus have two equations, (3.21) and (3.27), in two unknowns, dZ_Y and dZ_p, which are solved for dZ_p.

$$dZ_p = \frac{i\underline{r} \cdot \underline{J}[dZ_f + A_C dZ_Y]}{r^2 - A_C \underline{G} \cdot \underline{r} i} \qquad (3.28)$$

Expression (3.28) is now substituted into (3.22) to reduce the number of different complex increments by one:

$$-H \frac{\partial}{\partial t}[dZ_Y] = (A_w \underline{G} \cdot \underline{J} + i\underline{J} \cdot \underline{r})\, dZ_f + \left[A_w \underline{G} \cdot \underline{r} i - r^2\right]\left[\frac{i\underline{J} \cdot \underline{r}\, A_C dZ_y + i\underline{J} \cdot \underline{r}\, dZ_f}{r^2 - A_C \underline{G} \cdot \underline{r} i}\right] + \left[iA_w \underline{J} \cdot \underline{r} + A_w \underline{G} \cdot \underline{J}(A_w - 1)\right] dZ_Y \qquad (3.29)$$

Collecting terms:

$$-H\frac{\partial}{\partial t}dZ_Y = \left\{ A_w\underline{G}\cdot\underline{J} + i\underline{J}\cdot\underline{r} + \frac{i\underline{J}\cdot\underline{r}\left(A_w\underline{G}\cdot\underline{r}i - r^2\right)}{r^2 - A_C\underline{G}\cdot\underline{r}i} \right\} dZ_f + \left\{ i\underline{J}\cdot\underline{r}\left[A_w + \frac{A_C\left(A_w\underline{G}\cdot\underline{r}i - r^2\right)}{r^2 - A_C\underline{G}\cdot\underline{r}i} \right] + A_w\underline{G}\cdot\underline{J}(A_w - 1) \right\} dZ_Y \tag{3.30}$$

The following notations are introduced for convenience:

$$B_1(\underline{r}) = \frac{\left\{ i\underline{J}\cdot\underline{r}\left[A_w - A_C B_3(\underline{r})\right] + A_w\underline{G}\cdot\underline{J}(A_w - 1)\right\}}{H} \tag{3.31a}$$

$$B_2(\underline{r}) = \frac{-\left(A_w\underline{G}\cdot\underline{J} + i\underline{J}\cdot\underline{r} - i\underline{J}\cdot\underline{r}\, B_3(\underline{r})\right)}{H} \tag{3.31b}$$

$$B_3(\underline{r}) = \frac{r^2 - A_w\underline{G}\cdot\underline{r}i}{r^2 - A_C\underline{G}\cdot\underline{r}i} \tag{3.31c}$$

With these substitutions, (3.30) becomes:

$$\frac{\partial}{\partial t}dZ_Y + B_1(\underline{r})dZ_Y = B_2(\underline{r})dZ_f \tag{3.32}$$

SPECTRUM AND COVARIANCE OF LOG SATURATION AND PRESSURE

The differential equation (3.32) can be solved for dZ_Y:

$$dZ_Y = \frac{B_2(\underline{r})}{B_1(\underline{r})}\left[1 - \exp(-B_1(\underline{r})\, t)\right] dZ_f + dZ_Y(r{:}0)\, \exp\{-B_1(\underline{r})\, t\} \tag{3.33}$$

Here, we will study the behavior of saturation and, later, pressure under the assumption that the initial saturation profile is nonrandom. This makes the initial condition $dZ_Y(r{:}0) = 0$ and simplifies our solution. Since the saturation profile will change as flow occurs, the particular initial state may not be of great importance. This is particularly true for the steady state case, which is only approached after a long time period. Thus, for our steady state model, we are talking of a long time after the initial state, which makes the particular initial state rather unimportant.

The spectral density of $Y = \ell n\ S$ is given by:

$$S_{YY}(\underline{r}) = E\left\{ \left| dZ_Y \right|^2 \right\} = \left| \frac{B_2(\underline{r})}{B_1(\underline{r})} \right|^2 \left| 1 - \exp\{-B_1(\underline{r})\ t\} \right|^2 S_{ff}(\underline{r}) \quad (3.34)$$

The permeability spectral density model chosen was Mizell's spectral density B [Mizell, et al, 1982]. This is based on the Whittle spectrum for two-dimensional spatial processes. From this, spectral density B is a modification designed to yield a finite variance [Mizell, et al, 1982]. The Mizell spectral density B model is:

$$S_{ff}(\underline{r}) = S_B(\underline{r}) = \frac{3\sigma^2\alpha^2\left(r_1^2 + r_2^2\right)^2}{\pi\left(r_1^2 + r_2^2 + \alpha^2\right)^4} \quad (3.35)$$

where α = a parameter related to the integral scale

σ^2 = the variance of the permeability process

r_1, r_2 = spatial distance vector components in wave number space

To evaluate $S_{YY}(\underline{r})$ and, later, $S_{pp}(\underline{r})$, we make the assumption that $\underline{G}$ and $\underline{J}$ are parallel. This is a reasonable assumption, particularly for horizontal displacement of oil by water in a reservoir which was essentially at equilibrium before pumping began. We orient the axes so that r_1 is pointing in the direction of flow. Thus, r_1, $\underline{G}$, and $\underline{J}$ are mutually parallel and $\underline{G} = (G_1, 0)$, $\underline{J} = (J_1, 0)$.

From the spectral density, the covariance may be obtained using an inverse Fourier Transform [Lumley and Panofsky, 1964]:

$$C_{YY}(x_1, x_2) = \int_{-\infty}^{\infty} \int_{-\infty}^{\infty} e^{i\underline{r}\cdot\underline{x}}\ S_{YY}(\underline{r})\ dr_1 dr_2 \quad (3.36)$$

While this type of integral could be analytically integrated in the case of a simple spectrum, the expression obtained for S_{YY} did not appear amenable to direct integration. Thus, the covariance field was

obtained using a two-dimensional Fast Fourier Transform algorithm on a digital computer. Fourier transformation techniques and applications are described in Weaver (1983), for example. This code was written in FORTRAN 77 and is listed in Appendix I. The behavior of the correlation function associated with Mizell's spectral density B is shown in Figure 3.1.

This particular study is concerned with the steady-state case, which is approached as $t \to \infty$. Thus, for this case, (3.34) becomes

$$S_{YY}(\underline{r}) = \left| \frac{B_2(\underline{r})}{B_1(\underline{r})} \right|^2 S_{ff}(\underline{r}) \qquad (3.37)$$

The spectral density of pressure is obtained using relation (3.28).

$$S_{pp}(\underline{r}) = \left| \frac{i\underline{r} \cdot \underline{J}}{r^2 - A_C \underline{G} \cdot \underline{r} i} \right|^2 \left| 1 + A_C \frac{B_2(\underline{r})}{B_1(\underline{r})} \right|^2 S_{ff}(\underline{r}) \qquad (3.38)$$

where we incorporate the steady-state version of $S_{YY}(\underline{r})$, (3.37).

Again, Cov $(P(\underline{x}), P(\underline{x} + \underline{y}))$ is evaluated using the numerical FFT algorithm mentioned above.

$$C_{pp}(x_1, x_2) = \int_{-\infty}^{\infty} \int_{-\infty}^{\infty} e^{i\underline{r} \cdot \underline{x}} S_{pp}(\underline{r}) dr_1 dr_2 \qquad (3.39)$$

The results of computer code runs were verified by several means. The code was written in FORTRAN 77 and is listed in Appendix I. The following methods of verification were used:

* Set G = 0 and execute the code. This results in a variance for P equal to the variance corresponding to Mizell's spectral density B.
* Set $A_C = 0$ and run the code. This results in a variance for P equal to that corresponding to Mizell's spectral density B.

* S_{YY} and S_{pp} were hand-calculated at a few values of r_1 and r_2 to see that each term was being correctly computed by the code.

The results of these computer runs, discussion and figures are presented in Chapter 5.

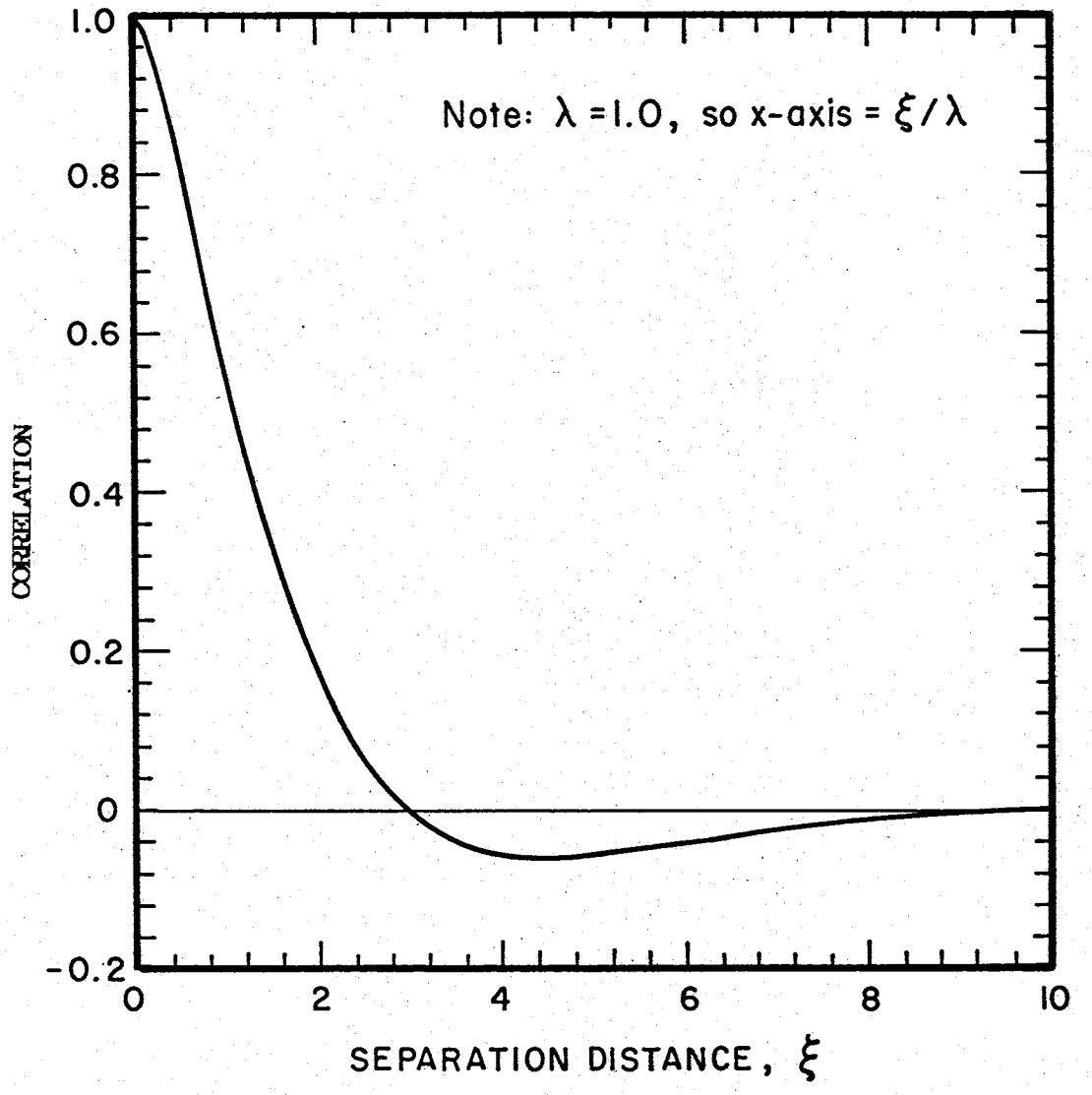

Figure 3.1. Correlation Function: Mizell B

4. THE THREE-DIMENSIONAL CASE AND EFFECTIVE VELOCITY

THE THREE-DIMENSIONAL MODEL

The two-dimensional spectral density model is easily extended to the three-dimensional case, since (3.34) and (3.35) are expressed in vector form. Now, $\underline{r}$ is a three-dimensional instead of a two-dimensional wave number vector.

Layering is very common in natural geologic formations. Reservoirs are almost always made up of sedimentary rocks, most often sandstone, limestone, or shale, generally of moderate relief, and typically quite extensive [Amyx, et al, 1960]. Due to horizontal layering at the time of formation of sedimentary rocks, low to moderate relief means that, in general, layers remain predominantly horizontal, or much closer to being horizontal than vertical. Therefore, starting from a given point, traveling a given distance in any of three coordinate directions (2 horizontal, 1 vertical), one would, on the average, cross more layers in the vertical direction than in either of the horizontal directions. From an elementary knowledge of geology, we know that correlation of rock properties along one layer is greater than correlation between different layers. Therefore, correlation lengths traveling within one layer are larger than correlation lengths going across layers.

Because of the large differences in correlation lengths across layers vs. within layers, it was deemed appropriate to incorporate this difference into the model. In most geological formations, the permeabilities of various layers differ considerably. Typically, some layers have very low permeabilities, meaning that flow rates across such a

layer would be quite low. Thus, in most cases, flow occurs much more readily in the horizontal directions than in the vertical. Therefore, gravity is less important. By neglecting gravity, we are able to use a model very similar to the two-dimensional case.

All assumptions are identical to the assumptions made for the two-dimensional case, except that some vertical flow occurs. However, vertical flow is considered to be small enough for gravity to be negligible.

Because the spectral density model previously used for permeability was proposed for two-dimensional processes, as well as the fact that it is an isotropic model, the following spectral density model for permeability in three dimensions was used.

$$S_{ff} = \frac{\lambda_1\lambda_2\lambda_3\sigma_f^2}{\pi^2\left[1 + \lambda_1^2 r_1^2 + \lambda_2^2 r_2^2 + \lambda_3^2 r_3^2\right]^2} \tag{4.1}$$

This represents a three-dimensional anisotropic exponential process and has been used by Yeh, et al. [1985]. Our general forms of the models are still identical to the two-dimensional versions. They are reproduced here for convenience.

$$S_{YY}(\underline{r}) = \left| \frac{B_2(\underline{r})}{B_1(\underline{r})} \right|^2 S_{ff}(\underline{r}) \tag{3.37}$$

$$S_{pp}(\underline{r}) = \left| \frac{i\underline{r}\cdot\underline{J}}{r^2 - A_C\underline{G}\cdot\underline{r}i} \right|^2 \left| 1 + A_C \frac{B_2(\underline{r})}{B_1(\underline{r})} \right|^2 S_{ff}(\underline{r}) \tag{3.38}$$

However, these differences exist:

For the two-dimensional case:

* $\underline{r}$ is a two-dimensional vector
* S_{ff} is Mizell's spectral density B, equation (3.35)

For the three-dimensional case:

* $\underline{r}$ is a three-dimensional vector
* S_{ff} is the spectral density model shown above in (4.1)

In full detail, $S_{YY}(\underline{r})$ is:

$$S_{YY}(\underline{r}) = \frac{\lambda_1\lambda_2\lambda_3\sigma_f^2}{\pi^2\left[1 + \lambda_1^2 r_1^2 + \lambda_2^2 r_2^2 + \lambda_3^2 r_3^2\right]^2} \cdot \frac{GA_w r^2 + (A_C - A_w)Gr_1^2 + (A_C A_w G^2)^2 r_1^2}{\left[A_w(A_w-1)G\right]r^2 + r_1^2\left[(A_w-A_C)r^2 - A_C A_w(A_w-1)G^2\right]^2} \tag{4.2}$$

where we have assumed that $\underline{G}$ and $\underline{J}$ are in the r_1 direction. This means that $G = |\underline{G}|$ and $J = |\underline{J}|$.

For the three-dimensional case, only the variance was computed. Simple numerical integration was used to compute the variances since an analytical expression for the variance was not available. A finely-discretized numerical integration of (4.2) in three dimensions requires a large amount of computer time. It was observed that if (4.2) was suitably transformed, it could be analytically integrated with respect to one variable, and, thus only two-dimensional numerical integration would be required.

A suitable transformation is to a cylindrical coordinate system, but oriented so that the z axis of the cylindrical system corresponds to r_i in our Cartesian system. The transformation was done in this manner because this particular orientation of the z axis was required for the analytical integration, and it was desired to retain the standard coordinate designations in the cylindrical system. A description of the cylindrical corrdinate system can be found in most standard algebra or calculus texts. For our transform, the following correspondences are used:

$$r_1 = z$$
$$r_2 = \rho \cos\theta \qquad ((4.3)$$
$$r_3 = \rho \sin\theta$$

Substitution of (4.3) into (4.2) yields:

$$S_{YY}(\underline{r}) = \frac{\lambda_1\lambda_2\lambda_3\sigma_f^2}{\pi^2\left[1 + \lambda_1^2z^2 + \lambda_2^2\rho^2\cos^2\theta + \lambda_3^2\rho^2\sin^2\theta\right]^2} \cdot \tag{4.4}$$

$$\left\{ \frac{GA_w(\rho^2 + z^2) + A_C - A_w)Gz^2 + (A_CA_wG^2)^2z^2}{\left[A_w(A_w-1)G\right]^2\left[\rho^2+z^2\right] + z^2\left[(A_w-A_C)(\rho^2+z^2) - A_CA_w(A_w-1)G^2\right]^2} \right\}$$

Because of the reorientation of the cylindrical coordinate system, it should be kept in mind that the "z" does not refer to vertical distance, but rather is a horizontal distance in what would normally be the r_1, or "x" direction. The letter "z" was used in order to maintain the almost universal convention of using the letters ρ, θ, and z as the three variables in the cylindrical coordinate system.

It will be assumed that the correlation lengths in the two horizontal directions are equal, that is, $\lambda_1 = \lambda_2$. The correlation length in the vertical direction will vary, generally being much smaller than, but never greater than, the correlation lengths in the horizontal directions. The anisotropy ratio is defined as:

$$A = \frac{\lambda_1}{\lambda_3} = \frac{\lambda_2}{\lambda_3} \tag{4.5}$$

Clearly, θ appears in much fewer terms in (4.4) than either ρ or z. Consequently, analytical integration will be performed with respect to θ.

Substituting $\lambda_1 = \lambda_2$ and $1 - \cos^2\theta = \sin^2\theta$ into the first factor of (4.4):

$$S_{ff} = \frac{\lambda_1^2\lambda_3\sigma_f^2}{\pi^2\left[1 + \lambda_1^2z^2 + \lambda_3^2\rho^2 + \left(\lambda_1^2-\lambda_3^2\right)\rho^2\cos^2\theta\right]^2} \tag{4.6}$$

For convenience, the following terms are defined:

$$A_1 = \frac{\lambda_1^2 \lambda_3 \sigma_f^2}{\pi^2} \cdot \left\{ \frac{GA_w(\rho^2 + z^2) + (A_c - A_w)Gz^2 + (A_c A_w G^2)^2 z^2}{[A_w(A_w-1)G]^2[\rho^2+z^2] + z^2[(A_w-A_c)(\rho^2+z^2) - A_c A_w (A_w-1)G^2]^2} \right\} \rho \tag{4.7a}$$

$$A_2 = 1 + \lambda_1^2 z^2 + \lambda_3^2 \rho^2 \tag{4.7b}$$

$$A_3 = \left(\lambda_1^2 - \lambda_3^2\right)\rho^2 \tag{4.7c}$$

We will only consider the case where $\lambda_1 > \lambda_3$, both λ_1 and λ_3 positive. Therefore A_2 and A_3 will always be positive for $\rho > 0$. Using (4.7) in (4.6) and (4.4):

$$\sigma_Y^2 = \int_0^\infty \int_{-\infty}^\infty \left\{ \int_0^{2\pi} \frac{A_1 \, d\theta}{\left[A_2 + A_3 \cos^2\theta\right]^2} \right\} dz d\rho \tag{4.8}$$

Multiplying by (4.8) by $\left(\frac{1}{A_3^2}\right) \Big/ \left(\frac{1}{A_3^2}\right)$:

$$\sigma_Y^2 = \int_0^\infty \int_{-\infty}^\infty \left\{ \int_0^{2\pi} \frac{\frac{A_1}{A_3^2} \, d\theta}{\left[A_2/A_3 + \cos^2\theta\right]^2} \right\} dz d\rho \tag{4.9}$$

Again, for convenience, the following terms are defined:

$$D_1 = \frac{A_1}{A_3^2} \tag{4.10a}$$

$$D_2 = \frac{A_2}{A_3} \tag{4.10b}$$

Because A_2 and A_3 are always positive, D_2 is always positive. Note also that as $\rho \to 0$, $\frac{A_2}{A_3}$ approaches $\frac{1 + \lambda^2 z^2 + \lambda_3^2}{\lambda_2^2 - \lambda_3^2}$ which is always positive and nonzero. To avoid A_3 in the denominator being zero, we must exclude the origin from the evaluation of the integral, and so ρ is always positive. This allows us to render (4.9) in its canonical form:

$$\int_0^\infty \int_{-\infty}^\infty \left\{ \int_0^{2\pi} \frac{D_1 d\theta}{\left[D_2 + \cos^2\theta\right]^2} \right\} dz d\rho \tag{4.11}$$

The following relation appears in a table of definite integrals [see e.g. Formula 2.5.18.2, Prudnikov, et al., 1984]:

$$\int_0^{\pi} \frac{d\theta}{a + \sin^2\theta} = \frac{\pi}{\sqrt{a^2 + a}} \tag{4.12}$$

Additionally,

$$\int_0^{\pi} \frac{d\theta}{a + \sin^2\theta} = \int_0^{\pi} \frac{d\theta}{a + \cos^2\theta} \tag{4.13}$$

Therefore, by relations (4.12) and (4.13):

$$\int_0^{2\pi} \frac{D_1 d\theta}{D_2 + \cos^2\theta} = \frac{2\pi D_1}{\sqrt{D_2^2 + D_2}} \tag{4.14}$$

Differentiating both sides of (4.14) with respect to D_2:

$$\int_0^{2\pi} \frac{D_1 d\theta}{\left[D_2 + \cos^2\theta\right]^2} = \frac{\pi D_1 [2D_2 + 1]}{\left[D_2^2 + D_2\right]^{3/2}} \tag{4.15}$$

Thus the variance is now:

$$\sigma_Y^2 = \int_0^{\infty}\int_{-\infty}^{\infty} \frac{\pi D_1 (2D_2 + 1)}{\left(D_2^2 + D_2\right)^{3/2}} \, dz d\rho \tag{4.16}$$

After re-introducing the expressions for the D's and A's and simplifying, (4.16) becomes:

$$\sigma_Y^2 = \int_0^{\infty}\int_{-\infty}^{\infty} \frac{\lambda_1^2 \lambda_3 \sigma_f^2}{\pi\left[\left(\lambda_1^2 - \lambda_3^2\right)\rho^2\right]^2} \cdot$$

$$\left\{ \frac{GA_w(\rho^2 + z^2) + (A_c - A_w)Gz^2 + (A_c A_w G^2)^2 z^2}{\left[A_w(A_w-1)G\right]^2\left[\rho^2+z^2\right] + z^2\left[(A_w-A_c)(\rho^2+z^2) - A_c A_w (A_w-1)G^2\right]^2} \right\} \rho \cdot$$

$$\left\{ \frac{2\left(1 + \lambda_1^2 z^2 + \lambda_3^2 \rho^2\right) + \left(\lambda_1^2 - \lambda_3^2\right)\rho^2}{\left[\left(1 + \lambda_1^2 z^2 + \lambda_3^2 \rho^2\right)^2 + \left(1 + \lambda_1^2 z^2 + \lambda_3^2 \rho^2\right)\left[\left(\lambda_1^2 - \lambda_3^2\right)\rho^2\right]\right]^{3/2}} \right\} \tag{4.17}$$

A listing of the code written to compute these is shown in Appendix II. In this code, the numerical integration is performed analytically.

The output of this code was verified by the following means:

* Sensitivity analysis behavior was compared to that for the two-dimensional case. In particular, as the correlation in the vertical direction became very small, behavior approached that for two dimensions.
* Numerical integration over three variables in Cartesian coordinates was carried out in a separately-written code.
* Numerical integration over three variables in cylindrical coordinates was carried out in a separately-written code.

TWO-DIMENSIONAL EFFECTIVE VELOCITY OF WATER

Velocities vary over a large range in flow through porous media - in fact, over many orders of magnitude [Freeze and Cherry, 1979]. Here, we are concerned with velocity variations due to specific features of real porous media flow, as well as our model. One type of velocity variation is due to reservoir heterogeneities, which generally means that there are differences in permeabilities in different parts of the formation. Another very important source of velocity differences is the fact that velocity is a function of saturation. For practical computation of flow velocities, it is desirable to use an effective velocity. Here, effective water velocity will be derived.

All assumptions are the same as those stated in Chapter 3 for two-dimensional flow. However, products of perturbations are retained in this derivation and only third-order and higher order terms are being dropped.

The formulation for effective velocity can be derived from equation (1.2a). Here, P_0 is shown substituted for P_w. Less detail is

shown here than was shown in earlier derivations. The steps are similar to the derivation of two-phase pressure and saturation relations.

$$\underline{V}_w = \frac{-kk_{rw}}{\mu_w} \nabla P_o \qquad (1.2a')$$

Introducing perturbations (2.9) and (3.5), and rearranging factors:

$$\underline{V}_w = -\frac{1}{\mu_w} e^F e^{C_w} e^{A_w \bar{Y}} \left[e^f e^{A_w Y'} \right] \left[\underline{J} + \nabla P_o' \right] \qquad (4.18)$$

Effective velocity is defined as the expected value of velocity. Note that the use of the word "effective" here may differ in meaning from its use in connection with permeability as customarily used in the petroleum literature. Using a second-order Taylor series approximation of $\exp(f + A_w Y')$, substituting in (4.18), expanding, taking expected values, and dropping terms with expected values equal to zero and terms of order higher than two:

$$\frac{-\mu_w E(\underline{V}_w)}{e^F e^{C_w} e^{A_w \bar{Y}}} = \underline{J} + E\left[f \nabla P_o' \right] + A_w E\left[Y' \nabla P_o' \right] + \frac{\underline{J}}{2} E[f^2] + A_w \underline{J} E[f Y'] + \frac{\underline{J} A_w^2}{2} E[(Y')^2] \qquad (4.19)$$

The following integral is a representation of two terms in (4.19):

$$E\left[\left(f + A_w Y' \right) \nabla P_o' \right] = \int_{-\infty}^{\infty} \underline{J} \cdot \underline{r} \, (i r_1) \left[\frac{1 + A_c \frac{B_2(\underline{r})}{B_1(\underline{r})}}{r^2 - i r_1 G A_c} \right] \cdot \left[1 + A_w \frac{B_2(\underline{r})}{B_1(\underline{r})} \right]^* S_{ff}(\underline{r}) d\underline{r} \qquad (4.20)$$

where * represents complex conjugate.

$$dZ_y = \frac{B_2(\underline{r})}{B_1(\underline{r})} dZ_f \qquad (4.21a)$$

$$dZ_p = \frac{\underline{J} r_1 \left[1 + A_c \frac{B_2(\underline{r})}{B_1(\underline{r})} \right]}{r^2 - i r_1 G A_c} dZ_f \qquad (4.21b)$$

Noting that $E(f^2) = \sigma_f^2$, $E[(Y')^2] = \sigma_Y^2$ and $E(fY') = \mathrm{Cov}(f, Y')$, (4.20) can be rewritten as:

$$E[\underline{V}_w] = \frac{-\exp\left(F + C_w + A_w \bar{Y}\right)}{\mu_w} \cdot \underline{J} \cdot \left[1 + I + \frac{\sigma_f^2}{2} + \frac{A_w^2 \sigma_Y^2}{2} + A_w \, \mathrm{Cov}\,(f,Y)\right] \tag{4.22}$$

where I is the integral in (4.20) with J factored out.

Cov(f,Y) is obtained by Fourier transformation of the cross-spectral density.

The cross-spectral density is defined analogously to the auto-spectral density [Lumley and Panofsky, 1964] and by an extension of the spectral representation theorem.

$$E\left[dZ_u\,(\underline{r}_1)\,dZ_v\,(\underline{r}_2)\right] = \begin{cases} 0, & \underline{r}_1 \neq \underline{r}_2 \\ S_{uv}(\underline{r}), & \underline{r}_1 = \underline{r}_2 = \underline{r} \end{cases} \tag{4.23}$$

Then, the cross-covariance is related to the cross-spectral density in the same way as for the autocovariance, as shown in the statement of the Spectral Representation Theorem in Chapter 3.

$$C_{uv}\,(\underline{x}) = \int_{-\infty}^{\infty} e^{i\underline{r}\cdot\underline{x}}\, S_{uv}\,(\underline{r})\,d\underline{r} \tag{4.24}$$

The integral I and the other terms in (4.5) were evaluated by using a numerical integration scheme. Results obtained using this code, discussion and figures are presented in Chapter 5.

A listing of the code to compute effective velocity is shown in Appendix III. Verification of this code was done using the following methods:

* Approximate comparison with hand calculations
* Setting $\underline{G} = \underline{0}$ results in some terms being zero.

An expression for effective velocity of oil can also be developed, using equation (1.2b). However, the functional form used to represent k_{ro}, equation (2.12), results in a very lengthy and unwieldy expression.

A more concise result would require that a different representation of k_{r0} be developed.

5. DISCUSSION AND CONCLUSIONS

DISCUSSION OF RESULTS

In this chapter, a discussion of the results obtained using the models derived in the last two chapters is presented. Conclusions are then drawn from this discussion, and, finally, directions for future research are suggested.

Spectral Densities

The spectral density of a process is simply the Fourier transform of the process. Basically, the spectral density shows how variability is distributed along various frequencies. In a sense, it is the inverse to the covariance in that frequencies are highest where correlation is zero between regions of positive and negative correlation. Figure 5.1 shows the spectral densities of Y, the log-saturation field, at two different values of the log-saturation gradient. The spectral densities of Y were calculated using relations (3.34) and (3.35). Figure 5.2 shows the correlation fields of Y, calculated from (3.36) using a Fast Fourier Transform of (3.34), which corresponds to these spectral densities. Correlation is simply a normalized covariance, obtained by dividing all covariance values by the variance. Figures 5.3 and 5.4 display the spectral density and covariance fields of pressure in a fashion similar to that for log saturation. Note that the spectral/covariance results for $Y = \ell nS$ are normalized by σ_f^2 and independent of J, while the results for p are normalized by $\sigma_f^2 J^2$.

In practice, the spectral density serves as a mathematical tool which enables us to calculate covariances. Although we utilize spectral

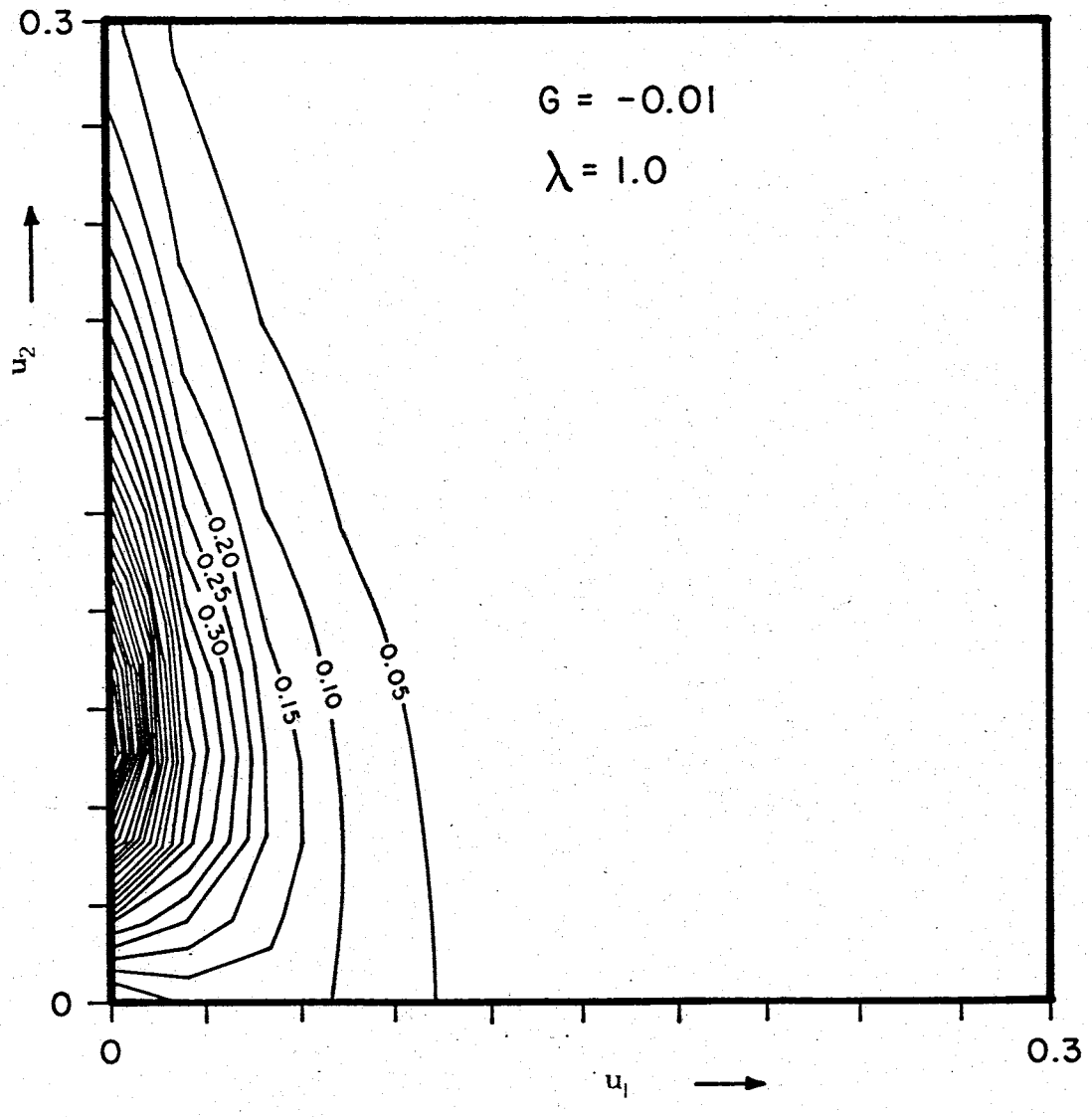

$r_1 = 2\pi u_1$, $r_2 = 2\pi u_2$

Figure 5.1a. Contours of Spectral Density for $Y = \ell nS$
2-D Model: Normalized by σ_f^2, Independent of J
$A_w = 3.0$, $A_c = 2.6$, $\lambda = 1$, $G = E(\nabla Y) = -.01$

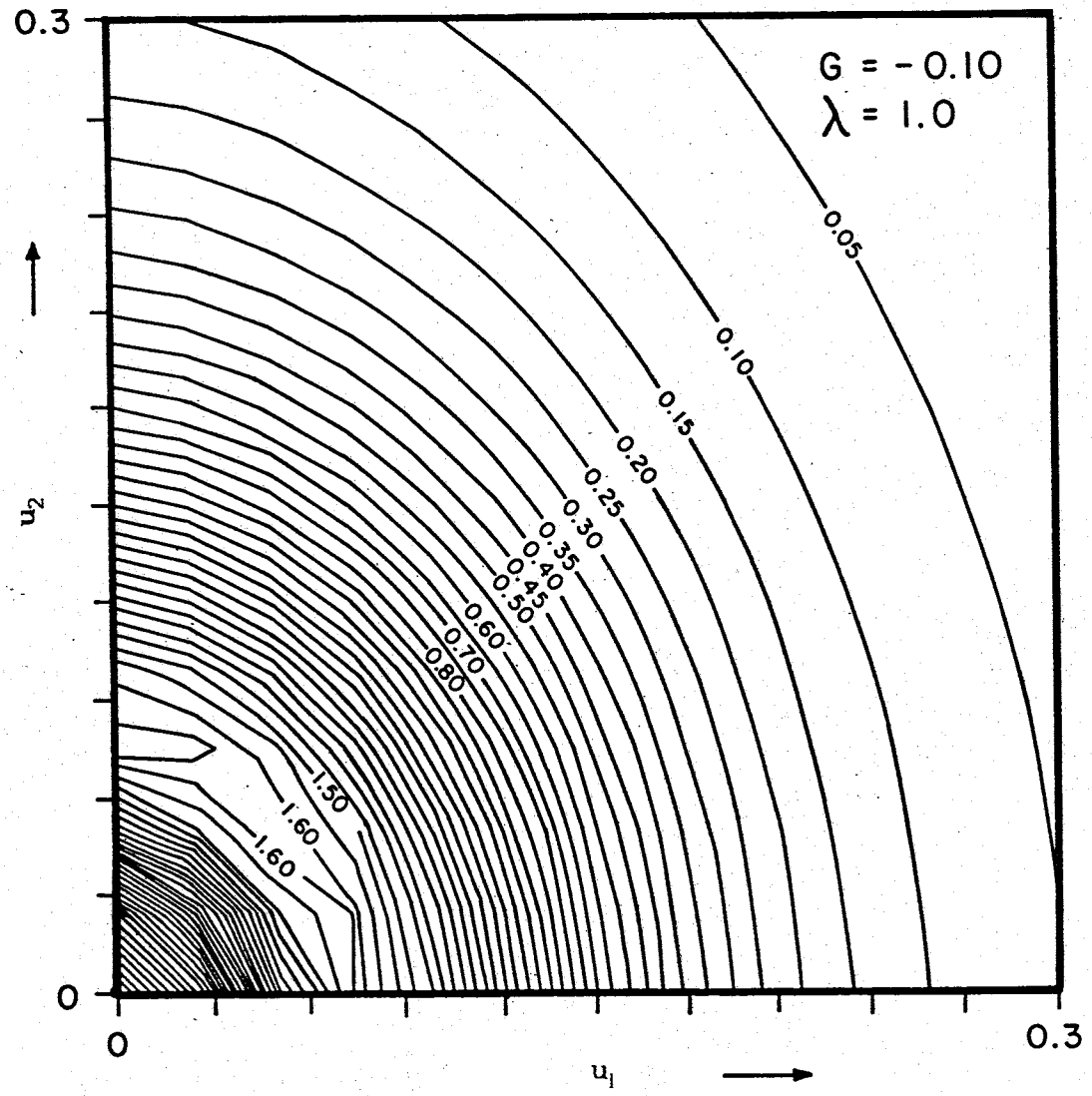

$r_1 = 2\pi u_1$, $r_2 = 2\pi u_2$

Figure 5.1b. Contours of Spectral Density for $Y = \ell nS$
2-D Model: Normalized by σ_f^2, Independent of J
$A_w = 3.0$, $A_c = 2.6$, $\lambda = 1$, $G = E(\nabla Y) = -.10$

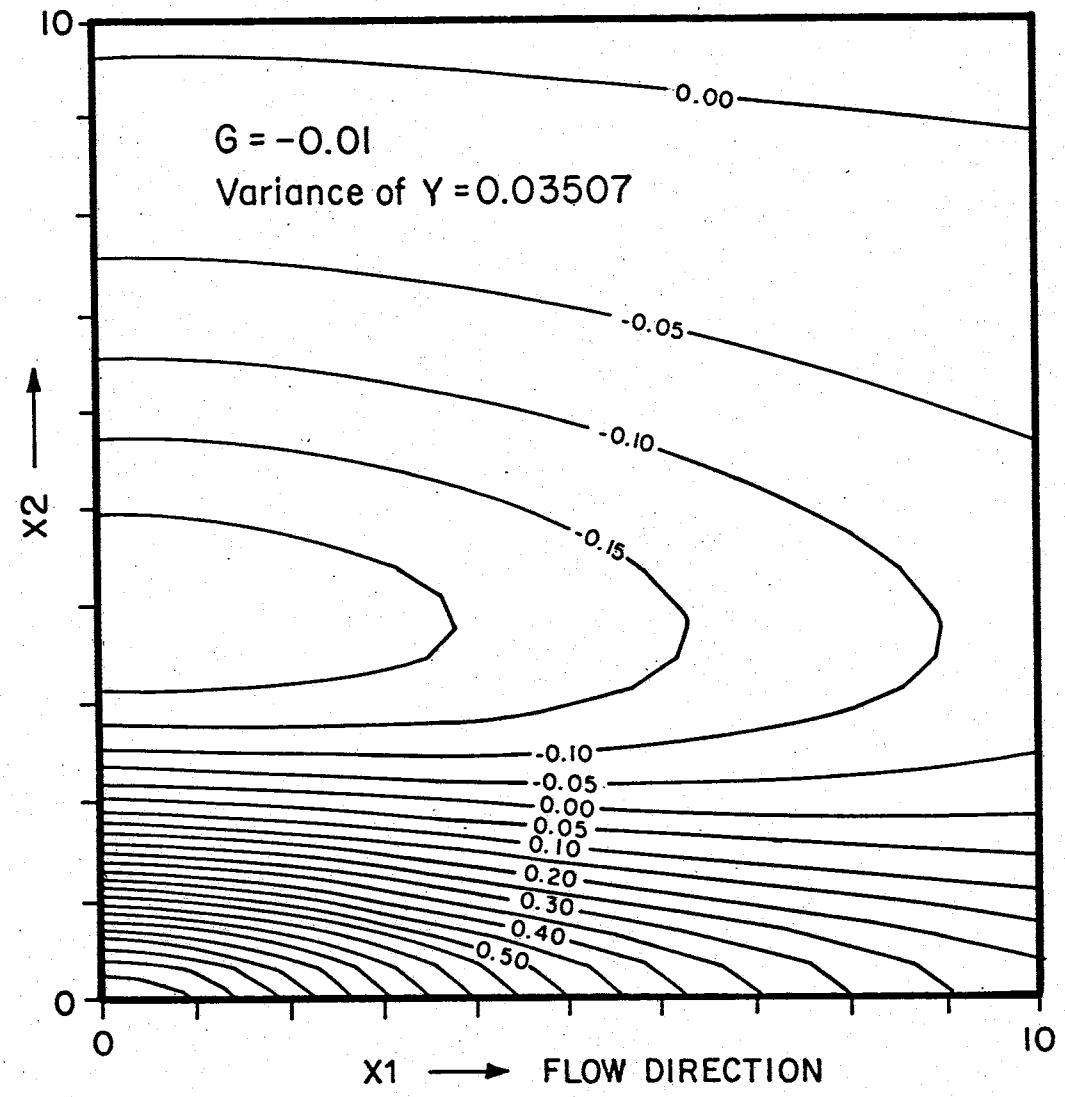

Figure 5.2a. Contours of Correlation Function for Y = ℓnS
2-D Model: Independent of J
A_w = 3.0, A_c = 2.6, λ = 1, G = E(∇Y) = -.01

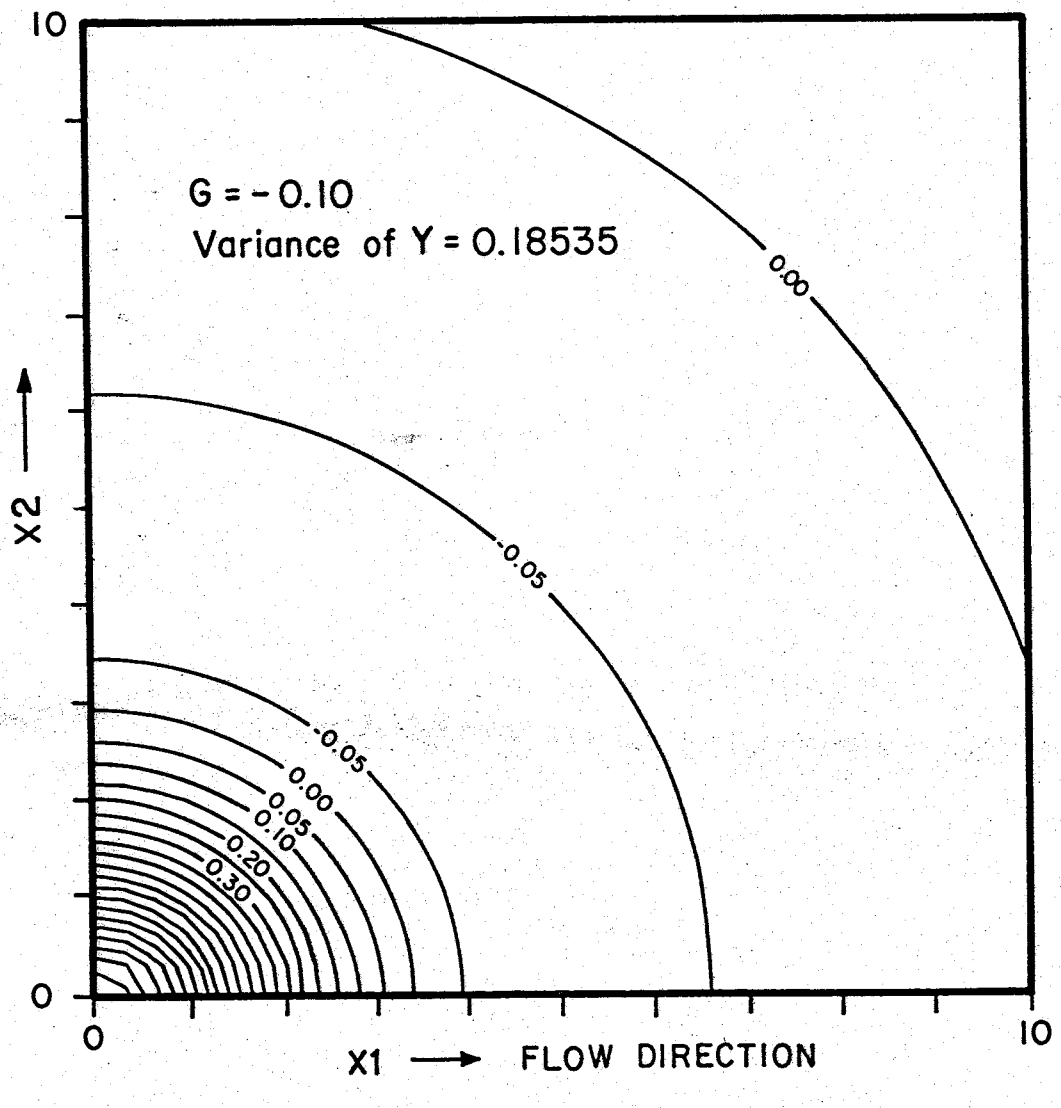

Figure 5.2b. Contours of Correlation Function for Y = ℓnS
2-D Model: Independent of J
A_w = 3.0, A_c = 2.6, λ = 1, G = E(∇Y) = -.1

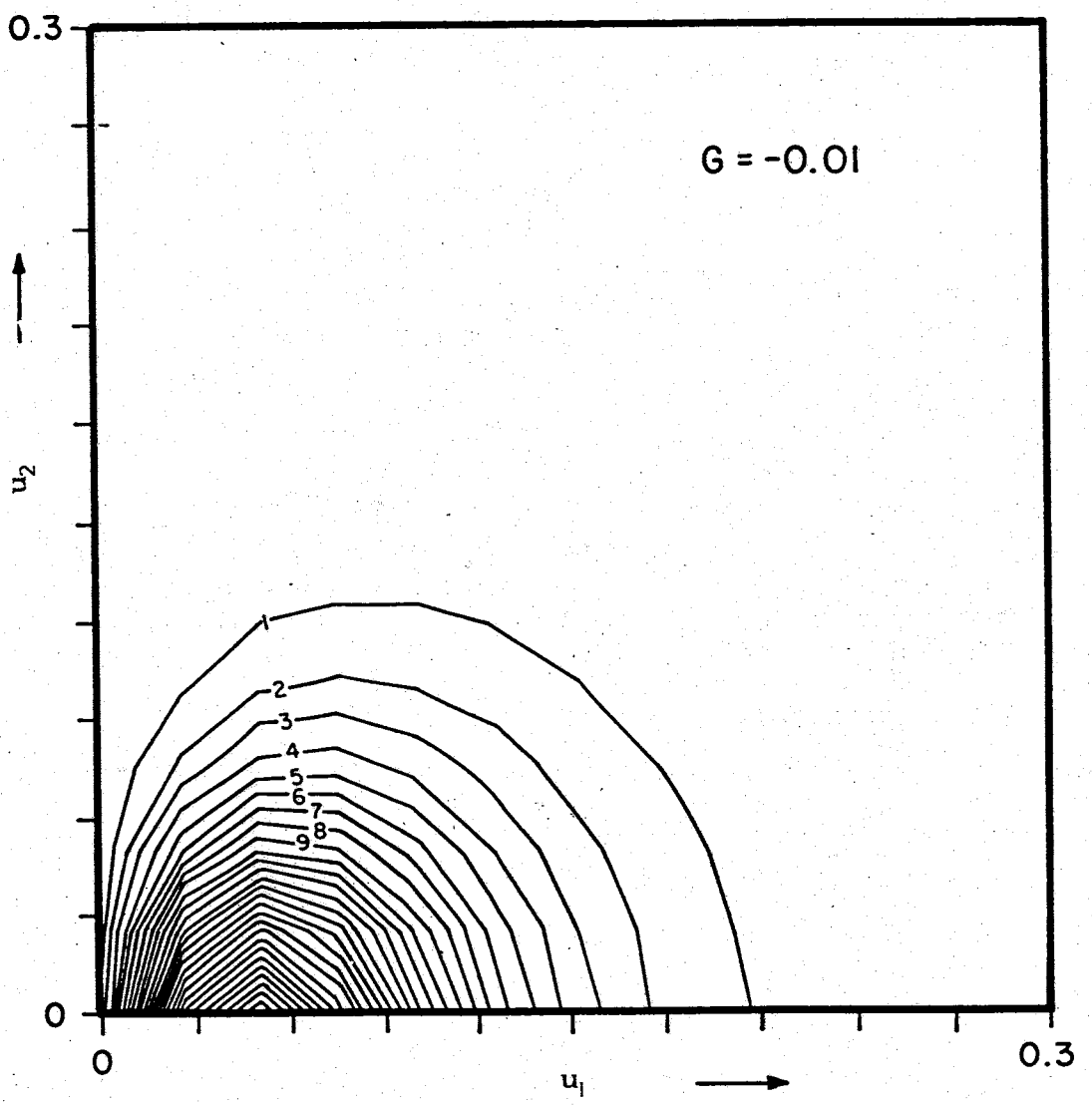

$r_1 = 2\pi u_1$, $r_2 = 2\pi u_2$

Figure 5.3a. Contours of Spectral Density for P
2-D Model: Normalized by $\sigma_f^2 J^2$
$A_w = 3.0$, $A_c = 2.6$, $\lambda = 1$, $G = E(\nabla \ell n S) = -.01$

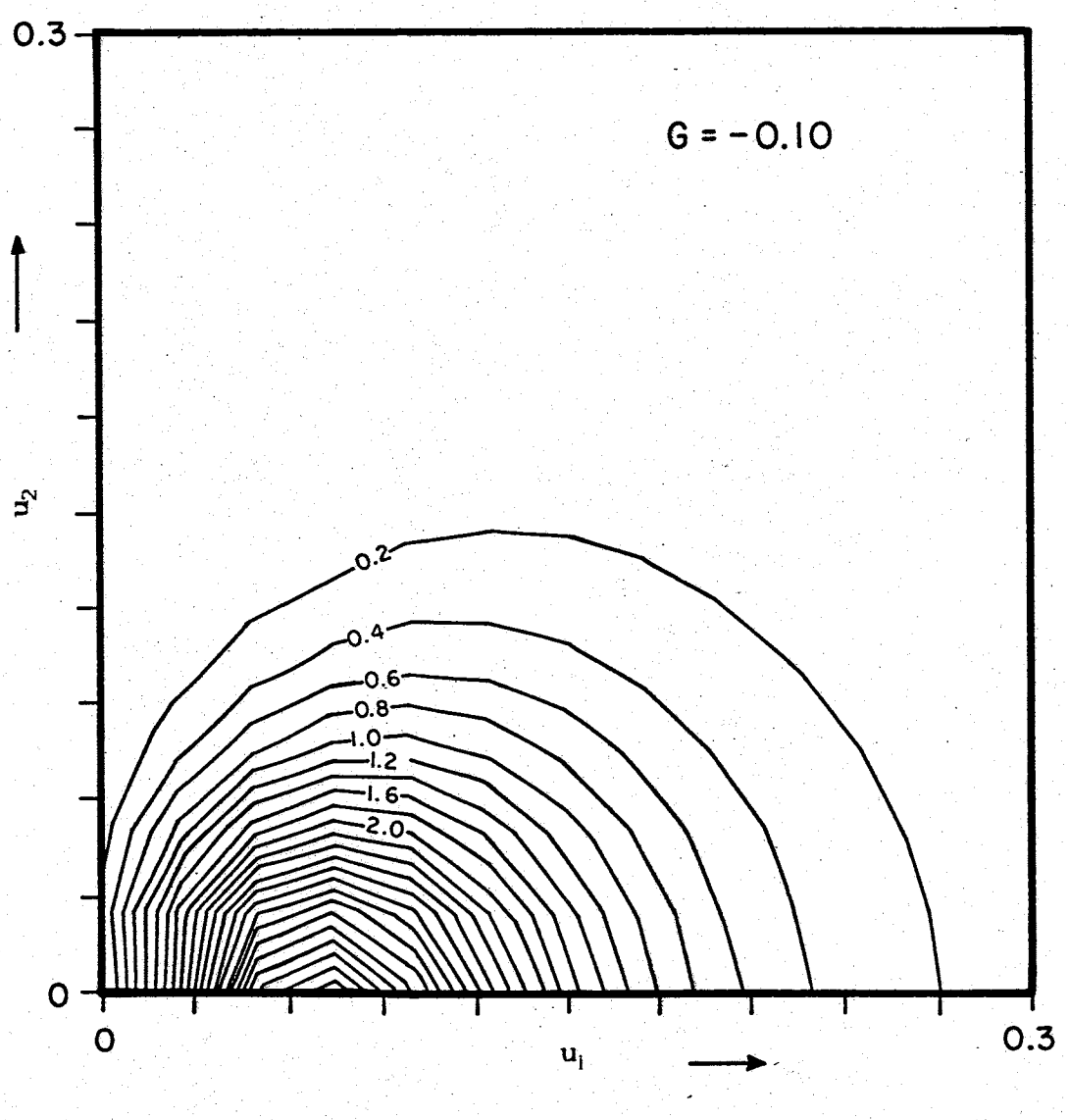

$r_1 = 2\pi u_1$, $r_2 = 2\pi u_2$

Figure 5.3b. Contours of Spectral Density for P
2-D Model: Normalized by $\sigma_f^2 J^2$
$A_w = 3.0$, $A_c = 2.6$, $\lambda = 1$, $G = E(\nabla \ell n S) = -.1$

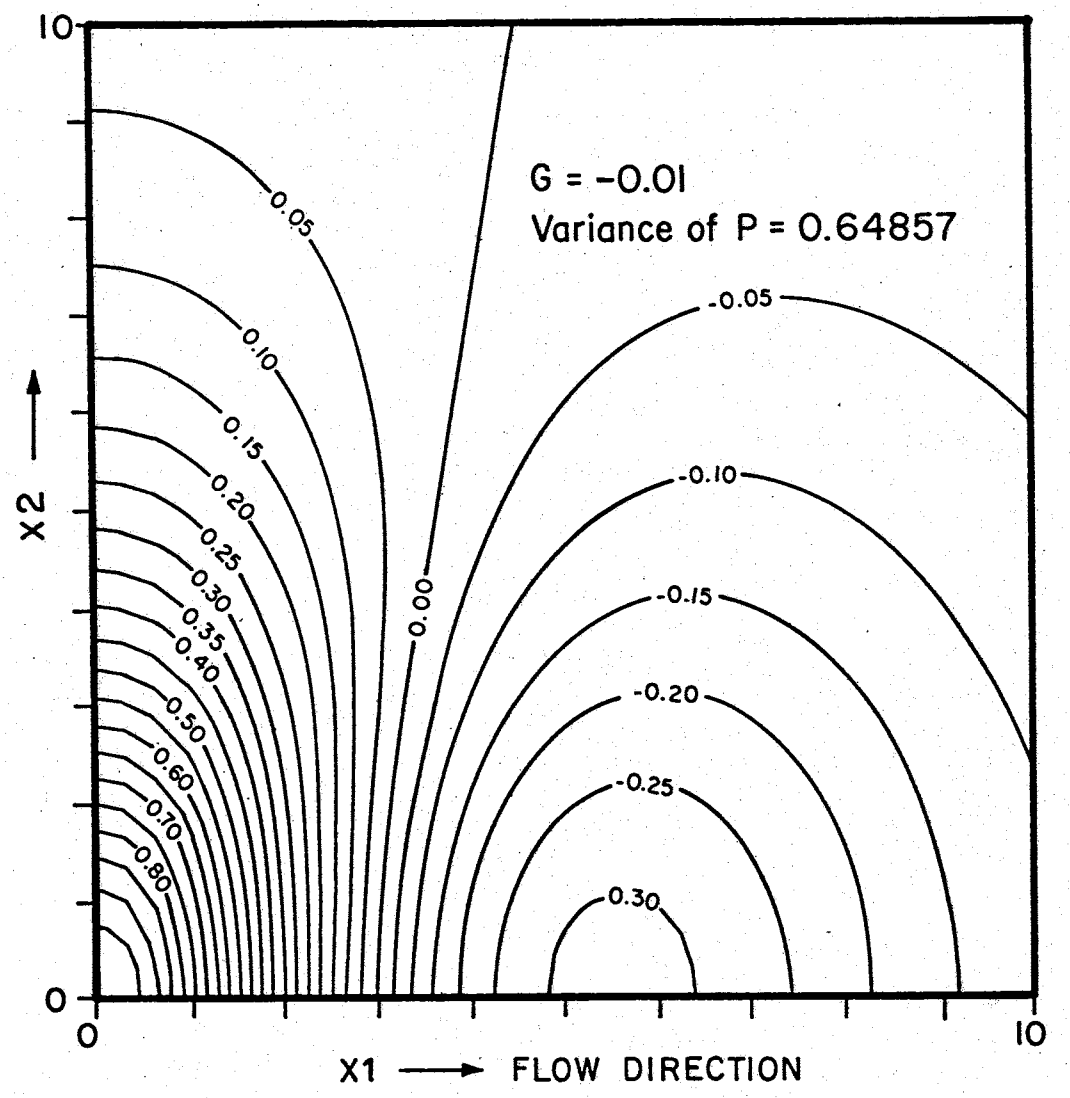

Figure 5.4a. Contours of Correlation Function for Pressure
2-D Model
$A_w = 3.0$, $A_c = 2.6$, $\lambda = 1.0$, $G = E(\nabla Y) = -.01$

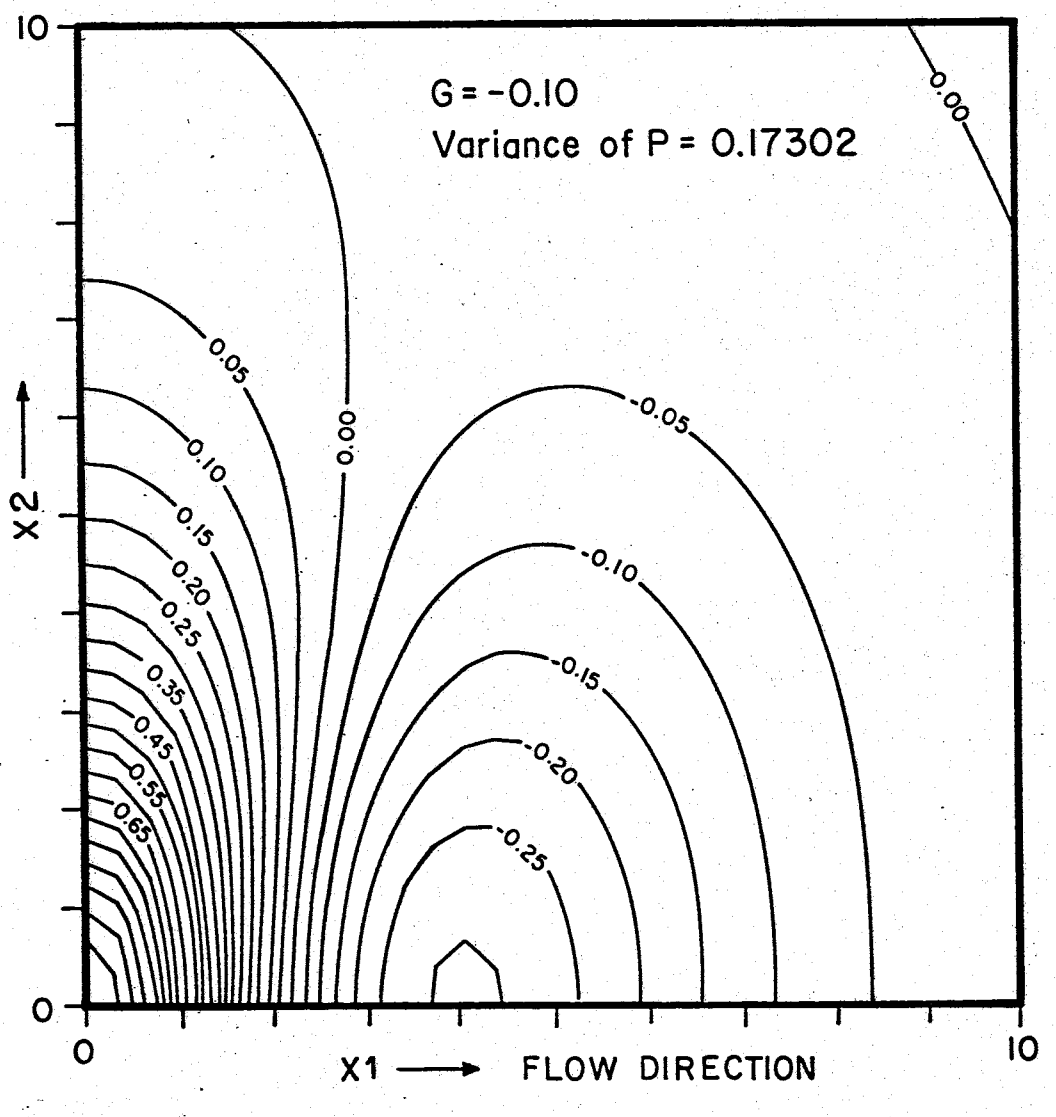

Figure 5.4b. Contours of Correlation Function for Pressure
2-D Model
$A_w = 3.0$, $A_c = 2.6$, $\lambda = 1.0$, $G = E(\nabla Y) = -.1$

analysis to achieve our results, our goal is to obtain the covariance fields. Covariances are more easily and naturally related to real physical processes. Therefore, Figures 5.1 and 5.3 have been included simply to illustrate the relationship of spectral density fields to covariance fields.

Two-Dimensional Flow

Covariances of Pressure and Saturation

Figure 5.2 shows that the correlation length of the saturation field is much larger in the direction of flow than transverse to it. Correlation length is the distance from (0,0) in the correlation field in which there is an e-fold drop in correlation, i.e. the distance between the location in the field at which correlation equals one and a point at which correlation equals 1/e. This distance is a function of direction. Figure 5.2 indicates that correlation length anisotropy is more pronounced at low values of the saturation gradient than at higher values.

This anisotropy can be explained by the presence of zones of differing saturations being elongated in the direction of flow. This occurs because the direction of flow plays a role in causing zones of differing saturations to be elongated in this way. Now, as the saturation gradient increases, correlation length decreases in the direction of flow, and, thus, the ratio of correlation length parallel to flow to correlation length transverse to flow decreases. Consequently, anisotropy decreases.

Heterogeneities in permeability tend to increase the prevalence and importance of zones of different saturations for at least two reasons.

First, zones of differing permeabilities will tend to retain different proportions of the original fluid (oil) when a second fluid (water) is flowing through. Second, the changing permeabilities mean that flow velocities are also changing. This also has a bearing on the proportion of the original fluid that is dislodged from the pore spaces. During imbibition (the initial movement of a wetting fluid into a formation containing mostly nonwetting fluid), the velocity of the displacing fluid may be higher in low-permeability media. Later during the flow, as steady state is approached, low-permeability media will tend to have lower flow velocities than high-permeability media. Lower flow velocities may tend to leave a higher proportion of the original fluid (oil) in place.

The elongated nature of zones of differing velocities (and thus differing saturations) can be illustrated by a simple schematic drawing of one single circular zone of low permeability, shown in Figure 5.5. Immediately upstream and downstream of this zone, flow velocities are lower because flow through the zone is impeded, and diverging and converging of flows occur well upstream and downstream of the low-permeability zone. On the other hand, immediately transverse to the zone, there are higher than average velocities as flow is constricted and concentrated, and thus the flow is at a higher velocity through a relatively narrow space.

Fingering is of serious concern in waterflood oil recovery. In most oil reservoirs in the real world, oil recovery is greatly reduced due to water flowing to recovery wells along preferential flowpaths, while the bulk of the oil is left behind [Ewing, 1983]. Once water

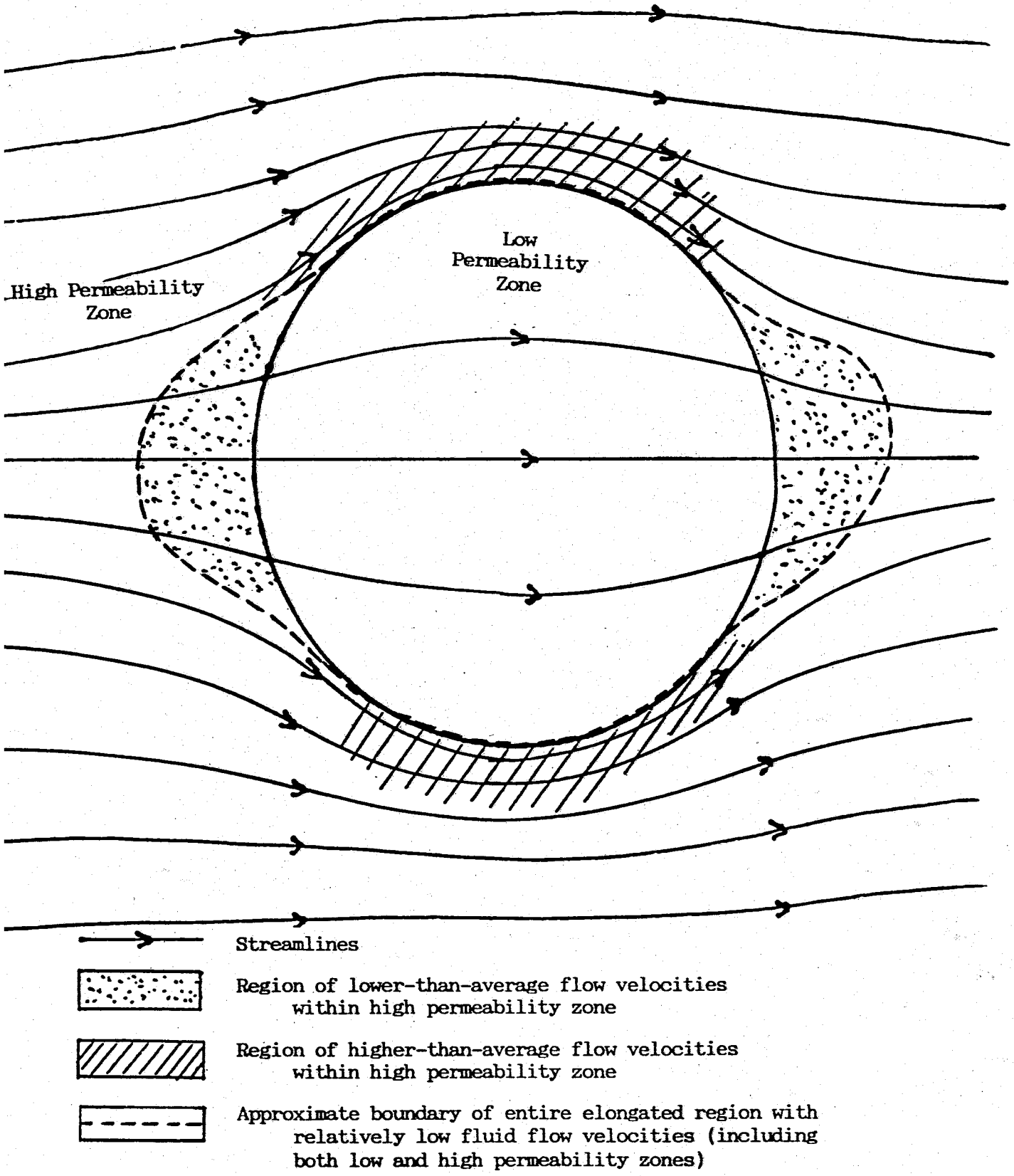

Figure 5.5. Flow Patterns Around Circular Low-Permeability Zone Showing Elongated Low-Velocity Region

reaches the production well, steady state is approached and oil production declines substantially. It is this situation that we are modeling. Oil production is generally halted before true steady state is reached. However, near the injection wells, the situation will be very nearly steady state while closer to the production wells it will be farther from it when the wells are shut down.

The correlation length of pressure perpendicular to flow is much larger than parallel to flow, as shown in Figure 5.4. This is expected, since equal pressure lines are perpendicular to flow in homogeneous media, and nearly so in most real media.

The correlation length of pressure perpendicular to flow appears to trend lower as the saturation gradient increases. It can be surmised that large saturation gradients may tend to occur more when substantial differences in pressure occur, perhaps in a complex pattern such that pressures in a straight line do not correlate over as long a distance.

Variance of Log Saturation and Saturation

Figure 5.6 shows that the variance of log saturation increases rapidly toward an asymptotic value, 0.25, with an increase in the log-saturation gradient. A large saturation gradient means that water saturation would tend to decrease rapidly over a short distance, most likely in the direction of flow, and, thus, it is reasonable to believe that its variance would be substantial. That is, there is almost certainly a large variation in the values of saturation in a direction parallel to flow. However, saturation is a physical process having possible values only between 0 and 1.

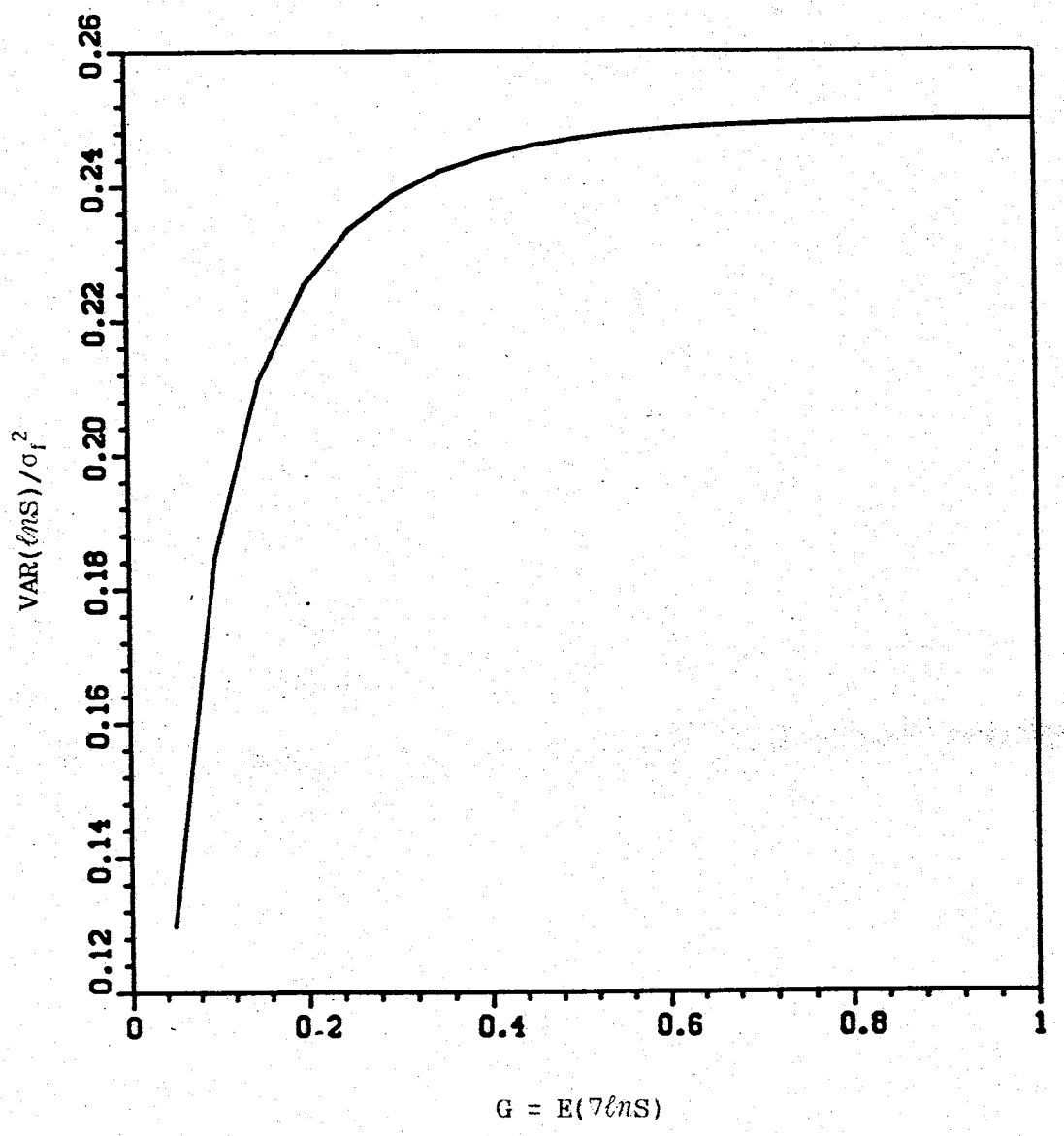

Figure 5.6. Variance of Y = ℓnS vs E($\nabla \ell nS$)
2-D Model: Normalized by σ_f^2, Independent of J
A_w = 3.0, A_c = 2.6, λ = 1.0

For $Y = \ln(S)$, the possible range of values is from $-\infty$ to 0. However, since we are assuming that water saturation remains between 0.25 and 0.8, the possible range of values for Y is from -1.386 to -0.223. From the definition of variance, it is clear that there must be an upper bound to the possible variance values, and, thus, it is not surprising that an asymptotic value is approached.

Now, suppose we consider the case of the mean of S = 0.50, and assume that S is log-normally distributed. We also know that the variance of Y approaches 0.25 asymptotically. The logarithm of saturation was used throughout this study because it allowed simplification of the mathematical relationships developed. We want to know the variance of saturation, σ_S^2, rather than the variance of the log of saturation. From Chapter 2, we have the following definition:

$$Y = \ln S \tag{2.9b}$$

From this, we have:

$$e^Y = S \tag{5.1}$$

The mean of Y is the expected value:

$$E(Y) = E(\ln S) \tag{5.2}$$

Now, having the values of σ_Y^2 and μ_S, the variance of S can be computed using the following relationship, which is derived from the probability density function for a normal distribution:

$$\sigma_S^2 = e^{2\mu_Y} e^{\sigma_Y^2} \left(e^{\sigma_Y^2} - 1 \right) \tag{5.3a}$$

while

$$\mu_S = e^{\mu_Y} e^{\sigma_Y^2/2}. \tag{5.3b}$$

Hence

$$\sigma_S^2 = \mu_S^2 \left[e^{\sigma_Y^2} - 1 \right]$$

and $\mu_S = .5$, $\sigma_Y^2 = .25$ implies $\sigma_S^2 = .25(e^{.25} - 1) = .071$

Variance of Pressure with Log Saturation Gradient

Figure 5.7 shows that the variance of pressure decreases dramatically with an increasing log-saturation gradient, particularly if the pressure gradient is large. With a small saturation gradient, the distribution of saturation and pressure values is likely to be irregular, and thus subject to considerable variability. A large saturation gradient would most likely occur with a well defined oil-water front moving through. In this case, the pressure distribution would be almost deterministic, exhibiting little variability. Also, with a small pressure gradient, the range of pressures encountered would be small, making the variance small. Conversely, a higher pressure gradient means that pressures occur over a larger range, making the variance larger.

Distances Over Which Significant Variability Occurs

Another way to compare and contrast the variances of pressure and saturation is to consider the distances over which substantial differences in pressure and saturation values exist. With a small saturation gradient, zones of varying saturations will exist over considerable distances parallel to flow. Pressure is subject to some variation as we cross these zones of differing saturation, which are likely to be zones of differing permeabilities. As the saturation gradient increases, the range of saturations encountered over a short distance in the direction of flow will tend to increase. Because pressures are easily transmitted over short distances, pressure variance decreases as the saturation gradient increases. It must be kept in mind, however, that we are working under the assumption of a zero capillary pressure. Thus, these interpretations must be taken with caution, particularly where

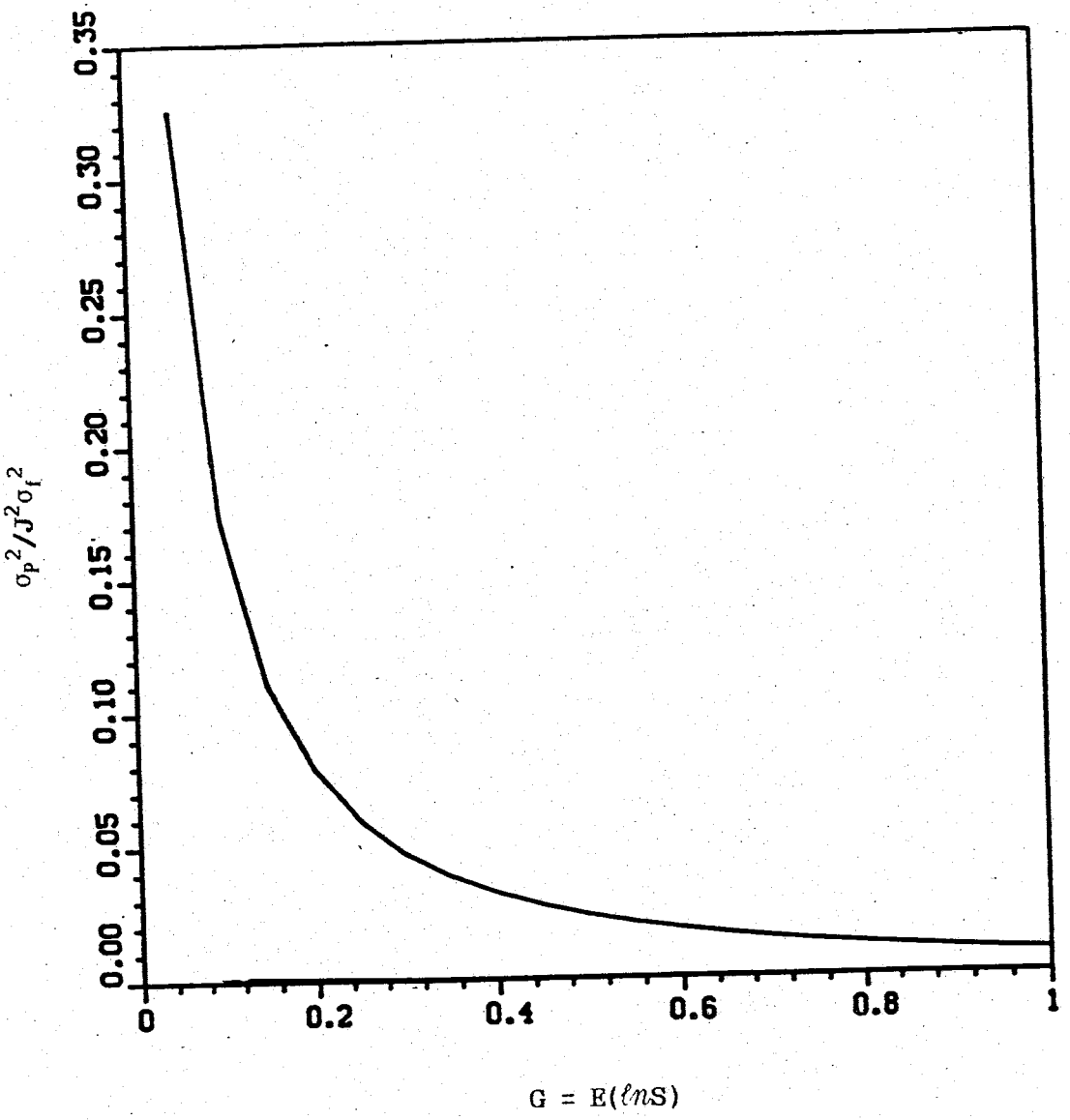

Figure 5.7. Variance of P vs E ($\nabla \ell n$S)
2-D Model: Normalized by $J^2\sigma_f^2$
A_w - 3.0, A_c = 2.6, λ = 1

capillary pressures are likely to be large or otherwise of importance because of the situation we are dealing with.

Variability of Saturation and Pressure with Correlation Length

The variance of log saturation appears to decrease very slightly and then levels off with increasing correlation length, as shown in Figure 5.8. The very small magnitude of change in its value casts doubt on whether this is significant or not. Pressure, on the other hand, exhibits an increase and then leveling off with increasing correlation length. Larger correlation length implies that there are fewer and larger zones of similar properties and values present. Since saturation physically takes on only a limited range of values, fewer zones within a region of interest may result in slightly lower variance (imagine two rolls of a die compared to a hundred - two rolls will not cover all possible values, but a hundred almost certainly will). Pressure, being a quantity with unbounded values, will tend to have more widely differing values if we have fewer, more widely-separated zones of differing permeabilities, velocities, saturations, and pressures. Figure 5.9 indicates that the variability of pressure increases with correlation length and then levels off. As correlation lengths continue to increase to the length of our model and beyond, we will eventually tend to be within one transition zone between regions of differing pressure, and, thus, pressure variability increase with increasing correlation length levels off.

Sensitivity to Relative Permeability and Mobility Parameters

Other sensitivity analysis runs show that the variances of both saturation and pressure are rather sensitive to choices of values of

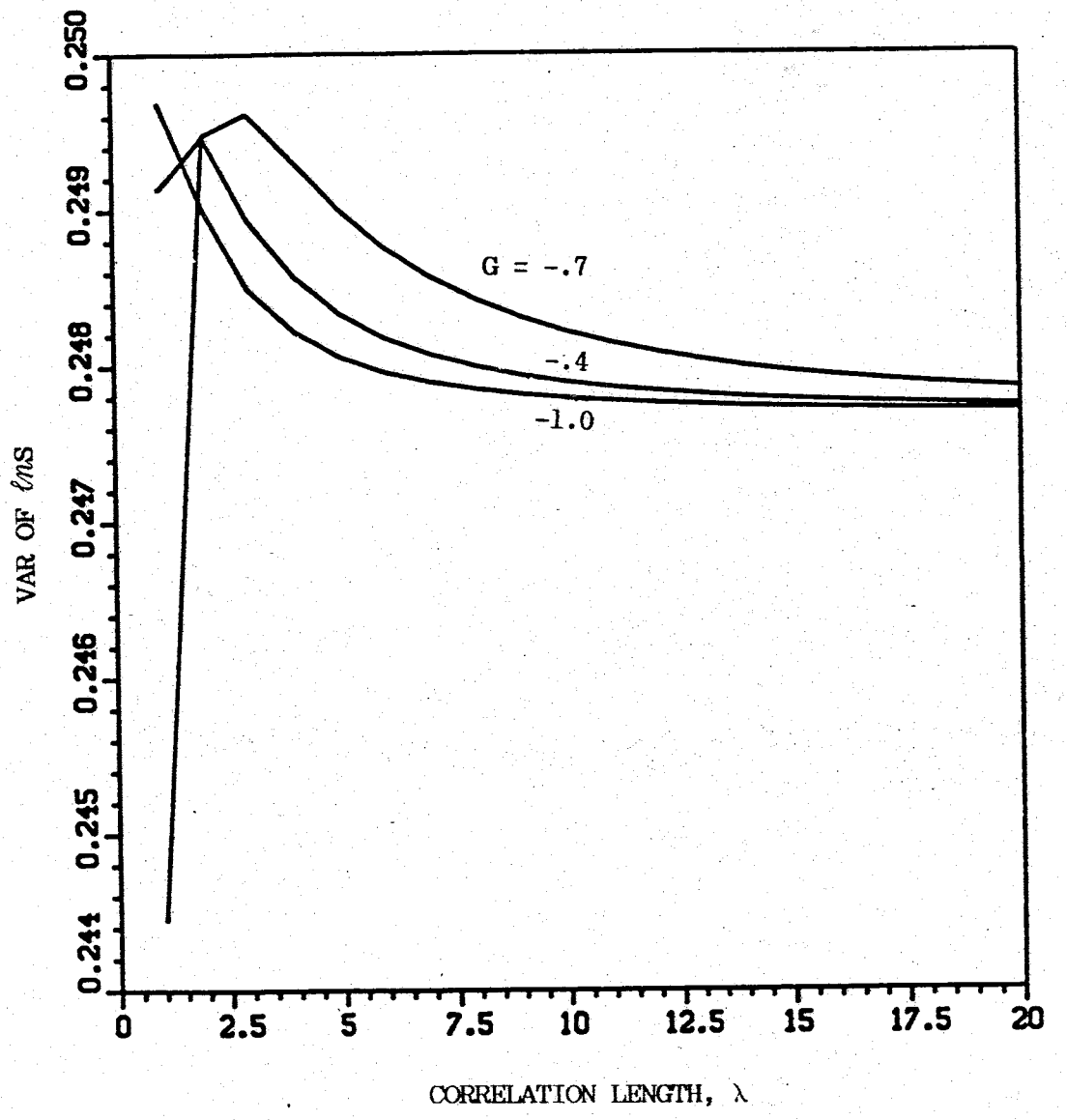

Figure 5.8. Variance of ℓnS vs Correlation Length, λ
2-D Model: Normalized by σ_f^2, Independent of J
$A_w = 3.0$, $A_c = 2.6$, $G = E(\nabla \ell nS)$

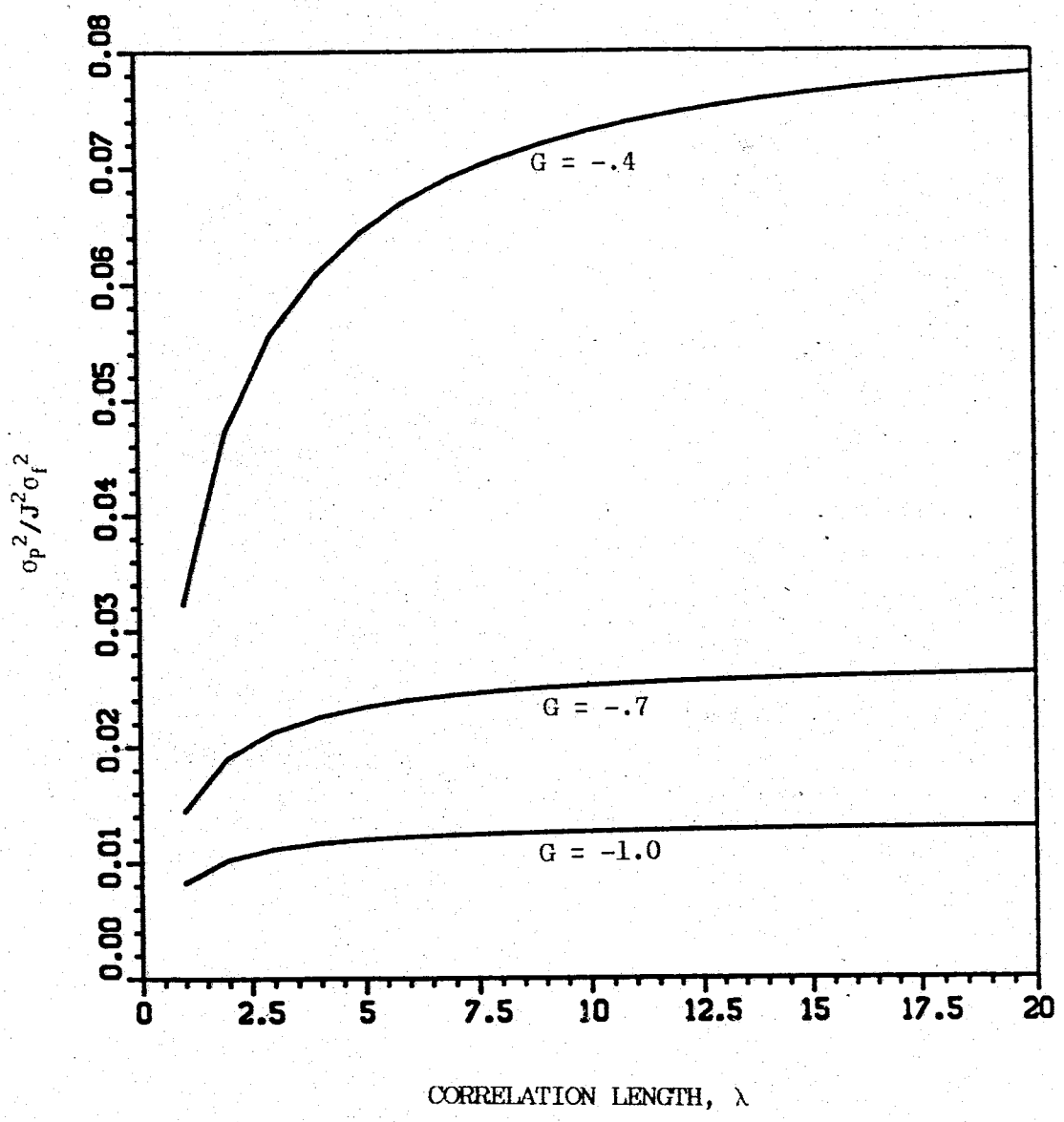

Figure 5.9. Variance of Pressure vs Correlation Length, λ
2-D Model: Normalized by $J^2\sigma_f^2$
$A_w = 3.0$, $A_c = 2.6$, $G = E(7\ell nS)$

A_c and A_w. These are parameters in the approximating functions for relative permeability of water and total mobility, respectively. This finding indicates that determining the most suitable functional forms for approximating these relations as well as finding appropriate values for the function parameters may be worthwhile topics for additional research.

The variance of log saturation is much more sensitive to the value of A_w than to values of A_c, as shown in Figure 5.10. However, Figure 5.11 reveals that the variance of pressure is quite sensitive to values of both A_c and A_w. Since A_c and A_w are not fundamental physical quantitites, but rather are parameters in somewhat arbitrary approximating functions, the specific nature of the variances' sensitivities to their values will not be further discussed.

The shape of the water relative permeability curve does not vary greatly from one medium to another. Furthermore, the exponential function which was fit to this curve provided quite a good fit. Therefore, it is likely that the value of A_w used was a good approximation which is not likely to vary much. However, oil viscosities vary widely, which means that oil relative permeability values will vary widely, and, consequently, total mobility values will differ considerably under different reservoir conditions. Furthermore, the fit of an exponential function to this curve was not as good a fit as it was for the water relative permeability curve. A substantially different total mobility curve may make an exponential function a very poor fit. Thus, values of A_c may vary over quite a large range, and a more realistic model may actually require a function of a different form.

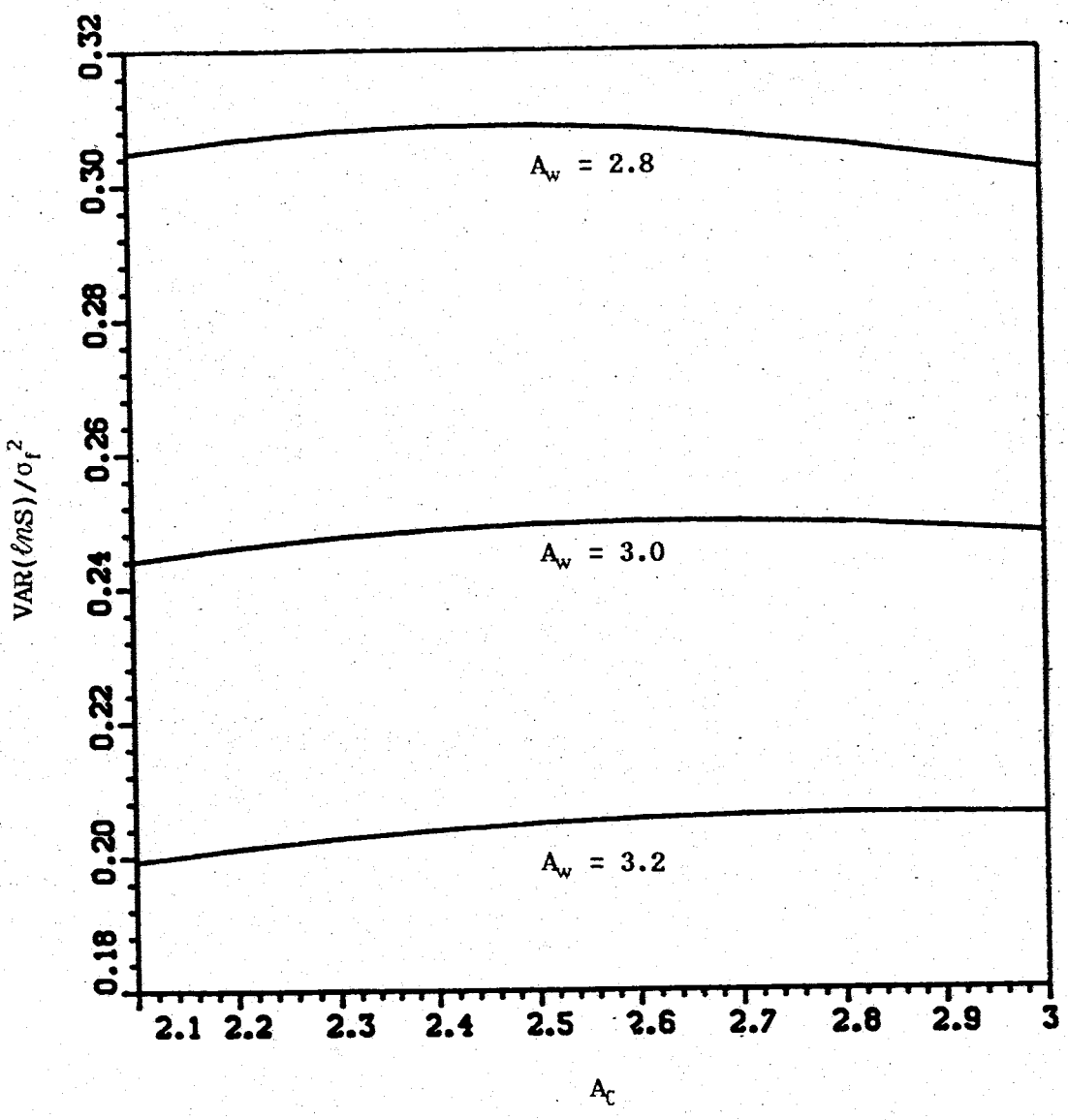

Figure 5.10. Sensitivity of Variance of ℓnS to A_c and A_w
2-D Model: Normalized by σ_f^2, Independent of J
$E(\nabla \ell nS) = -1$

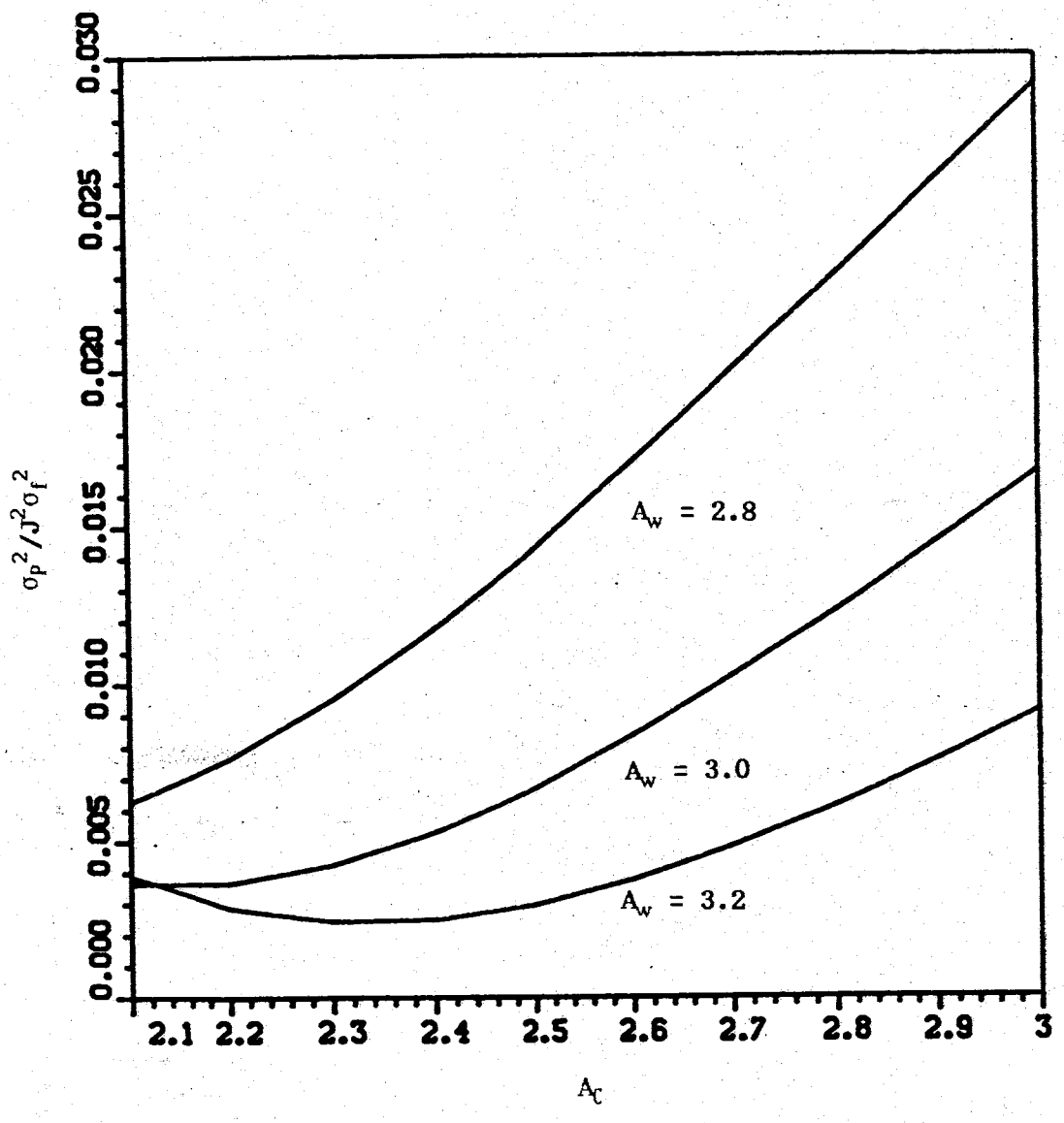

Figure 5.11. Sensitivity of Variance of P to A_c and A_w
2-D Model: Normalized by $J^2\sigma_f^2$
$E(\nabla \ell n S) = -1$

It can be concluded that the variance of log saturation was probably not seriously affected if our choices of functions or their parameter values for water relative permeability and total mobility were rather poor. However, the pressure variance's sensitivity to A_c, in particular, casts some uncertainty on our observations of the behavior of this variance.

The Three-Dimensional Model

The sensitivity of the variance of log saturation to the log-saturation gradient was quite similar to the two-dimensional case, as shown in Figure 5.12. This was not surprising, as the anisotropic model used describes a situation in which flow is likely to be predominantly horizontal, and, thus, flow does not differ greatly from the two-dimensional case.

The variance of log saturation approaches the two-dimensional variance for a large anisotropy ratio, as expected. A large anisotropy ratio means that the vertical correlation length is much smaller than that in the horizontal directions. This is caused by layers of substantially differing permeabilities, which, as discussed earlier, generally results in little vertical flow. Thus, as the anisotropy ratio increases, the flow approaches the two-dimensional case.

As the anisotropy ratio approaches one, the variance of log saturation approaches its limiting value much more slowly with increasing correlation length. This is so because the freer vertical movement implied by the lower anisotropy ratio (meaning a relatively larger vertical correlation length) allows saturation differences to more effectively reach equilibrium in the vertical direction in addition to the horizontal directions, thereby reducing its variability.

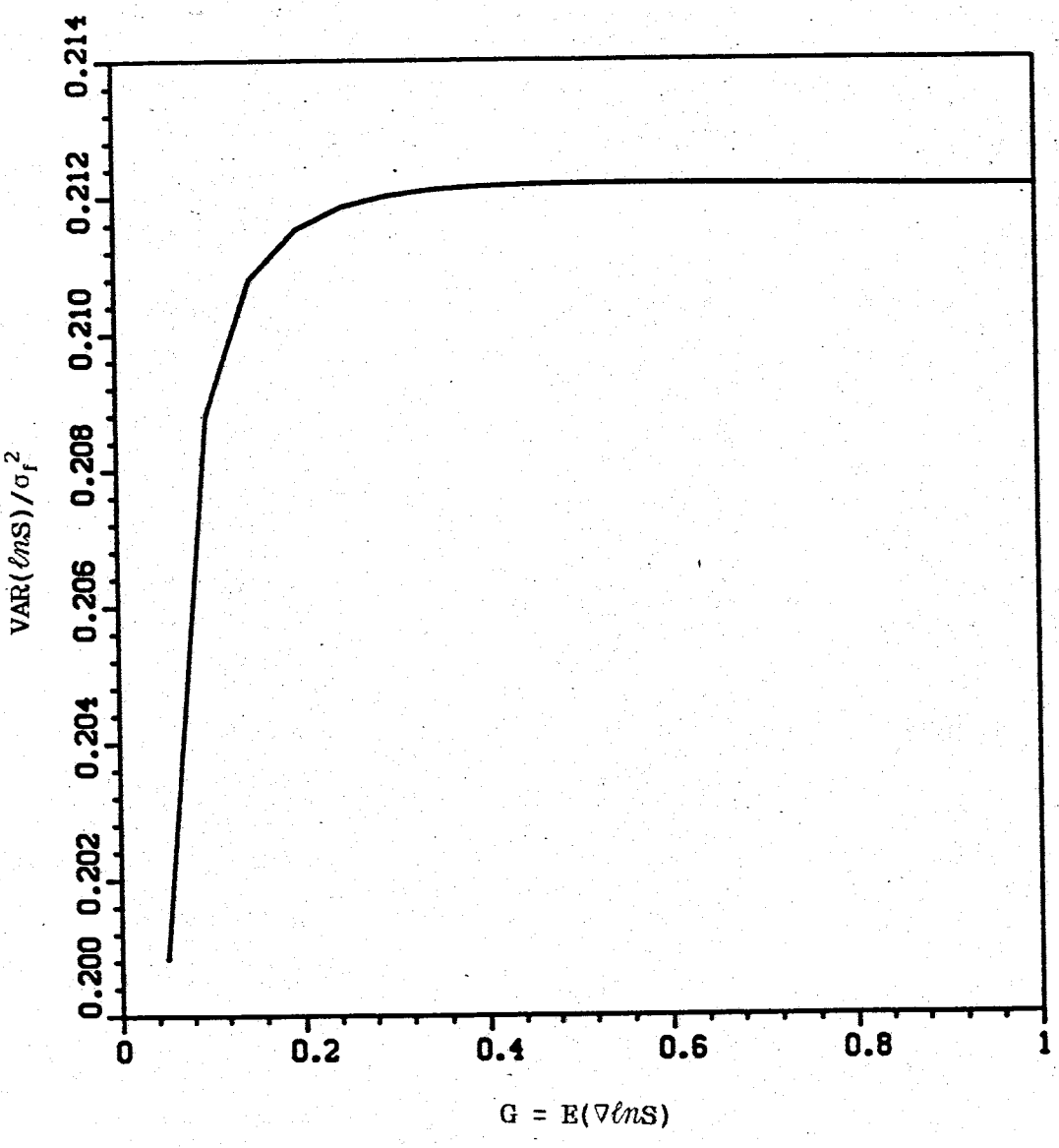

Figure 5.12. Variance of Y = ℓnS vs E($\nabla \ell n$S)
3-D Isotropic Model: Normalized by σ_f^2, Independent of J
A_w = 3.0, A_c = 2.6, λ = 1

However, results for a small anisotropy ratio should be interpreted with caution, as our model did not incorporate gravity effects. A small anisotropy ratio implies that vertical flow may be relatively important, which means that the role of gravity is more important.

The behavior of the variance of pressure with varying log-saturation gradient is almost identical to that for the two-dimensional case, at first falling rapidly and then more slowly as the log-saturation gradient increases. This is shown in Figure 5.13. Because pressures reach equilibrium over distances more quickly than do differing saturations, the net effect of a third dimension being present does not influence pressures much.

The variance of saturation increases with increasing correlation length, approaching an asymptotic value, as shown in Figure 5.14. This can be explained by the likelihood of longer correlation lengths to imply the presence of fewer and larger zones of differing permeabilities (and, thus, differing saturations). This, in turn, means that preferential flowpaths exhibiting higher flow velocities will tend to be of more substantial length, and thus of greater importance. Therefore, zones of substantially different saturations will exist, which means that the variance of saturation is larger. As explained previously, because of the limited range of possible values for saturation, the variance approaches a limiting value.

The variance of pressure increases without bound as correlation length increases (Figure 5.15). Increasing correlation length implies fewer, larger zones of differing pressures. Substantial differences in pressure are more likely to be maintained over larger distances than

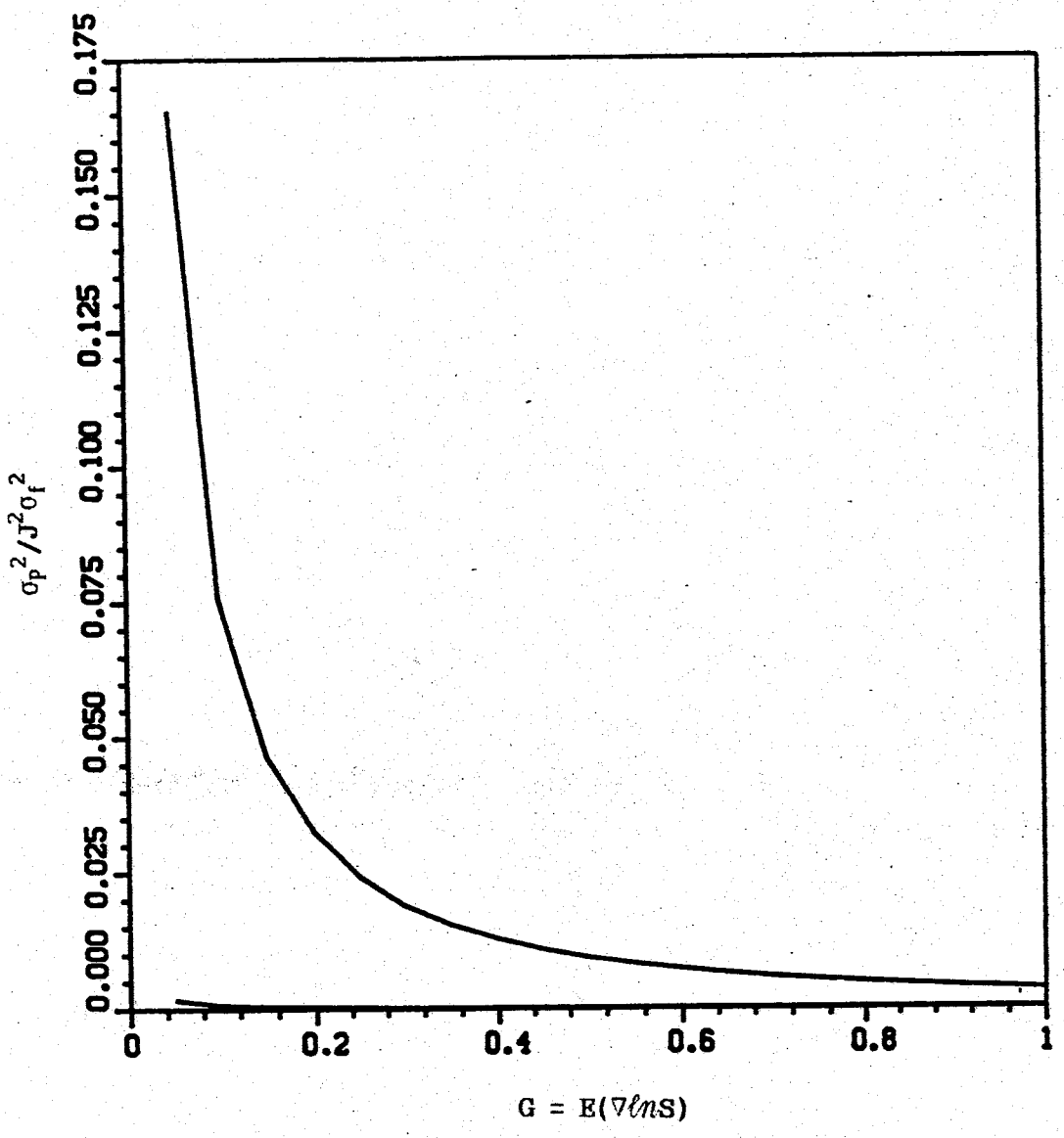

Figure 5.13. Variance of P vs E(ℓnS)
3-D Isotropic Model: Normalized by $J^2\sigma_f^2$
A_w = 3.0, A_c = 2.6, λ = 1

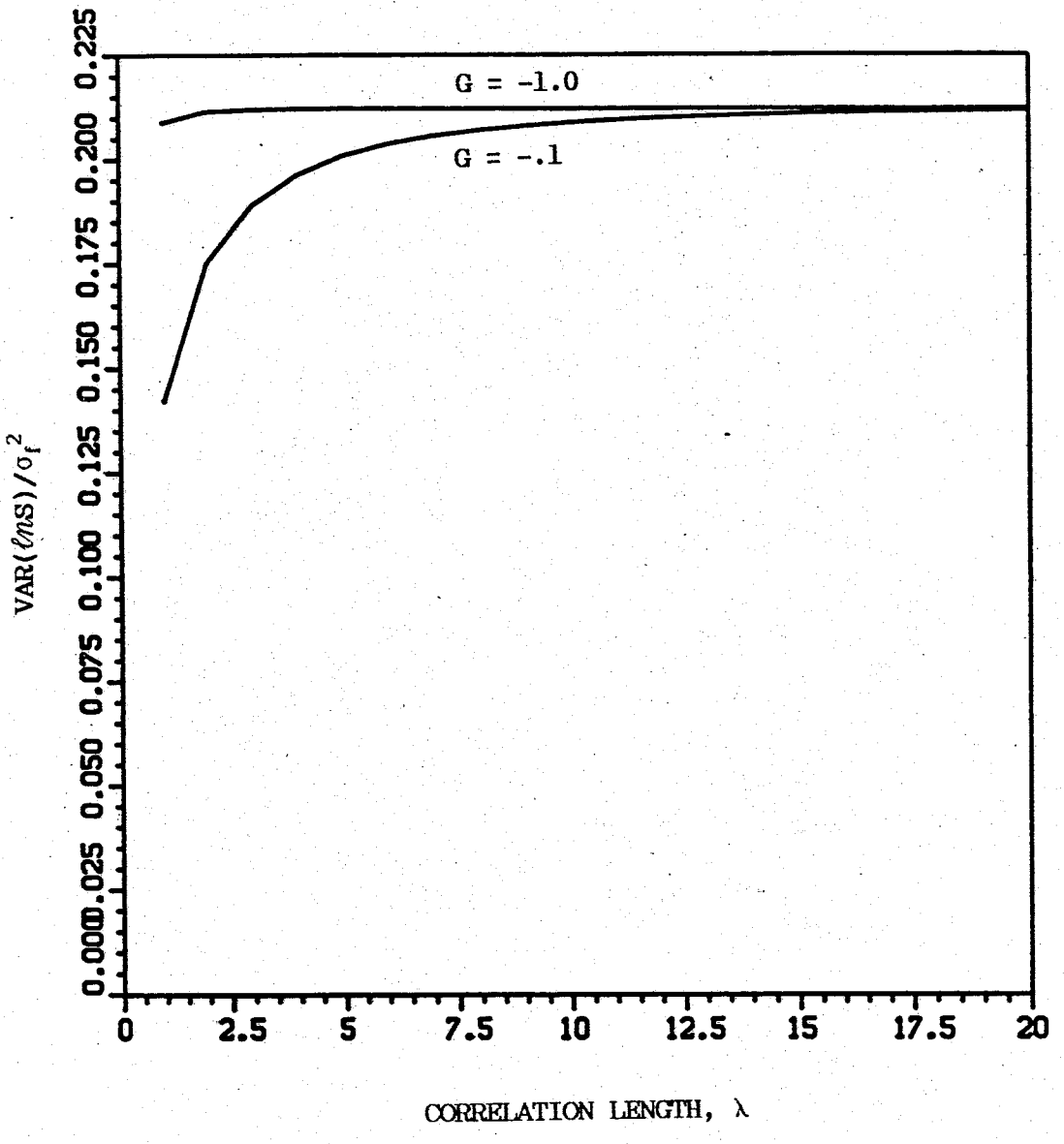

Figure 5.14. Variance of ℓnS vs Correlation Length, λ
3-D Isotropic Model: Normalized by σ_f^2, Independent of J
$A_w = 2.6$, $A_c = 2.6$, $G = E(\nabla \ell nS)$

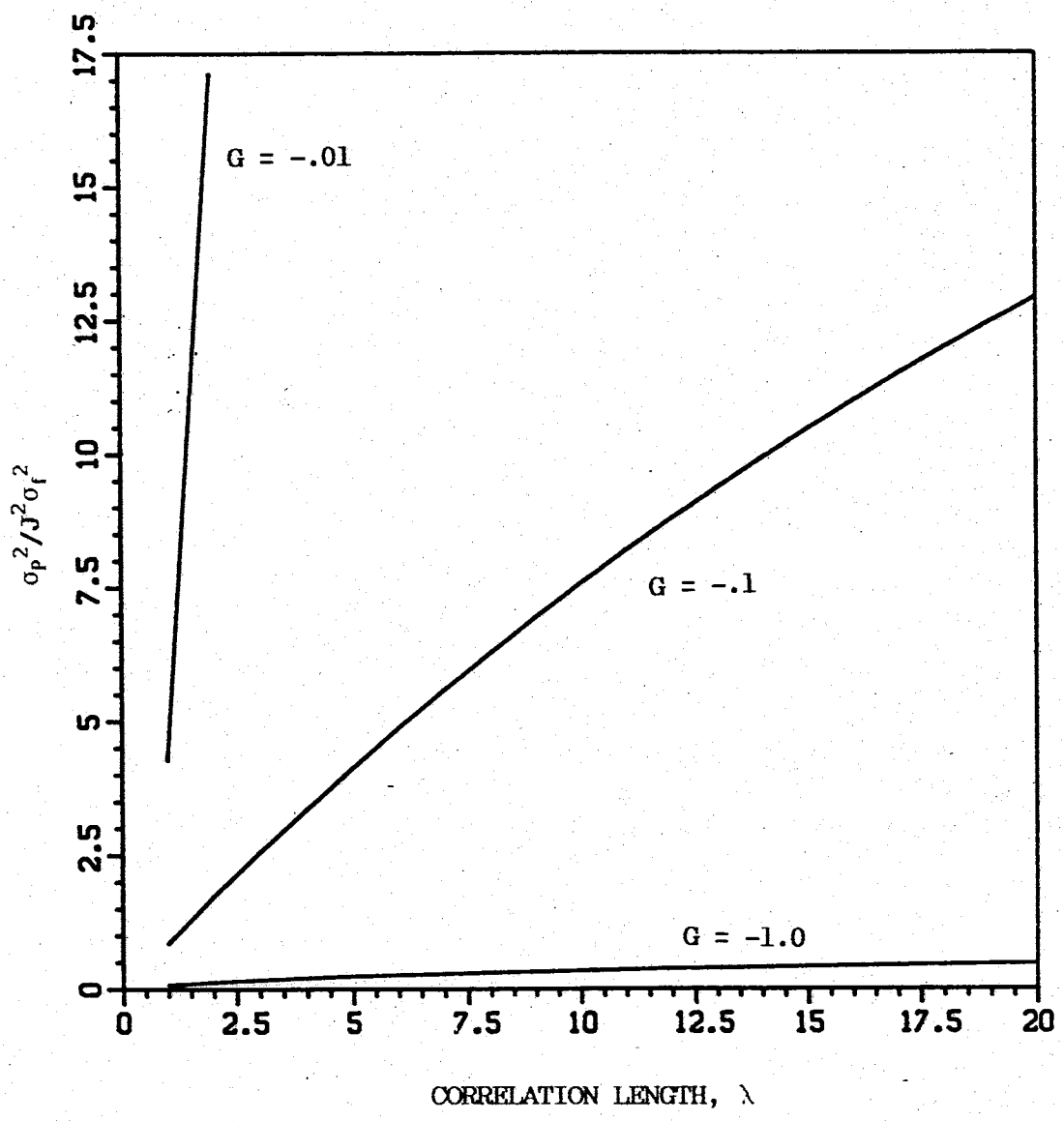

Figure 5.15. Variance of P vs Correlation Length, λ
3-D Isotropic Model: Normalized by $J^2\sigma_f^2$
$A_w = 3.0$, $A_c = 2.6$, $G = E(\nabla \ell n S)$

over short distances. Therefore, variance increases with increasing correlation length. Since there is no upper bound for pressure values, its variance also increases without bound.

The variance of log of saturation decreases almost linearly with an increase in the anisotropy ratio (Figure 5.16). The variance of pressure also decreases substantially with increasing anisotropy ratio (Figure 5.17). Basically, these curves reflect a transition from substantially three-dimensional flow to essentially two-dimensional, horizontal flow. In three-dimensional flow, these properties are likely to vary considerably as one moves transverse to the flow direction.

Effective Velocity of Water

Effective water velocity was found to increase slightly with increasing correlation length, as seen in Figure 5.18. Low correlation lengths imply that many small zones of varying permeabilities exist. Chances are that there would not be enough small high permeability zones interconnected to allow a significantly long flowpath to develop. At higher correlation lengths, these zones will generally be larger. Even a few such zones interconnected may be sufficiently long enough to allow significantly increased flow rates. A significant increase in flow velocities along certain pathways would result in some rise in effective velocity.

Effective velocity also exhibited a small increase with increasing saturation gradient (Figure 5.19). One possible explanation for this is that where saturation gradients are large, there is likely to be a full range of saturations ranging from predominantly oil-saturated to predominantly water-saturated. Furthermore, the predominantly water-

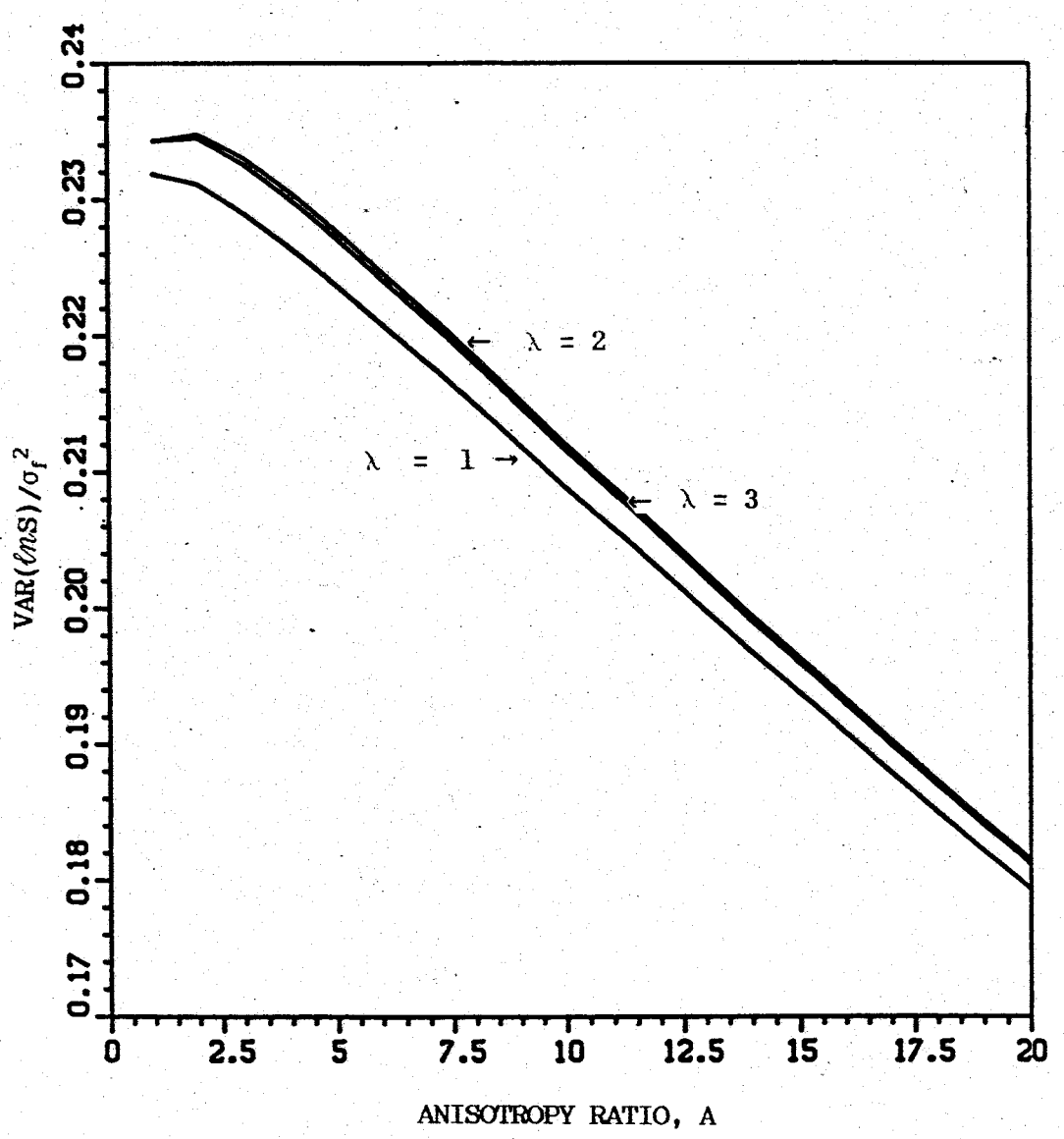

$A = \lambda_h/\lambda_v$
$\lambda_h = \lambda$ = horizontal correlation length
λ_v = vertical correlation length

Figure 5.16. Variance of ℓnS vs Anisotropy Ratio
3-D Model: Normalized by σ_f^2, Independent of J
$A_w = 3.0$, $A_c = 2.6$, $G = E(\nabla \ell nS) = -1.0$

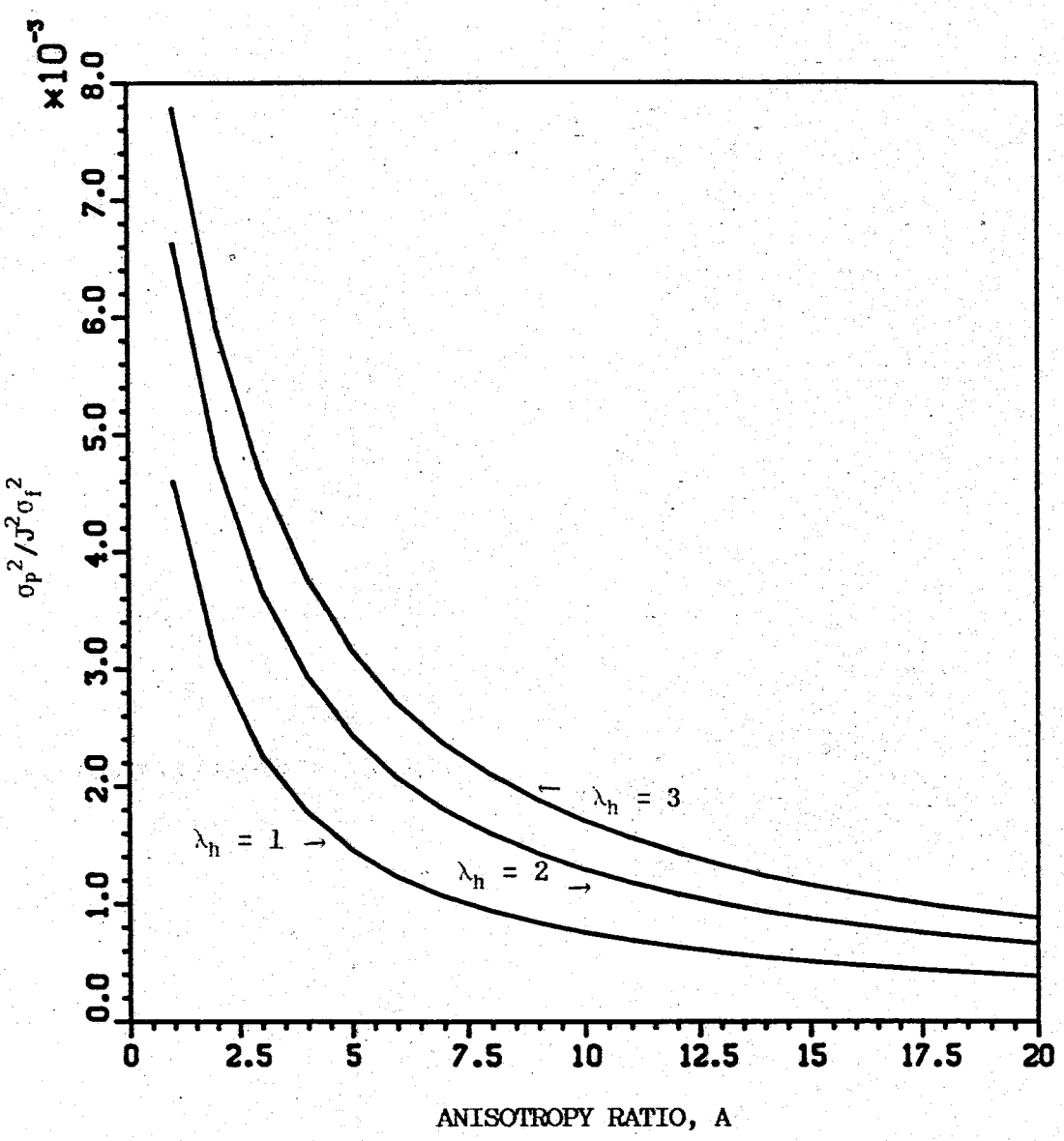

$A = \lambda_h/\lambda_v$
$\lambda_h = \lambda$ = horizontal correlation length
λ_v = vertical correlation length

Figure 5.17. Variance of P vs Anisotropy Ratio, A
3-D Model: Normalized by $J^2\sigma_f^2$
$A_w = 3.0$, $A_c = 2.6$, $G = E(\ell nS) = -1.0$

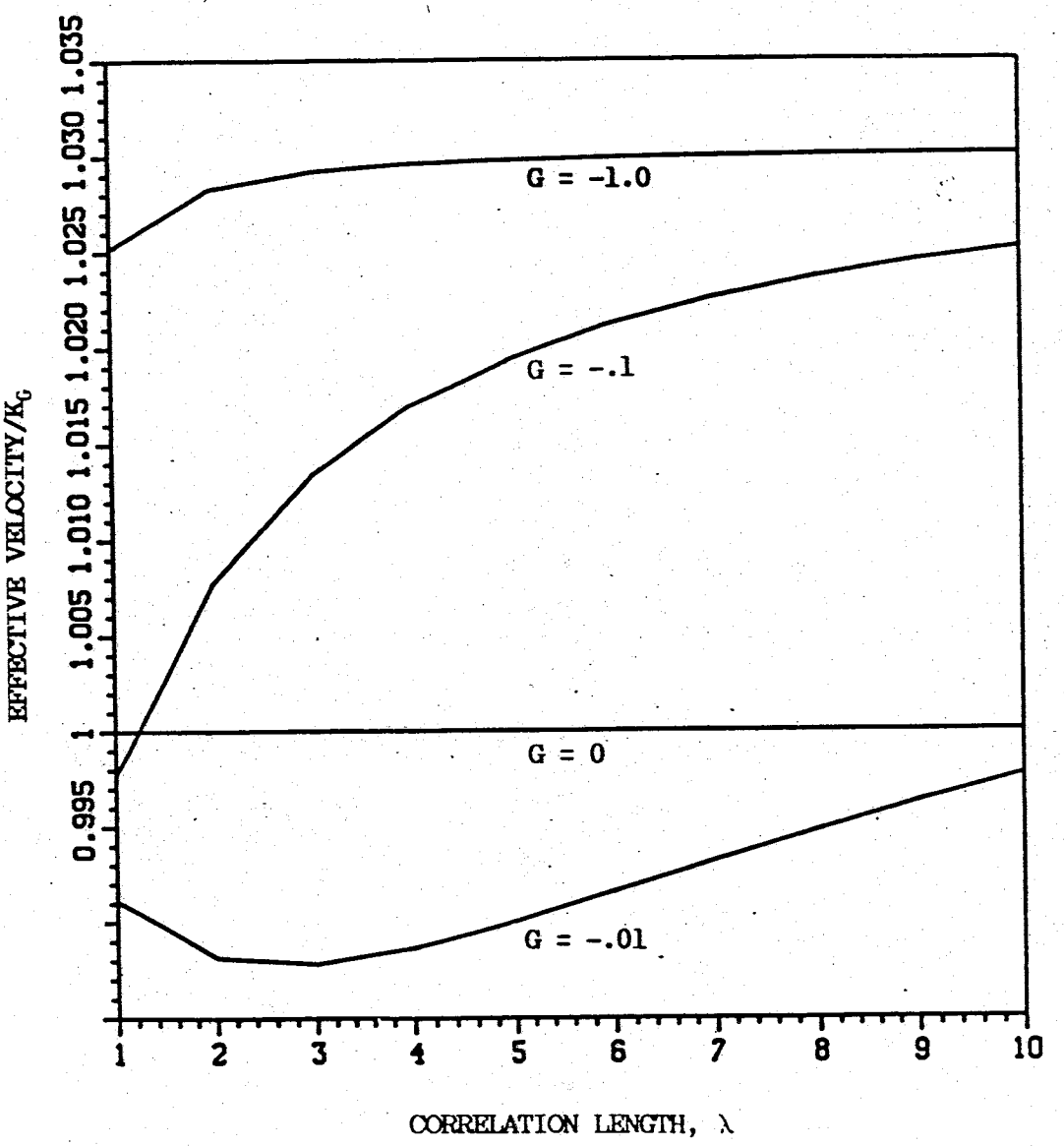

Figure 5.18. Effective Velocity vs Correlation Length, λ
2-D Model: Normalized by K_G
$A_w = 3.0$, $A_\zeta = 2.6$, $G = E(\nabla \ell n S)$

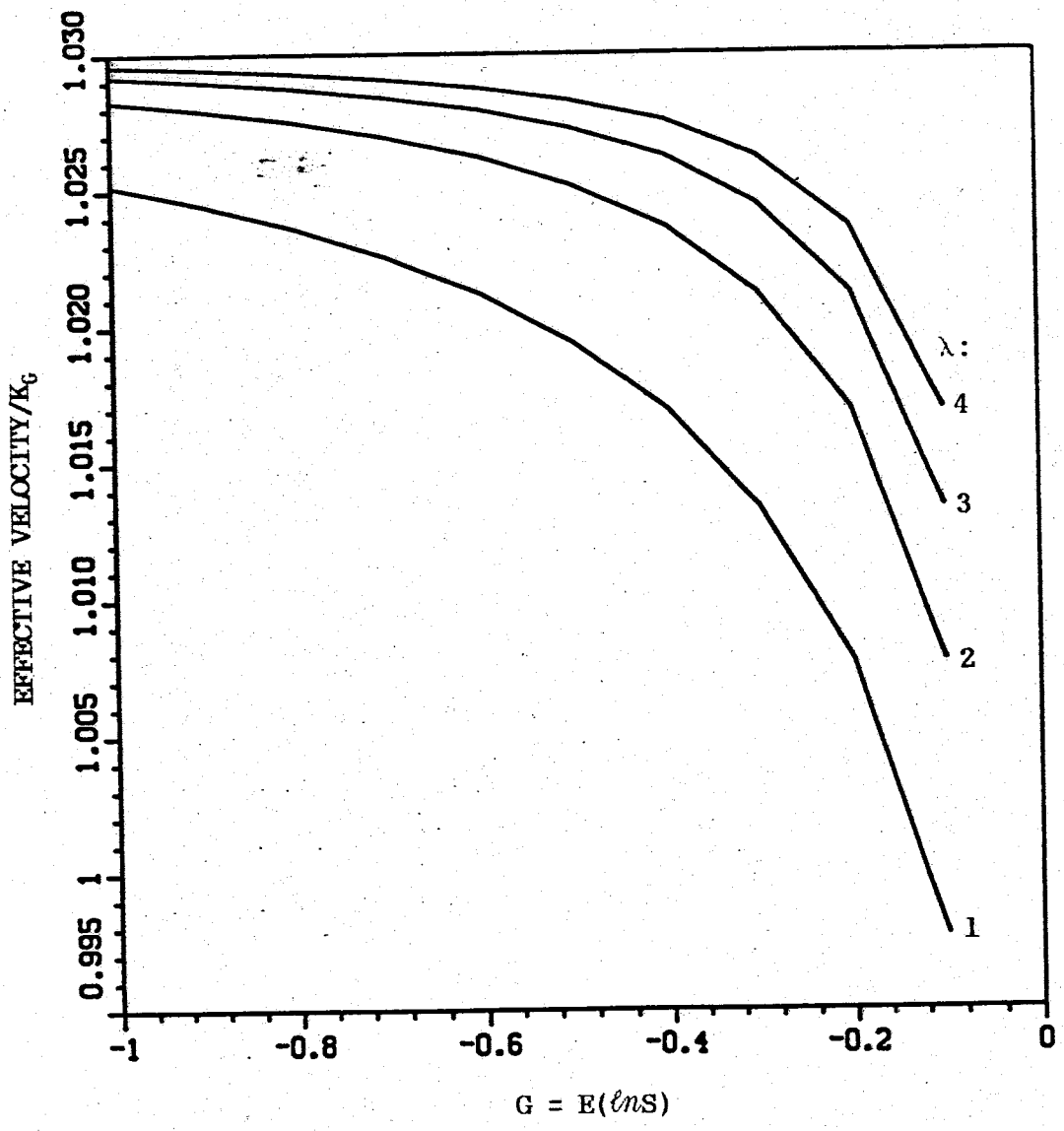

Figure 5.19. Effective Velocity vs G = E($\nabla \ell n$S)
2-D Model: Normalized by K_G
A_w = 3.0, A_C = 2.6, λ = Correlation Length

saturated zones are likely to occur in higher-permeability zones because in waterflooding of an oil reservoir, the higher-permeability pathways will be the main pathways where water will preferentially flow. Now, a medium with a high water saturation will have a higher effective water velocity at a given pressure gradient than will the same medium with lower water saturation (this is for a case such as in our model where the other fluid has higher viscosity). As mentioned earlier, this higher velocity along certain pathways will cause some rise in the overall effective velocity.

It is important to realize that, in general, oil and water effective velocities will differ, often greatly. With our assumption of an oil-water viscosity ratio of 30:1, water velocities will be greater than for oil for most values of saturation.

Effective Velocity of Oil

In this study, equations were not developed for effective oil velocity. The form of the approximating function for oil relative permeability was chosen for a good fit, but that form (Equation 2.12) would result in a very lengthy and cumbersome expression for effective oil velocity. Thus, it would be highly desirable to develop a different functional form for oil relative permeability. However, some general observations about effective oil velocity can be made.

In a medium with 50% water saturation and 50% oil saturation, each fluid behaves in some sense roughly as each fluid would in a similar porous medium, but with one-half the porosity. Thus, by Darcy's law, our much-higher-viscosity oil will have a substantially lower flow velocity than water. In fact, this oil velocity is so much lower that

it remains lower than for water over most of the saturation ranges expected to be encountered in real oil reservoirs. Therefore, effective water velocity is higher than effective oil velocity during virtually the entire time period of operation of a waterflooding process. The relative difference between these two effective velocities depends both on saturation and the oil-water viscosity ratio.

Strategies for Enhanced Recovery of Oil

An examination of the velocity equations (1.2) gives an insight into some strategies used in enhanced oil recovery methods. The goal, if waterflood oil recovery is being used, is to increase effective oil velocity relative to effective water velocity. The following are some strategies which have been employed in the search for more efficient oil recovery methods (Taber and Martin, 1983):

* Reduce oil viscosity to make the viscosity ratio μ_o/μ_w smaller, and thus make the velocity ratio, V_o/V_w, larger. This is done by addition of heat to oil, as in fireflooding or steam flooding.
* Increase water viscosity to make the velocity ratio, V_o/V_w, larger. This is accomplished by the addition of polymers to the injected water.
* Make water miscible with oil. This has as its goal the formation of a single fluid so that oil and water would flow together at the same velocities. Additives such as detergents and alcohol are used to achieve miscibility.
* Increase the permeability of a reservoir using fracturing methods. With larger passageways for fluids through fractures, the

viscosity difference between oil and water is relatively less important and effective velocities of oil and water are more nearly equal.

CONCLUSIONS

It is demonstrated that the spectral-perturbation method provides a useful tool for studying two-phase flow. The conclusions drawn from this model appear to correlate with findings using other methods. Thus, this method is submitted as being another valid and useful approach to two-phase flow modeling.

Variances for pressures and saturation are smaller for three dimensions than for two dimensions, this being in accord with the findings of previous researchers. In general, variance is reduced with each additional dimension. Variance of pressure is substantially reduced with an additional dimension, while the variance of saturation is also reduced, but to a much smaller extent. The degree of covariance anisotropy for pressure in the two-phase case can differ substantially from the single-phase saturated case.

The effect of the saturation gradient on the variances and covariance anisotropies of pressure and saturation is substantial. The pressure gradient only has a scaling effect on the variance and covariance values.

Because this work is an initial application of the spectral-perturbation method to two-phase flow, many simplifying assumptions have been made. There is much further research which should be done to make the model more nearly approximate real-world situations, as discussed in the next section.

The development of an expression for effective water velocity is an aid to judging the effectiveness of various enhanced oil recovery strategies. Subsequent development of an expression for effective oil velocity will further this effort.

In conclusion, the major contribution of this work is the introduction of a new technique, the spectral-perturbation method, to the modeling of two-phase flow. Further refinement of the conclusions resulting from application of the models can be expected after research which leads to eliminating or reducing some of the more restrictive assumptions made in this work.

RECOMMENDATIONS FOR FUTURE RESEARCH

The models developed in this work have made use of a number of simplifying assumptions. Many of these provide avenues for future research to develop models which reduce or eliminate the restrictiveness of some of the assumptions.

One major assumption was that capillary pressure was zero. However, capillary pressure is very important in many cases. It would be highly desirable to develop a model which takes capillary pressure into account. Also, the situations in which it is reasonable to neglect capillary pressure can be better determined. In a model which includes capillary pressure, one may also want to consider the possibility of a nonzero capillary pressure gradient.

The form of the approximating function for total mobility is worth investigating, particularly since the exponential form would be a very poor form for some viscosity ratios which may be encountered. For example, a constant plus an exponential expression would provide a better

fit than an exponential expression alone. Associated with this issue is the consideration of a different form for oil relative permeability. While the form used, Equation (2.12), provides a good fit, it results in a very long and cumbersome expression for the effective velocity of oil.

The inclusion of a gravity term should be considered for models in which vertical flow is expected to be significant. This includes the cases of three-dimensional flow, two-dimensional flow down an inclined plane, and two-dimensional flow in a vertical plane. Inclusion of a gravity term would facilitate comparison of modeling results to find ings made in vadose zone flow studies.

Another extension to this work could be the study of compressible flow. This would allow modeling of two-phase flow where gas was one of the fluids. Applications include modeling of gases in an oil reservoir and air in the vadose zone.

All of these ideas would involve changes in the governing equations, which would require re-deriving the perturbation and spectral relations. However, each of these improvements would allow the model to better represent real-world conditions. Related to the inclusion of these factors is a study under what circumstances it would be reasonable to neglect each of these considerations.

Another major extension would be transient modeling of two-phase flow. This would involve retaining the transient terms, including that in the boundary condition, in the solution of equation (3.32).

Yet another major area for future research is the extension of the spectral-perturbation method to other fluid flow modeling problems.

These could include three-phase flow and solute transport modeling, as well as other applications.

REFERENCES

Amyx, J. W., D. M. Bass, Jr., and R. L. Whiting, *Petroleum Reservoir Engineering*, McGraw-Hill, New York, 1960.

Bakr, A. A., L. W. Gelhar, A. L. Gutjahr, and J. R. MacMillan, Stochastic analysis of spatial variability in subsurface flows, 1, Comparison of one- and three-dimensional flows, *Water Resour. Res. 14(2)*, 262-271, 1978.

Bear, J., *Hydraulics of Groundwater*, McGraw-Hill, New York, 1979.

Collins, R. E., *Flow of Fluids Through Porous Materials*, Chapter 6, The Petroleum Publishing Company, Tulsa, Ok., 1976.

Craig, F., *The Reservoir Engineering Aspects of Waterflooding*, Society of Petroleum Engineers of AIME, New York, 1971.

Dagan, G., Statistical theory of Groundwater flow and transport: pore to laboratory, laboratory to formation, and formation to regional scale, *Water Resour. Res. 22(9)*, 120S-145S, 1986.

Dake, L. P., *Fundamentals of Reservoir Engineering*, Elsevier Scientific Publishing Co., Amsterdam, 1978.

Ewing, R. E., Problems arising in the modeling of processes for hydrocarbon recovery, in *The Mathematics of Reservoir Simulation*, edited by R. E. Ewing, Chapter 1, SIAM, Philadelphia, 1983.

Freeze, R. A. and J. A. Cherry, *Groundwater*, Prentice-Hall, Inc., Englewood Cliffs, NJ, 1979.

Gutjahr, A. L., L. W. Gelhar, A. A. Bakr, and J. R. MacMillan, Stochastic analysis of spatial variability in subsurface flows, 2, evaluation and application, *Water Resour. Res 14(5)*, 953-959, 1978.

Huyakorn, P. S. and G. F. Pinder, *Computational Methods in Subsurface Flow*, Academic Press, New York, 1983.

IMSL User's Manual, IMSL, Inc., Houston, Tx., 1984.

Lumley, J. L. and H. A. Panofsky, *The Structure of Atmospheric Turbulence*. Wiley-Interscience, New York, 1964.

Mizell, S. A., A. L. Gutjahr, and L. W. Gelhar, Stochastic analysis of spatial variability in two-dimensional steady groundwater flow assuming stationary and nonstationary heads, *Water Resour. Res. 18(4)*, 1053-1067, 1982.

Morel-Seytoux, H. J., Introduction of flow of immiscible liquids in porous media, in *Flow Through Porous Media* edited by R. M. DeWiest, Chapter 11, Academic Press, New York, 1969.

Prudnikov, A. P., Y. A. Brychkov and O. I. Marichev, *Integrals and Series: Vol. 1*, p. 798, Gordon & Breach, New York, New York, 1984.

Scheidegger, A. E., *The Physics of Flow Through Porous Media*. University of Toronto Press, Toronto, 1960.

Singh, S. P., Waterflood design (pattern, rate, timing), SPE Paper 10024, presented at International Petroleum Exhibition and Technical Symposium of the Society of Petroleum Engineers of AIME at Beijing, China, March 18-26, 1982.

Smith, P. J. and C. E. Brown, Stochastic modeling of two-phase flow in porous media in *Proceedings, 57th Annual Fall Technical Conference and Exhibition of the Society of Petroleum Engineers of AIME*, New Orleans, LA, Sept. 26-29, 1982.

Taber, J. J. and F. D. Martin, Technical screening guides for the enhanced recovery of oil, SPE Paper 12069, Society of Petroleum Engineers of AIME, Dallas, Texas, 1983.

Weaver, H., *Applications of Discrete and Continuous Fourier Analysis*, John Wiley & Sons, Inc., New York, 1983.

Welge, H. J., A simplified method for computing oil recovery by gas or water drive, *T. P. 3309, Petroleum Transactions AIME*, v. 195, 91-98, 1952.

Yeh, T.-C. J., L. W. Gelhar, and A. L. Gutjahr, Stochastic analysis of unsaturated flow in heterogeneous soils, 2, statistically anisotropic media with variable α, *Water Resour. Res. 21(4)*, 457-465, 1985.

A P P E N D I C E S

APPENDIX I

TWO-DIMENSIONAL COVARIANCE PROGRAM LISTING

```
OGRAM SDFFT3.FOR    "SPECTRAL DENSITY FAST FOURIER TRANSFORM CODE #3"
 INCORPORATE EXPONENTIALS TO ACCOUNT FOR OFFSET OF 0.5*DELU
 SET UP A SERIES OF SUMS TO FACILITATE FFT OF ISOTROPIC, AND ANISOTROPIC
   SPECTRAL DENSITIES
 SET UP TO COMPUTE COVARIANCES FROM SPECTRAL DENSITIES OF LOG OF
   SATURATION AND PRESSURE
 USING A NEW COMPLEX-VALUED FUNCTION FOR RATIO OF B2/B1
 USING AC AND AW VALUES DETERMINED FROM EXPONENTIAL REPRESENTATION
          OF RELATIVE PERMEABILITY CURVES
 INCLUDES SUBROUTINE WHICH CREATES CONTOUR PLOT FILES FOR COCARIANCES
 INCLUDES OPTION TO NORMALIZE COVARIANCE PLOTS (i.e., SET VAR = 1.0)
 HEADINGS WITH PARAMETER VALUES FOR CONTOUR PLOTS HAVE BEEN IMPLEMENTED
 INCLUDES OPTION TO AUTOMATICALLY PLOT SPECTRAL DENSITIES
 COMPLEX RATIO CALCULATION HAS BEEN CORRECTED AND SIMPLIFIED
==>> IMPLEMENT PRINTOUT OF LOCATION OF MAX VALUE ON SPECTRAL DENSITY
          PLOT AND MIN VALUE ON COVARIANCE PLOT
==>> TEST OUTPUT BY COMPARISON TO VARIANCE OF MIZELL'S S.D. "B"
          (COMPARISON CAN BE MADE IF AC = 0, OR G IS VERY SMALL)
-----------------------------------------------------------------------
   THIS CODE PERFORMS TWO FAST FOURIER TRANSFORMS ON TWO-DIMENSIONAL
PUT DATA.  SPECIFICALLY, IT TRANSFORMS SPECTRAL DENSITIES OF
(LN OF SATURATION, S), AND PRESSURE, P.  THIS RESULTS IN THE
VARIANCE FUNCTIONS OF THE GIVEN PROCESSES.
   RESULTS HAVE BEEN CHECKED BY:
) COMPARING SPECTRAL DENSITY EVALUATIONS WITH HAND CALCULATIONS OF SAME
) COMPARING NUMERICAL INTEGRATION WITH RCOV(0,0) TO CHECK VARIANCE CALC.

   VARIABLES USED:
LECT- FILENAME OF COVARIANCE OF "T" UNFORMATTED DATA
LECP- FILENAME OF COVARIANCE OF "P" UNFORMATTED DATA
LEST- FILENAME OF SPECTRAL DENSITY OF "T" UNFORMATTED DATA
LESP- FILENAME OF SPECTRAL DENSITY OF "P" UNFORMATTED DATA
IM -  PARAMETER INDICATING DIMENSIONED ARRAY SIZES
IZE - VARIABLE USED TO PASS VALUE "IDIM" TO SUBROUTINE
  -   THE ROW AND COLUMN DIMENSION OF THE DISCRETIZED SPECTRAL DENSITY
1  -  THE VALUE OF N MINUS 1
I1 -  ARRAY OF SPECTRAL DENSITY VALUES IN 1ST QUADRANT (M1, M2 BOTH +)
I2 -  ARRAY OF SPECTRAL DENSITY VALUES IN 2ND QUADRANT (+M1, -M2)
  -   A COMPLEX ARRAY SUITABLY DIMENSIONED FOR PASSING TO FFT3D SUBROUTINE
M1  - SIGN OF M1 INDEX
M2  - SIGN OF M2 INDEX
,M2 - INDICES REPRESENTING DISCRETIZED SPACING IN FREQUENCY DOMAIN
J1  - SIGN OF J1 INDEX
J2  - SIGN OF J2 INDEX
,J2 - INDICES REPRESENTING DISCRETIZED SPACING IN COVARIANCE FIELD
LU  - SPACING IN FREQUENCY DOMAIN
AX  - MAXIMUM VALUE OF U IN EITHER DIRECTION (I.E., EITHER U1 OR U2)
  -   VALUE OF FIRST  SPATIAL VARIABLE IN SPECTRAL DOMAIN
  -   VALUE OF SECOND SPATIAL VARIABLE IN SPECTRAL DOMAIN
LX -  SPACING IN COVARIANCE FIELD
```

```
[1 -  COMPLEX RESULTS OF FFT TRANSFORM OF 1ST QUAD OF S.D. ARRAY:
        CORRESPONDS TO SUM1 ON P.12 OF ALLAN'S NOTES OF 8/12/87
[3 -  COMPLEX RESULTS OF FFT TRANSFORM OF 4TH QUAD OF S.D. ARRAY:
        CORRESPONDS TO SUM3 ON P.12 OF ALLAN'S NOTES OF 8/12/87
)V -  REAL COVARIANCE VALUES RESULTING FROM TRANSFORM
:  -  VARIANCES OF T AND P
[AX - MAX VALUES IN SPECTRAL DENSITY FIELDS OF T AND P
[XU1- U1 VALUE AT MAX S.D. VALUE
[XU2- U2 VALUE AT MAX S.D. VALUE
:  -  SPECTRAL DENSITY RANGE FOR PLOTTING
)R -  INDEX RANGE CORRESPONDING TO SPECTRAL DENSITY RANGE FOR PLOTTING
'PLT- FLAG TO INDICATE COVARIANCE PLOT TO BE PREPARED
:IZE- DIMENSIONS OF COVARIANCE PLOT
:N -  MINIMUM VALUE ON COV P PLOT
:NX1- X1 COORDINATE VALUE CORRESPONDING TO MINIMUM VALUE ON COV P PLOT
:NX2- X2 COORDINATE VALUE CORRESPONDING TO MINIMUM VALUE ON COV P PLOT
.X -  VARIANCE OF P
:N -  MINIMUM VALUE ON COV T PLOT
:NX1- X1 COORDINATE VALUE CORRESPONDING TO MINIMUM VALUE ON COV T PLOT
:NX2- X2 COORDINATE VALUE CORRESPONDING TO MINIMUM VALUE ON COV T PLOT
.X -  VARIANCE OF T
  -   CHARACTER VARIABLE TO HOLD A DOLLAR SIGN
.D -  CHARACTER STRING TO HOLD TITLE OF PLOT
  -   NUMBER OF CHARACTERS IN STRING
 ..H4-CHARACTER STRINGS USED TO FORM HEADINGS
....LH4 - CHARACTER STRINGS (TYPE INTEGER) WHICH ARE THE HEADING LINES
    SUBROUTINES USED:
:P  - EVALUATES SPECTRAL DENSITIES OF LOG OF SATURATION AND PRESSURE
.OT - PREPARES COVARIANCE PLOTS FOR HP PLOTTER
-------------------------------------------------------------------------

 PARAMETER  IDIM = 128
 COMPLEX  AX(IDIM,IDIM), CEXPON, CWK(IDIM)
 COMPLEX  SUM1(0:IDIM-1,0:IDIM-1), SUM3(0:IDIM-1,0:IDIM-1)
 INTEGER  I, J, K, N, ISIZE
 INTEGER  IA1, IA2, N1, N2, N3, ISIGN, IWK(6*IDIM+150)
 INTEGER  NM1, ISJ1, ISJ2, J1, J2, ISM1, ISM2, M1, M2
 INTEGER  J1P1, J2P1, M1P1, M2P1
 INTEGER  LH1(20), LH2(20), LH3(20), LH4(20)
 REAL  RCOV(0:IDIM-1,0:IDIM-1), IMAG, RWK(6*IDIM+150), U1, U2
 REAL  PI, DELU, UMAX, TEMP, TOL, A, DELX, X1, X2, XI
 REAL  PHI1(0:IDIM-1,0:IDIM-1,2), PHI2(0:IDIM-1,0:IDIM-1,2)
 REAL  LAMBDA, G, JJJ, TMIN, TMAX, PMIN, PMAX
 REAL  AC, AW, SIGSQ, CPSIZE, VAR(2), SDMAX(2)
 REAL  SDMXU1(2), SDMXU2(2), TMINX1, TMINX2, PMINX1, PMINX2
 CHARACTER  FILEST*9, FILESP*9, FILECT*9, FILECP*9, COVQ*1, DS*1
 CHARACTER  COVPLT*1, NORMQ*1, H1*6, H2*6, H3*6, H4*6, HEAD*39
 CHARACTER  H5*10, H6*9, H7*8, H8*8, H9*12, H10*7, SDQ*1
```

```
FILEST = 'STUNF.DAT'
FILESP = 'SPUNF.DAT'
FILECT = 'CTUNF.DAT'
FILECP = 'CPUNF.DAT'
OPEN(UNIT=26,FILE='SUNT.DAT',STATUS='NEW',CARRIAGECONTROL='LIST')
OPEN(UNIT=27,FILE='SUNP.DAT',STATUS='NEW',CARRIAGECONTROL='LIST')
OPEN(UNIT=38,FILE='SDT.DAT',STATUS='NEW',CARRIAGECONTROL='LIST')
OPEN(UNIT=39,FILE='SDP.DAT',STATUS='NEW',CARRIAGECONTROL='LIST')
OPEN(UNIT=42,FILE=FILEST,FORM='UNFORMATTED',STATUS='NEW')
OPEN(UNIT=43,FILE=FILESP,FORM='UNFORMATTED',STATUS='NEW')
OPEN(UNIT=40,FILE=FILECT,FORM='UNFORMATTED',STATUS='NEW')
OPEN(UNIT=41,FILE=FILECP,FORM='UNFORMATTED',STATUS='NEW')

PI = 3.1415927
AW = 3.0
AC = 2.6
WRITE (5,*) ' AW SET AT ',AW,' AC = ',AC
SIGSQ = 1.0
TOL = 10.0 ** -10
ISIZE = IDIM
WRITE (5,*) ' ENTER DELU '
READ (5,*) DELU
WRITE (5,*) ' ENTER U MAX '
READ (5,*) UMAX
N = IFIX(UMAX/DELU)
NM1 = N - 1
A = DELU * FLOAT(N)

INPUT PARAMETER VALUES AND ANSWER QUESTIONS REGARDING OUTPUT ***

WRITE (5,*) ' ENTER G '
READ  (5,*) G
WRITE (5,*) 'ENTER J '
READ  (5,*) JJJ
WRITE (5,*) ' ENTER LAMBDA '
READ  (5,*) LAMBDA
WRITE (5,*) ' RANGE OF COV PLOT? <CR>=10x10; "N"=NO ==>DIFF.RANGE'
READ (5,'(A)') COVQ
IF (COVQ .EQ. 'n') COVQ = 'N'
IF (COVQ .EQ. 'N') THEN
  WRITE (5,*) ' ENTER RANGE DESIRED '
  READ (5,*) CPSIZE
ELSE
  CPSIZE = 10.0
ENDIF
WRITE (5,*) ' NORMALIZE COVARIANCE VALUES ? "Y"=YES; <CR>=NO '
IF (NORMQ .EQ. 'y') NORMQ = 'Y'
READ  (5,'(A)') NORMQ
IF (NORMQ .EQ. 'y') NORMQ = 'Y'
```

```
WRITE (5,*) ' WANT PLOTS OF SPECTRAL DENSITIES? "Y"=YES; <CR>=NO'
READ  (5,'(A)') SDQ
IF (SDQ .EQ. 'y') SDQ = 'Y'
IF (SDQ .NE. 'Y') SDQ = 'N'
IF (SDQ .EQ. 'Y') THEN

  WRITE (5,*) ' ENTER RANGE OF S.D. FIELD TO BE PLOTTED'
  SDR = 100.0 * DELU
  SDR = MIN(SDR,UMAX)
  WRITE (5,*) ' RANGE MUST BE <= TO ',SDR,' (IN TERMS OF U)'
  READ  (5,*) SDR
  ISDR = IFIX (SDR / DELU)

ENDIF

SET UP CHARACTER CONSTANTS TO FORM HEADING LINES FOR CONTOUR PLOTS

DS = '$'
H1 = ' Aw = '
H2 = ' Ac = '
H3 = '  J = '
H4 = '  G = '
NC = 45
ENCODE (NC,500,LH2) H1, AW, H2, AC, H3, JJJ, H4, G, DS
FORMAT(4(A6,F5.2),A)
H5 = ' LAMBDA = '
H6 = ' SIGSQ = '
H7 = ' DELU = '
H8 = ' UMAX = '
NC = 56
ENCODE (NC,510,LH3) H5, LAMBDA, H6, SIGSQ, H7, DELU, H8, UMAX, DS
FORMAT(A10,F5.2,A9,F4.1,A8,F6.4,A8,F5.2,A)
H10 = ' MIN = '

PRINT HEADINGS AND PARAMETER VALUES FOR NUMERICAL ARRAY OUTPUTS ***

WRITE (38,211)
FORMAT (10X,'LOG OF SATURATION (T) SPECTRAL DENSITY FIELD ',/)
WRITE (39,212)
FORMAT (//,10X,'PRESSURE (P) SPECTRAL DENSITY FIELD ',/)
WRITE (38,213) DELU, UMAX, N
WRITE (39,213) DELU, UMAX, N
FORMAT(5X,'DELU = ',F6.3,'   UMAX = ',F6.2,'   N = ',I3,/)
WRITE (38,214) G, JJJ, LAMBDA
FORMAT(5X,'G = ',F7.4,'   J = ',F7.4,'   LAMBDA = ',F6.2,/)
WRITE (38,216) AW, AC, SIGSQ
FORMAT(5X,'AW = ',F6.2,'   AC = ',F6.2,' SIGSQ = ',F6.2,/)
FORMAT (100F9.6)
```

```
* EVALUATE SPECTRAL DENSITY FUNCTION TO BE USED; PLACE IN ARRAY FOR FFT3D;
      PRINT OUT VALUES OF THIS ARRAY; COMPUTE PARAMETERS FOR FFT3D  ***

 ISM2 = 1
 CALL SDTP (PHI1,N,DELU,ISM2,ISIZE,G,JJJ,LAMBDA,AC,AW,SIGSQ)

 THIS NEEDED ONLY FOR CASES WHERE S(U1,U2) IS NOT EQUAL TO S(U1,-U2) +++
  ISM2 = -1
  CALL SDTP (PHI2,N,DELU,ISM2,ISIZE,G,JJJ,LAMBDA,AC,AW,SIGSQ)

 IA1 = IDIM
 IA2 = IDIM
 N1 = N
 N2 = N
 N3 = 1
 ISIGN = 1
 DO 5  K = 1, 2

   SDMAX(K) = 0.0
   DO 10  M2 = NM1, 0, -1

     M2P1 = M2 + 1
     DO 15  M1 = 0, NM1

       PHI1(M1,M2,K) = 4.0 * PI * PI * PHI1(M1,M2,K)
       IF (PHI1(M1,M2,K) .GT. SDMAX(K)) THEN

         SDMAX(K) = PHI1(M1,M2,K)
         SDMXU1(K) = (FLOAT(M1) + 0.5) * DELU
         SDMXU2(K) = (FLOAT(M2) + 0.5) * DELU

       ENDIF
       AX(M1+1,M2P1) = CMPLX(PHI1(M1,M2,K),0.0)

     CONTINUE
     IF (K .EQ. 1) THEN

       IF (M2 .LT. 11) WRITE (38,210) (PHI1(M1,M2,K),M1=0,11)

     ELSE IF(K .EQ. 2) THEN

       IF (M2 .LT. 11) WRITE (39,210) (PHI1(M1,M2,K),M1=0,11)

     ENDIF

   CONTINUE
```

```
 CREATE PLOT FILES FOR SPECTRAL DENSITY CONTOUR PLOTS ***

   IF (SDQ .EQ. 'N') GO TO 410
   DO 399  M2 = 0, ISDR

     IF (K .EQ .1) WRITE (42) (PHI1(M1,M2,1),M1=0,ISDR)
     IF (K .EQ. 2) WRITE (43) (PHI1(M1,M2,2),M1=0,ISDR)

   CONTINUE
   FORMAT (4X,12F6.3,/)

* TAKE FFT OF "A" FIELD AND PLACE RESULTS BACK INTO SUM1 ARRAY ***

   CALL FFT3D(AX,IA1,IA2,N1,N2,N3,ISIGN,IWK,RWK,CWK)
   DO 22  J1 = 0, NM1

     J1P1 = J1 + 1
     DO 23  J2 = 0, NM1

       SUM1(J1,J2) = AX(J1P1,J2+1)

     CONTINUE

   CONTINUE

+ THIS NEEDED ONLY IF S(U1,U2) IS NOT EQUAL TO S(U1,-U2) ++++
* NOW COMPUTE S.D. ARRAY FOR 4TH QUADRANT; PLACE IN AX ARRAY FOR FFT3D;
     CALL FFT3D TO TRANSFORM S.D.;    *****
    DO 28  M1 = 0, NM1
     M1P1 = M1 + 1
     DO 29  M2 = 0, NM1
       PHI2(M1,M2,K) = 4.0 * PI * PI * PHI2(M1,M2,K)
       AX(M1P1,M2+1) = CMPLX(PHI2(M1,M2,K),0.0)
     CONTINUE
    CONTINUE
    CALL FFT3D(AX,IA1,IA2,N1,N2,N3,ISIGN,IWK,RWK,CWK)
```

```
*  PLACE TRANSFORMED ARRAY INTO SUM3 -- REARRANGING TO FORM CORRECT SUM ***

      DO 30  J1 = 0, NM1

        J1P1 = J1 + 1
        DO 31  J2 = 0, NM1

          IF (J2 .EQ. 0) THEN
            SUM3(J1,0) = AX(J1P1,1)
          ELSE
            SUM3(J1,J2) = AX(J1P1,N-J2+1)
          ENDIF

        CONTINUE

      CONTINUE

*     MULTIPLY EACH SUM TIMES THE APPROPRIATE IMAGINARY EXPONENTIAL FACTOR;
          ADD THE TWO SUMS; MULTIPLY BY APPROPRIATE CONSTANTS; OUTPUT RESULTS

      DELX = 1.0 / A
      IF (K .EQ. 1) WRITE (38,221)
      FORMAT (/,10X,'COVARIANCE FIELD FOR LOG OF SATURATION (T)',/)
      IF (K .EQ. 2) WRITE (39,222)
      FORMAT (/,10X,'COVARIANCE FIELD FOR PRESSURE (P)',/)
      IF (K .EQ. 1) WRITE (38,223) DELX
      IF (K .EQ. 2) WRITE (39,223) DELX
      FORMAT('    DELX  =  ',F7.4,/)

    COMPUTE PARAMETERS FOR CONTOUR PLOTTING ***

      IF (K .EQ. 1) THEN

        TMIN = 0.0
        TMAX = 0.0
        PMIN = 0.0
        PMAX = 0.0

      ENDIF
      MAXJ = IFIX(CPSIZE/DELX)
      DELR = DELU * 2.0 * PI
      IF (MAXJ .GT. NM1) MAXJ = NM1
      IF (K .EQ. 1) WRITE(5,*) ' PLOT N = ',MAXJ+1
      DO 33 J2 = NM1, 0, -1

        DO 35  J1 = 0, NM1
```

```
TIPLY TERMS BY IMAGINARY EXPONENTIAL FACTOR REFLECTING OFFSET FROM AXES

      JJ = J1 + J2
      IMAG = FLOAT(ISIGN) * PI * FLOAT(JJ) / FLOAT(N)
      SUM1(J1,J2) = CEXP(CMPLX(0.0,IMAG)) * SUM1(J1,J2)
      JJ = J1 - J2
      IMAG = FLOAT(ISIGN) * PI * FLOAT(JJ) / FLOAT(N)
      SUM3(J1,J2) = CEXP(CMPLX(0.0,IMAG)) * SUM3(J1,J2)
      RCOV(J1,J2) = 2.0 * (SUM1(J1,J2) + SUM3(J1,J2))*DELU*DELU
      TMAX = RCOV(0,0)
      PMAX = RCOV(0,0)
      IF ((J1 .LE. MAXJ) .AND. (J2 .LE. MAXJ)) THEN

        IF ((K .EQ. 1) .AND. (RCOV(J1,J2) .LT. TMIN)) THEN

          TMIN = RCOV(J1,J2)
          TMINX1 = FLOAT(J1) * DELX
          TMINX2 = FLOAT(J2) * DELX

        ELSE IF ((K .EQ. 2) .AND. (RCOV(J1,J2) .LT. PMIN)) THEN

          PMIN = RCOV(J1,J2)
          PMINX1 = FLOAT(J1) * DELX
          PMINX2 = FLOAT(J2) * DELX

        ENDIF

      ENDIF

    CONTINUE
    IF (K .EQ. 1) THEN

      IF (J2 .LE. 11) WRITE (38,210) (RCOV(J1,J2),J1=0,11)

    ELSE IF(K .EQ. 2) THEN

      IF (J2 .LE. 11) WRITE (39,210) (RCOV(J1,J2),J1=0,11)

    ENDIF

  CONTINUE

* WRITE OUT UNFORMATTED COVARIANCE DATA FOR CONTOUR PLOTTING ***
* WRITE OUT DATA FOR SHADE PLOTTING ON SUN COMPUTERS ***

  IF (K. EQ. 1) WRITE (26,240) TMIN, TMAX
  IF (K .EQ. 2) WRITE (27,240) PMIN, PMAX
  VAR(K) = RCOV(0,0)
```

```
  DO 40  J2 = 0, NM1

    DO 45  J1 = 0, NM1

      IF (K .EQ. 1) WRITE (26,260) RCOV(J1,J2)
      IF (K .EQ. 2) WRITE (27,260) RCOV(J1,J2)

    CONTINUE
    IF (NORMQ .EQ. 'Y') THEN
      DO 47  J1 = 0, MAXJ
        RCOV(J1,J2) = RCOV(J1,J2) / VAR(K)
      CONTINUE
    ENDIF
    IF ((K.EQ.1).AND.(J2.LE.MAXJ))WRITE(40)(RCOV(J1,J2),J1=0,MAXJ)
    IF ((K.EQ.2).AND.(J2.LE.MAXJ))WRITE(41)(RCOV(J1,J2),J1=0,MAXJ)

  CONTINUE

CONTINUE
WRITE(5,*) ' G = ',G,' VAR T = ',VAR(1),' VAR P = ',VAR(2)
FORMAT(2F9.6)
FORMAT(1X,F9.6)
VARB = (8.0/(3.0*PI))**2 * JJJ*JJJ * SIGSQ * LAMBDA*LAMBDA
WRITE(5,*) ' VARIANCE OF MIZELL"S FIELD "B" = ',VARB

CLOSE (UNIT = 26)
CLOSE (UNIT = 27)
CLOSE (UNIT = 38)
CLOSE (UNIT = 39)
CLOSE (UNIT = 40)
CLOSE (UNIT = 41)
CLOSE (UNIT = 42)
CLOSE (UNIT = 43)

CREATE HEADINGS; PLOT SPECTRAL DENSITY FIELDS ***

IF (SDQ .EQ. 'Y') THEN

  HEAD = ' CONTOURS OF THE SPECTRAL DENSITY OF Y '
  NC = 40
  ENCODE (NC,540,LH1) HEAD, DS
  H9 = ' S.D. MAX = '
  NC = 39
  ENCODE (NC,520,LH4) H9, SDMAX(1), SDMXU1(1), SDMXU2(1), DS
  COVPLT = 'S'
  CALL CPLOT (FILEST,COVPLT,ISDR+1,SDR,LH1,LH2,LH3,LH4)
```

```
  HEAD = ' CONTOURS OF THE SPECTRAL DENSITY OF P '
  NC = 40
  ENCODE (NC,540,LH1) HEAD, DS
  NC = 39
  ENCODE (NC,520,LH4) H9, SDMAX(2), SDMXU2(1), SDMXU2(2), DS
  COVPLT = 'R'
  CALL CPLOT (FILESP,COVPLT,ISDR+1,SDR,LH1,LH2,LH3,LH4)

ENDIF
FORMAT(A12,F8.4,' @ (',F6.4,',',F6.4,')',A)

CREATE HEADINGS; PLOT COVARIANCE FIELDS ***

MAXJ = MAXJ + 1
COVPLT = 'T'
NC = 40
HEAD = ' CONTOURS OF COVARIANCE FUNCTION OF  Y '
IF(NORMQ .EQ. 'Y')HEAD ='CONTOURS OF CORRELATION FUNCTION OF  Y '
ENCODE (NC,540,LH1) HEAD, DS
H9 = ' VAR OF Y = '
NC = 54
ENCODE (NC,550,LH4) H9, VAR(1), H10, TMIN, TMINX1, TMINX2, DS
CALL CPLOT (FILECT,COVPLT,MAXJ,CPSIZE,LH1,LH2,LH3,LH4)
IF (NORMQ .EQ. 'Y') WRITE (5,295) COVPLT, VAR(1)
FORMAT(5X,' VAR OF ',A,' = ',F10.7)
COVPLT = 'P'
HEAD = ' CONTOURS OF COVARIANCE FUNCTION OF  P '
IF(NORMQ .EQ. 'Y')HEAD ='CONTOURS OF CORRELATION FUNCTION OF  P '
NC = 40
ENCODE (NC,540,LH1) HEAD, DS
H9 = ' VAR OF P = '
NC = 54
ENCODE (NC,550,LH4) H9, VAR(2), H10, PMIN, PMINX1, PMINX2, DS
FORMAT(A39,A)
FORMAT(A12,F8.5,A7,F8.5,' @ (',F6.3,',',F6.3,')'A)
CALL CPLOT (FILECP,COVPLT,MAXJ,CPSIZE,LH1,LH2,LH3,LH4)
IF (NORMQ .EQ. 'Y') WRITE (5,295) COVPLT, VAR(2)
IF (SDQ .EQ. 'Y') WRITE (5,*) 'S.D. PLOT FILES: CSDT.POP;CSDP.POP'

STOP ' PROGRAM SDFFT3 FIN"D: TO PLOT: "PLOTA CCOVT.POP; CCOVP.POP'
END
```

```
SUBROUTINE SDTP(SDTPAR,N,DELU,ISR2,IDIM,G,J,LAMBDA,AC,AW,SIGSQ)
-----------------------------------------------------------------
  THIS SUBROUTINE EVALUATES THE SPECTRAL DENSITIES OF LOG OF
TURATION (T) AND PRESSURE (P).
-----------------------------------------------------------------

COMPLEX  CFACT, I, RATIO, VRATB, DZP
REAL  SFF, SPP, STT, H1, H, J, PI, TOL2, RDEN
REAL  READIN, R, R1, R2, SIGSQ, LAMBDA, RATSD, INTEGR
REAL  AC, AW, G, TOL, STPI2, SBF, SBFV, PORS, FACTSQ
REAL  DELU, INTT, INTP, VARP, VART, SDTPAR(0:IDIM-1,0:IDIM-1,2)
REAL  MUW, TBAR, F, CW, SDOFT, PINT, HDELR
INTEGER  II, III, JJ, K, N, ISR2, NM1

TOL = 1.0 / 10000.0
I = CMPLX (0.0, 1.0)
PI = 3.141592654

VALUES FOR USE IN TIME-VARYING CALCULATIONS ***
 MUW = 1.0; TBAR = -.693; CW = -.22; PORS = .3; F = 4.605
 H = MUW * PORS * EXP(-(F + CW + (AW - 1) * TBAR))

** LOOPS TO VARY R1, R1: CALCULATE SPACE-DEPENDENT-ONLY TERMS ******

ALPHA = 3.0 * PI / (16.0 * LAMBDA)
NM1 = N - 1
WRITE (5,*) ' NM1 = ',NM1
RDEN = AW * G * (AW - 1.0)
DO 10 II = 0, NM1

  R1 = (FLOAT(II) + 0.5) * DELU * 2.0 * PI
  DO 20 JJ = 0, NM1

    R2 = FLOAT(ISR2) * (FLOAT(JJ) + 0.5) * DELU * 2.0 * PI

COMPUTE THE VALUE OF SPECTRAL DENSITY "B" ***

    SFF = SB (ALPHA, R1, R2, SIGSQ)
    RSQ = R1 * R1  +  R2 * R2
```

```
COMPUTE THE VALUE OF THE SPECTRAL DENSITY OF LOG OF SATURATION (T) ***

    IF (RSQ .GT. TOL) THEN

      VRATB = RATIO (AC,AW,G,RSQ,R1,RDEN)
      RATV = REAL(VRATB * CONJG(VRATB))
      SDTPAR(II,JJ,1) = SFF * RATV
      CFACT = I * R1 * J / (RSQ  -  AC * G * R1 * I)

    ELSE

      SDTPAR(II,JJ,1) = 0.0
      VRATB = CMPLX(0.0,0.0)
      CFACT = CMPLX (0.0, 0.0)

    ENDIF

COMPUTE THE VALUE OF THE SPECTRAL DENSITY OF PRESSURE (P) ***

    FACTSQ = REAL(CFACT * CONJG(CFACT))
    CFACT = CMPLX(1.0,0.0) + AC * VRATB
    FACTSQ = FACTSQ * REAL(CFACT * CONJG(CFACT))
    SDTPAR(II,JJ,2) = FACTSQ * SFF

  CONTINUE

CONTINUE

RETURN
END
```

```
REAL FUNCTION SB (ALPHA, K1, K2, SIGSQ)
C-----------------------------------------------------------------------
C  THIS FUNCTION COMPUTES THE SPECTRAL DENSITY B IN MIZELL'S PAPER
C(R 18 (4), pp. 1053-2067) FORMULA 13.
C-----------------------------------------------------------------------

      REAL ALPHA, K1, K2, SIGSQ
      PI = 3.141592654

      SB = 3.0 * ALPHA * ALPHA * SIGSQ * (K1 * K1  +  K2 * K2) ** 2
      SB = SB / (PI * (K1 * K1  +  K2 * K2  +  ALPHA * ALPHA) ** 4)

      RETURN
      END


      COMPLEX FUNCTION RATIO(AC, AW, G, RSQ, R1, RDEN)
C-----------------------------------------------------------------------
C  THIS FUNCTION CALCULATES THE RATIO OF B2(R) OVER B1(R),
C-----------------------------------------------------------------------

      REAL  AC, AW, G, R1, RSQ, RDEN
      COMPLEX  I, RTNEW, B3, DEN

      I = CMPLX(0.0,1.0)
      B3 = CMPLX(RSQ,-AW*G*R1) / CMPLX(RSQ,-AC*G*R1)
      RTNEW = CMPLX(AW*G,R1) - R1 * B3 * I
      DEN = I*R1*(AW - AC*B3) + CMPLX(RDEN,0.0)
      RATIO = -RTNEW / DEN

      RETURN
      END
```

```
SUBROUTINE CPLOT(FILE,COVPLT,NX,PLTSIZ,LH1,LH2,LH3,LH4)
-----------------------------------------------------------------------
SUBROUTINE TO PREPARE DATA FOR PLOTTING ON HP PLOTTER
-----------------------------------------------------------------------
  REAL  P(10000), PLTSIZ, XMAX, YMAX, INC, TEMP, RANGE
  CHARACTER  FILE*9,ANS*3, COVPLT*1, COVFIL*10
  INTEGER  NX, NY, IINC, I, J, LH1(20), LH2(20), LH3(20), LH4(20)
  COMMON  WORK(50000)
  COMMON     /CNTURP/ ZMIN,ZINC,NLBC

  OPEN(UNIT=97,FILE=FILE,FORM='UNFORMATTED',STATUS='OLD')
  OPEN(UNIT=99,NAME='DISPLAY.MSG',STATUS='NEW')

  CALL COMPRS
  CALL SETDEV(99,99)
  CALL NOBRDR
  CALL SETCPR(2,0,0,0)
  IF (COVPLT .EQ. 'T') THEN
    COVFIL = 'CCOVT.POP'
  ELSE IF (COVPLT .EQ. 'P') THEN
    COVFIL = 'CCOVP.POP'
  ELSE IF (COVPLT .EQ. 'S') THEN
    COVFIL = 'CSDT.POP'
  ELSE IF (COVPLT .EQ. 'R') THEN
    COVFIL = 'CSDP.POP'
  ENDIF
  OPEN(UNIT=2,NAME=COVFIL,STATUS='NEW',FORM='UNFORMATTED')
  WRITE (5,*) ' OUTPUT DISK PLOT FILE: ',COVFIL
  NY = NX
  CALL PAGE(8.5,11.)
CALL INTAXS
IXTIX = 10
IYTIX = 10
CALL XTICKS(IXTIX)
CALL YTICKS(IYTIX)
IF ((COVPLT .EQ. 'S') .OR. (COVPLT .EQ. 'R')) THEN
  CALL XNAME(' U  --------> $',100)
  CALL YNAME(' U  --------> $',100)
ELSE IF ((COVPLT .EQ. 'T') .OR. (COVPLT .EQ. 'P')) THEN
  call xname('                X  ------> $',100)
  call yname('                X  ------> $',100)
ENDIF
  CALL AREA2D(5.5,5.5)
  CALL COMPLX
XMAX = PLTSIZ
YMAX = PLTSIZ
  CALL GRAF(0.,XMAX,XMAX, 0.,YMAX,YMAX)
  CALL GRACE(0.0)
```

```
CALL HEADIN(LH1,100,-1.25,4)
CALL HEADIN(LH2,100,1.0,4)
CALL HEADIN(LH3,100,1.0,4)
CALL HEADIN(LH4,100,1.0,4)
  CALL THKFRM(0.015)
  CALL FRAME

  DO 10  IX = 1, NX

          ibeg=(ix-1)*NX+1
          iend=ibeg+NX-1
          read(97)(p(iy),iy=ibeg,iend)

  CONTINUE
  NXNY = NX * NY
  PMIN = P(1)
  PMAX = P(1)
  SUM = 0.0
  DO 20  I = 1, NXNY

    PMIN = MIN(PMIN,P(I))
    PMAX = MAX(PMAX,P(I))
    SUM = SUM + P(I)

  CONTINUE
  AVE = SUM / NXNY
  WRITE(5,290) COVPLT, PMAX
  FORMAT(5X,A1,'MAX = ',F8.4)
  WRITE(5,291) COVPLT, PMIN
  FORMAT(5X,A1,'MIN = ',F8.4)
  write(5,*)'ave=',ave
  RANGE = PMAX - PMIN
  IF (RANGE .LT. .001) WRITE(5,*)' ***** WARNING: RANGE < .001 **'
  IF (RANGE .GT. 10.0) WRITE(5,*)' ***** WARNING: RANGE > 10 ****'
  INC = RANGE / 20.0
  J = 0
  TEMP = INC
  IF (TEMP .LE. 2.0) THEN

    DO 30  I = 1, 10

      TEMP = TEMP * 10.0
      J = J + 1
      IF (TEMP .GT. 2.0) GO TO 400

    CONTINUE

  ENDIF
```

```
IINC = IFIX(TEMP)
IF (IINC .GT. 5) IINC = IINC - MOD(IINC,5)
IF (IINC .EQ. 3) IINC = 2
IF (IINC .EQ. 4) IINC = 5
INC = FLOAT(IINC) / (10.0 ** J)
IF (PMIN .LT. 0.0) ISIGN = -1
IF (PMIN .GE. 0.0) ISIGN = 1
ZMIN = 0.0
DO 40  I = 1, 40

  IF ((ZMIN .GE. PMIN).AND.(ABS(ZMIN-PMIN) .LT. INC)) GO TO 410
  ZMIN = ZMIN + FLOAT(ISIGN) * INC

CONTINUE
ZINC = INC
nlbc=0
WRITE (5,*) ' ZMIN = ',ZMIN,' INC = ',INC

CALL HEIGHT(.06)
CALL CONMIN(1.5)
CALL CONANG(90.)
CALL CONTHN(0.0)
CALL BCOMON(50000)

CALL ZBASE(ZMIN)
CALL CONMAK(P,NX,NY,ZINC)
CALL CONLIN(0,'SOLID','LABELS',1,10)
DO 50 I=1,NLBC
CALL CONLIN(I,'DASH','NOLABELS',1,9)
NCON = NLBC + 1
CALL CONTUR(NCON,'LABELS','DRAW')
CALL ENDPL(0)
CALL DONEPL
CLOSE(UNIT=1)
CLOSE(UNIT=2)

RETURN
END
```

APPENDIX II

THREE-DIMENSIONAL VARIANCE PROGRAM LISTING

```
)GRAM INT3D.FOR  "NUMERICAL INTEGRATION OF 3-D SPECTRAL DENSITY OF T"
------------------------------------------------------------------------
   THIS PROGRAM PERFORMS A NUMERICAL INTEGRATION OF THE SPECTRAL DENSITY
 T IN THREE DIMENSIONS.  THE VALUE OF THIS INTEGRAL REPRESENTS THE
E VARIANCE OF T IN THREE DIMENSIONS.  THIS SPECTRAL DENSITY IS FOR
E CASE WHERE CORRELATION LENGTHS IN THE TWO HORIZONTAL DIRECTIONS ARE
JAL, WHILE THE CORRELATION LENGTH IN THE VERTICAL DIRECTION IS
NSIDERABLY SHORTER.  GRAVITY IS NEGLECTED.
   SINCE THE NUMBER OF VARIABLES CAN BE REDUCED TO TWO BY TRANSFORMING
 CYLINDRICAL COORDINATES AND INTEGRATING WITH RESPECT TO THETA, THIS
S BEEN DONE.  IN PARTICULAR, THE CHANGE OF COORDINATES IS PERFORMED
TH THE Z AXIS CORRESPONDING TO THE R1 AXIS, AND THE THETA = 0 AXIS
RRESPONDING TO THE R2 AXIS.
   VARIABLES USED:
LRHO - INCREMENTS OF RADIAL DISTANCE (i.e., THE VARIABLE RHO)
LZ   - INCREMENTS IN THE Z DIRECTION
HO   -  NUMBER OF INCREMENTS OF RHO TAKEN
   -    NUMBER OF INCREMENTS OF Z TAKEN
J,K  - LOOP INDICES
   -    EXPONENT IN FUNCTION REPRESENTING MOBILITY
   -    EXPONENT IN FUNCTION REPRESENTING RELATIVE PERMEABILITY OF WATER.
   -    SATURATION GRADIENT
GMSQ - VARIANCE OF 3-D SPECTRAL DENSITY FUNCTION USED.
MB1 -  CORRELATION LENGTH IN R1 DIRECTION
MB2 -  CORRELATION LENGTH IN R2 DIRECTION
MB3 -  CORRELATION LENGTH IN R3 DIRECTION
O  -   RADIAL DISTANCE VARIABLE (FROM Z-AXIS = R1-AXIS)
  -    Z-AXIS DISTANCE VARIABLE (CORRESPONDS TO R1 AXIS)
FV  -  VALUE OF 3-D SPECTRAL DENSITY FN USED
TSDV - VALUE OF RATIO OF B2(R)/B1(R) AFTER ABSOLUTE VALUE TAKEN & SQUARED
XVR -  MAX VALUE OF SPECTRAL DENSITY AT MAXIMUM RADIAL DISTANCE USED
XVZ -  MAX VALUE OF SPECTRAL DENSITY FN AT MAXIMUM Z DISTANCE USED
R   -  VARIANCE COMPUTED
   SUBPROGRAMS USED:
F  -   FUNCTION TO COMPUTE SPECTRAL DENSITY USED
TSD -  FUNCTION TO COMPUTE THE RATIO B2(R)/B1(R), ABS VALUE & SQUARED

------------------------------------------------------------------------

 REAL  DELRHO, DELZ, AC, AW, G, SIGSQ, LAMB1, LAMB2, LAMB3
 REAL  RHO, Z, SFFV, RATSDV, HDELZ, MAXVR, MAXVZ, VAR, PI, SUM
 REAL  SFF, RATSD
 INTEGER  I, J, K, NRHO, NZ

 PI = 3.1415927
 DELRHO = 0.2
 DELZ = 0.2
 HDELZ = DELZ/2.0
 NRHO = 100
 NZ = 25
```

```
AC = 2.6
AW = 3.0
G = -1.0
SIGSQ = 1.0
LAMB1 = 10.0
LAMB2 = 10.0
LAMB3 = 1.0
SUM = 0.0
MAXVR = 0.0
MAXVZ = 0.0
DELTH = PI / 12.5
NTH = 25

DO 5  II = 1, NTH

  THETA = FLOAT(II) * DELTH

  DO 10  I = 0, NRHO

    RHO = FLOAT(I) * DELRHO
    Z = -HDELZ
    DO 20  J = 1, NZ

      Z = Z + DELZ
      SFFV = SFF (SIGSQ, THETA, RHO, Z, LAMB1, LAMB2, LAMB3)
      RATSDV = RATSD (RHO, Z, AC, AW, G)
      VALUE = SFFV * RATSDV
      SUM = SUM + VALUE
      IF (I .EQ. NRHO) THEN
        IF (VALUE .GT. MAXVR) MAXVR = VALUE
      ENDIF
      IF (J .EQ. NZ) THEN
        IF (VALUE .GT. MAXVZ) MAXVZ = VALUE
      ENDIF

    CONTINUE

  CONTINUE

CONTINUE

VAR = 2.0 * SUM * DELRHO * DELZ * DELTH
WRITE (5,*) ' VAR = ',VAR
WRITE (5,*) ' MAXVR = ',MAXVR,' MAXVZ = ',MAXVZ

STOP
END
```

```
 REAL FUNCTION SFF(SIGSQ, THETA, RHO, Z, LAMB1, LAMB2, LAMB3)
C-----------------------------------------------------------------------
C   THIS FUNCTION EVALUATES THE THREE-DIMENSIONAL SPECTRAL DENSITY
CED AS A BASIS FOR OUR SPECTRAL DENSITY.  REFERENCE: _____________
C   VARIABLES USED:
CSQ  - VARIANCE OF FIELD
C    -  RADIAL DISTANCE VARIABLE
C    -    AXIAL DISTANCE VARIABLE
CMB1  - CORRELATION LENGTH IN R1 DIRECTION (Z-DIRECTION HERE)
CMB2  - CORRELATION LENGTH IN R2 DIRECTION
CMB3  - CORRELATION LENGTH IN R3 DIRECTION
CN  -   DENOMINATOR
CM  -   NUMERATOR
C-----------------------------------------------------------------------

 REAL  SIGSQ, RHO, Z, LAMB1, LAMB2, LAMB3, DEN, NUM, THETA

 PI = 3.1415927
 NUM = SIGSQ * LAMB1 * LAMB2 * LAMB3
 DEN = 1.0 + Z * Z * LAMB1 * LAMB1
 DEN = DEN + RHO*RHO*((LAMB2*COS(THETA))**2+(LAMB3*SIN(THETA))**2)
 DEN = DEN * DEN * PI * PI
 SFF = NUM / DEN
 RETURN
 END

 REAL FUNCTION RATSD(RHO, Z, AC, AW, G)
C-----------------------------------------------------------------------
C   THIS FUNCTION EVALUATES THE RATIO B2(R)/B1(R), IN ITS
CUARED FORM AFTER TAKING ITS ABSOLUTE VALUE.  THIS RATIO IS COMPUTED
C A THREE-DIMENSIONAL SPACE.
C   VARIABLES USED:
CSQ  - VARIANCE OF FIELD
C    -  RADIAL DISTANCE VARIABLE
C    -   EXPONENT IN FUNCTION REPRESENTING MOBILITY
C    -   EXPONENT IN FUNCTION REPRESENTING RELATIVE PERMEABILITY OF WATER.
C    -   SATURATION GRADIENT
CN  -   DENOMINATOR
CM  -   NUMERATOR
C-----------------------------------------------------------------------

 REAL  RHO, Z, AW, AC, G, DEN, NUM

 R1SQ = Z * Z
 RSQ = RHO * RHO  +  R1SQ
 NUM = (G * AW * RSQ  +  (AC - AW) * G * R1SQ) ** 2
 NUM = (NUM  +  (AC * AW * G * G) ** 2 * R1SQ) * RHO
 DEN = (AW * (AW - 1.0) * G) ** 2 * RSQ * RSQ
 DEN = DEN + R1SQ * ((AW - AC)*RSQ - AC * AW * (AW - 1.0)*G*G)**2
 RATSD = NUM / DEN
 RETURN
 END
```

APPENDIX III

EFFECTIVE VELOCITY PROGRAM LISTING

```
)GRAM EFFV6.FOR  "EFFECTIVE VELOCITY PROGRAM #6"
\DD SOME CONVENIENCE I/O, COMPUTATION FEATURES
=> IMPLEMENT LOOPING TO VARY PARAMETERS
=> DIVIDE THRU BY H (EXPONENTIAL DIV BY MUW)  11/22
=> IMPLEMENT GRID SPACING AS A FUNCTION OF LAMBDA  -  12/1
-----------------------------------------------------------------------
   THIS PROGRAM NUMERICALLY COMPUTES EFFECTIVE WATER VELOCITY IN THE
)-PHASE FLOW CASE IN TWO HORIZONTAL DIMENSIONS.  THE EQUATIONS ARE THE
;ULT OF PERTURBATIONS, SPECTRAL REPRESENTATION OF RANDOM VARIABLES, AND
TAYLOR SERIES APPROXIMATION OF EXPONENTIALS REPRESENTING VARIABILITIES
 PERMEABILITY AND SATURATION.  SINCE EFFECTIVE VELOCITY IS THE EXPECTED
LUE OF VELOCITY, TAKING THE EXPECTED VALUE RESULTS IN SEVERAL STOCHASTIC
TEGRALS.  EVALUATING THESE INTEGRALS RESULTS IN VARIANCES AND CROSS-
/ARIANCES.  THESE INTEGRALS ARE NUMRICALLY EVALUATED IN THIS CODE.

   VARIABLES USED:
   -    INPUT: EXPONENT IN FUNCTION REPRESENTING MOBILITY
   -    INPUT: EXPONENT IN FUNCTION REPRESENTING RELATIVE PERM. OF WATER.
   -    INPUT: A CONSTANT IN EXPONENTIAL REPRES. OF REL PERM. OF WATER
   -    INPUT: SATURATION GRADIENT
T  -    INPUT: PRESSURE GRADIENT
;FSQ - INPUT: VARIANCE OF HYDRAULIC HEAD (MODELED BY MIZELL'S S.D. "B")
MBDA - INPUT: CORRELATION LENGTH IN ANY HORIZONTAL DIRECTION
V  -    INPUT: THE DYNAMIC VISCOSITY OF WATER
   -    INPUT: THE MEAN OF THE NATURAL LOG OF INTRINSIC PERMEABILITY
\R -    INPUT: THE MEAN OF THE LOG OF WATER SATURATION
?HA -   A TERM WHICH IS A SCALED INVERSE OF CORRELATION LENGTH, LAMBDA
   -    SPATIAL VARIABLE IN FREQUENCY DOMAIN
   -    SPATIAL VARIABLE IN FREQUENCY DOMAIN
LR -    INCREMENTS IN R1 AND R2
ELR -   HALF OF DELR
   -    NUMBER OF INCREMENTS TAKEN IN R1 AND R2 ON EITHER SIDE OF AXES.
I,K -   LOOP INDICES
VG  -   A CONSTANT TERM WHICH IS A FUNCTION OF AW AND G
?V  -   VALUE OF 3-D SPECTRAL DENSITY FN USED
MR1 -   SUM OF COMPUTATIONS IN INTEGRATION W.R.T. R1
\TIO - VALUE OF RATIO B2(R)/B1(R) EVALUATED AT SOME PARTICULAR R1 AND R2
IR1 -   VALUE OF INTEGRATION OF E[f del Po'] + Aw E[T' del Po'] in R1 dir.
ICMB - VALUE OF INTEGRATION GIVING THE CROSS-COVARIANCE  COV(f,T')
NTI -   VALUE OF PART OF INTEGRAL "I" EVALUATED AT A PARTICULAR R1 AND R2
IR1 -   VALUE OF INTEGRAL "I" IN R1 DIRECTION EVAL AT A PARTIC. R1 AND R2
RMVF - VALUE OF TERM OF WHICH THE PRINCIPAL COMPONENT IS VAR OF f
RMVT - VALUE OF TERM OF WHICH THE PRINCIPAL COMPONENT IS VAR OF T'
RF  -   VARIANCE OF HEAD PROCESS
RT  -   VARIANCE OF LOG OF SATURATION PROCESS
CFT -   VALUE OF TERM IN CROSS-COV OF f, T' INTEGRAL AT A PARTIC. R1 AND R2
CFT -   SUM OF INDIVIDUAL EVALUATIONS OF CROSS-COV OF f, T' INTEGRAL
CFT -   VALUE OF INTEGRAL OF  CROSS-COV OF f, T'
MINT - SUM OF INTEGRATIONS PERFORMED AS PART OF COMPUTATION OF EFF VEL
```

```
FVEL - OUTPUT: THE EFFECTIVE VELOCITY
AIN -  INPUT: USER'S RESPONSE TO "DO YOU WANT ANOTHER RUN ?"
ONE -  INOUT: USER'S RESPONSE TO "SET SIGMA F EQUAL TO ONE ?"
   SUBPROGRAMS USED:
   -    FUNCTION TO COMPUTE SPECTRAL DENSITY OF HEAD (MIZELL'S "B")
FIO -  FUNCTION TO COMPUTE THE COMPLEX RATIO B2(R)/B1(R)
FI  -  FUNCTION TO COMPUTE THE MAJOR CALCULATIONS FOR INTEGRAL "I"
-----------------------------------------------------------------------

 REAL  AC, ALPHA, AW, CW, DELR, EFFVEL, F, G, ICCFT, INTR1
 REAL  JJJ, LAMBDA, MUW, PI, R1, R2, RSQ, SB, SFFV, SIGFSQ
 REAL  SUMINT, TAWG, TBAR, TERMVF, TERMVT, VARF, VART
 INTEGER  I, J, K, NR
 COMPLEX  INTI, RATIO, SCCFT, SUMR1, VCCFT, VINTI, VIIR1, VRATIO
 CHARACTER  AGAIN*1, SFONE*1

 WRITE (5,*) ' SET SIGMA F EQUAL TO ONE AGAIN? <CR>=YES;"N"=NO'
 READ (5,'(A1)') SFONE
 IF (SFONE .NE. 'N' .OR. 'n') SFONE = 'Y'
 AGAIN = 'N'
 PI = 3.1415927
 DELR = 0.10
 DELRO = DELR
 HDELR = DELR / 2.0
 HDELRO = HDELR
 F = 1.0
 CW = 0.0
 TBAR = -0.693
 MUW = 1.0
 NR = 100
 AC = 2.6
 AW = 3.0
 WRITE (5,*) ' ENTER G '
 READ  (5,*) G
 WRITE (5,*) ' ENTER J '
 READ  (5,*) JJJ
 SIGFSQ = 1.0
 DO 2  III = 1, 4

   IF (III .EQ. 1) G = 0.0
   IF (III .EQ. 2) G = -0.01
   IF (III .EQ. 3) G = -0.1
   IF (III .EQ. 4) G = -1.0
   DO 3 JJ = 1, 10

     LAMBDA = FLOAT(JJ)
     DELR = DELRO/LAMBDA
     HDELR = HDELRO/LAMBDA
```

```
      ALPHA = 3.0 * PI / (16.0 * LAMBDA)
      TAWG = AW * (AW - 1.0) * G
      SUMR1 = CMPLX(0.0,0.0)
      SCCFT = CMPLX(0.0,0.0)
      TERMVF = 0.0
      TERMVT = 0.0
      DO 10  I = -NR, NR-1

        R1 = FLOAT(I) * DELR + HDELR
        DO 20  J = -NR, NR-1

          R2 = FLOAT(J) * DELR + HDELR
          RSQ = R1 * R1  +  R2 * R2
          SFFV = SB (ALPHA, R1, R2, SIGFSQ)
          TERMVF = TERMVF + SFFV
          VRATIO = RATIO (AC, AW, G, RSQ, R1, TAWG)
          TERMVT = TERMVT + REAL(VRATIO * CONJG(VRATIO)) * SFFV
          VINTI = INTI (AC, AW, VRATIO)
          VIIR1 = CMPLX(SFFV,0.0) * VINTI / CMPLX(RSQ,-R1*G*AC)
          SUMR1 = SUMR1 + CMPLX(-R1*R1,0.0) * VIIR1
          SCCFT = SCCFT + VRATIO * SFFV

        CONTINUE

      CONTINUE
      INTR1 = REAL(SUMR1) * DELR * DELR
      VARF = TERMVF * DELR * DELR
      IF (SFONE .EQ. 'Y')    VARF = 1.0
      TERMVF = VARF / 2.0
      VART = TERMVT * DELR * DELR
      TERMVT = AW * AW * VART / 2.0
      ICCFT = AW * REAL(SCCFT) * DELR * DELR
      SUMINT = REAL(INTR1) + TERMVF + TERMVT + ICCFT

IDE THRU BY H

      EFFVEL = - JJJ * (1.0 + SUMINT)
      WRITE (5,*) ' EFFVEL = ',EFFVEL,' G = ',G,' LAMBDA=',LAMBDA
      WRITE (20,290) LAMBDA, EFFVEL

    CONTINUE
    WRITE (20,*) '  '

  CONTINUE
  FORMAT(F7.2,2X,F9.5)
  WRITE (5,*) ' DO YOU WANT ANOTHER RUN ? <CR> = NO; "Y" = YES '
  READ (5,'(A1)') AGAIN
  IF (AGAIN .EQ. 'Y' .OR. 'y') GO TO 400

  STOP ' PROGRAM EFFV6.FOR COMPLETED '
  END
```

```
REAL FUNCTION SB (ALPHA, K1, K2, SIGFSQ)
C-----------------------------------------------------------------------
C  THIS FUNCTION COMPUTES THE SPECTRAL DENSITY B IN MIZELL'S PAPER
CR 18 (4), pp. 1053-2067, FORMULA 13).
C-----------------------------------------------------------------------

      REAL ALPHA, K1, K2, SIGFSQ
      PI = 3.141592654

      SB = 3.0 * ALPHA * ALPHA * SIGFSQ * (K1 * K1  +  K2 * K2) ** 2
      SB = SB / (PI * (K1 * K1  +  K2 * K2  +  ALPHA * ALPHA) ** 4)

      RETURN
      END


      COMPLEX FUNCTION INTI(AC, AW, VRATIO)
C-----------------------------------------------------------------------
C  THIS FUNCTION CALCULATES THE RATIO OF B2(R)/B1(R), THEN COMPUTES
CRESULT WHICH IS A PRODUCT OF FUNCTIONS OF THIS RATIO.
C-----------------------------------------------------------------------

      REAL  AC, AW
      COMPLEX  VRATIO, RATIO1, RATIO2

      RATIO1 = 1.0  +  AC * VRATIO
      RATIO2 = 1.0  +  AW * VRATIO
      RATIO2 = CONJG(RATIO2)
      INTI = RATIO1 * RATIO2

      RETURN
      END


      COMPLEX FUNCTION RATIO(AC, AW, G, RSQ, R1, TAWG)
C-----------------------------------------------------------------------
C  THIS FUNCTION CALCULATES THE RATIO OF B2(R) OVER B1(R),
C-----------------------------------------------------------------------

      REAL  AC, AW, G, R1, RSQ, TAWG
      COMPLEX  I, RTNEW, B3, DEN

      I = CMPLX(0.0,1.0)
      B3 = CMPLX(RSQ,-AW*G*R1) / CMPLX(RSQ,-AC*G*R1)
      RTNEW = CMPLX(AW*G,R1) - R1 * B3 * I
      DEN = I*R1*(AW - AC*B3) + CMPLX(TAWG,0.0)
      RATIO = -RTNEW / DEN

      RETURN
      END
```